

NASA CR-159096



# NASA Contractor Report 159096

NASA-CR-159096  
1979 0021299

# Thermostructural Applications of Heat Pipes

FOR REFERENCE  
DO NOT REMOVE FROM THIS ROOM

M. E. Peeples, J. C. Reeder, and K. E. Sontag

McDonnell Douglas Astronautics Company-St. Louis Division  
St. Louis, Missouri 63166

Contract NAS 1-15554  
June 1979

**NASA**  
National Aeronautics and  
Space Administration  
**Langley Research Center**  
Hampton, Virginia 23665

**LIBRARY COPY**

SEP 6 1979

LANGLEY RESEARCH CENTER  
LIBRARY, NASA  
HAMPTON, VIRGINIA



|   |  |  |            |
|---|--|--|------------|
| 1. Report No.<br>NASA CR 159096   | 2. Government Accession No.                          | 3. Recipient's Catalog No.                                 |            |
| 4. Title and Subtitle<br>Thermostructural Applications of Heat Pipes  |  | 5. Report Date<br>June 1979                                |            |
|   |  | 6. Performing Organization Code                            |            |
| 7. Author(s)<br>M. E. Peeples, J. C. Reeder, and<br>K. E. Sontag  |  | 8. Performing Organization Report No.                      |            |
|   |  | 10. Work Unit No.  |            |
| 9. Performing Organization Name and Address<br>McDonnell Douglas Astronautics Company-<br>St. Louis Division<br>Post Office Box 516<br>St. Louis, Mo. 63166   |  | 11. Contract or Grant No.<br>NAS 1-15554                   |            |
|   |  | 13. Type of Report and Period Covered<br>Contractor Report |            |
|   |  | 14. Sponsoring Agency Code                                 |            |
| 12. Sponsoring Agency Name and Address<br>NASA Langley Research Center<br>Hampton, VA 23665   |  |  |            |
| 15. Supplementary Notes<br>FINAL REPORT<br>Langley Technical Monitor: Charles J. Camarda  |  |  |            |
| 16. Abstract<br><p>The feasibility of integrating heat pipes in high temperature structure to reduce local "hot spot" temperature is evaluated for a variety of hypersonic aerospace vehicles. From an initial list of twenty-two potential applications, the Single Stage to Orbit (SSTO) wing leading edge showed the greatest promise and was selected for preliminary design of an integrated heat pipe thermostructural system. The design consisted of a Hastelloy-X assembly with sodium heat pipe passages aligned normal to the wing leading edge. A D-shaped heat pipe cross-section was determined to be optimum from the standpoint of structural weight.</p> |  |  |            |
| 17. Key Words (Suggested by Author(s))<br>Heat Pipes<br>Thermal Protection Systems<br>Space Transportation Systems  |  | 18. Distribution Statement<br>Unclassified - Unlimited     |            |
| 19. Security Classif. (of this report)<br>Unclassified  | 20. Security Classif. (of this page)<br>Unclassified | 21. No. of Pages<br>116                                    | 22. Price* |

\* For sale by the National Technical Information Service, Springfield, Virginia 22151

N79-29470 #



## FOREWORD

This report was prepared by the McDonnell Douglas Astronautics Company, St. Louis Division, for the Langley Research Center of the National Aeronautics and Space Administration.

The purpose of this study was to investigate the feasibility of employing heat pipes in an integrated thermostructural subsystem together with evaluation of two specific heat pipe concepts provided by NASA. The program was conducted in accordance with the requirements and instructions of NASA Contract NAS1-15554, with minor revisions mutually agreed on by NASA and MDAC-St. Louis. Customary units were used for the principal measurements and calculations. Results were converted to the International System of Units (SI) for the final report.

Mr. M. E. Peeples was the MDAC-St. Louis Program Manager and was responsible for the thermodynamic analyses. Mr. K. E. Sontag was responsible for design engineering and Mr. J. C. Reeder was responsible for the detailed strength analyses.



TABLE OF CONTENTS

| <u>SECTION</u> | <u>TITLE</u>  | <u>PAGE</u> |
|----------------|---|-------------|
| 1.0            | SUMMARY.....  | 1           |
| 2.0            | INTRODUCTION.....   | 3           |
| 3.0            | SURVEY OF POTENTIAL APPLICATIONS.....                       | 5           |
|                | 3.1 Candidate Vehicles.....                                 | 5           |
|                | 3.2 Candidate Screening.....                                | 7           |
|                | 3.2.1 First Screening.....                                  | 7           |
|                | 3.2.2 Second Screening.....                                 | 9           |
|                | 3.3 APPLICATION SELECTED FOR FURTHER STUDY.....             | 32          |
| 4.0            | SSTO WING LEADING EDGE HEAT PIPE DESIGN.....                | 33          |
|                | 4.1 SSTO Baseline Description.....                          | 33          |
|                | 4.2 Design Environments.....                                | 38          |
|                | 4.3 Heat Pipe Design.....                                   | 41          |
|                | 4.3.1 Definition of Heat Pipe Length.....                   | 42          |
|                | 4.3.2 Transient Analysis.....                               | 45          |
|                | 4.3.3 Radial and Axial Heat Transfer Rates.....             | 49          |
|                | 4.3.4 Heat Pipe Limits.....                                 | 54          |
|                | 4.4 Leading Edge Design.....                                | 57          |
|                | 4.4.1 Heat Pipe Cross-Section Design.....                   | 58          |
|                | 4.4.2 Strength Analysis.....                                | 64          |
|                | 4.4.3 System Weight.....                                    | 71          |
| 5.0            | CONCLUSIONS.....  | 73          |
| 6.0            | APPENDIX A - LEADING EDGE PARAMETRIC STUDIES.....           | 75          |
|                | A.1 Heat Pipe Limits and Analytical Methods.....            | 75          |
|                | A.2 Leading Edge Heat Pipe Design Parameters.....           | 79          |
| 7.0            | APPENDIX B - HEAT PIPE COOLED HONEYCOMB SANDWICH PANEL..... | 107         |
|                | B.1 NASA Design Concept.....                                | 107         |
|                | B.2 Design Assessment.....                                  | 109         |
| 8.0            | REFERENCES.....   | 115         |

## LIST OF ILLUSTRATIONS

| <u>Figure</u> | <u>Title</u>   | <u>Page</u> |
|---------------|--|-------------|
| 1             | Representative Vehicle Configurations.....                                 | 6           |
| 2             | Potential Thermostructural Applications of Heat Pipes .....                | 8           |
| 3             | Wing Leading Edge - Single Stage to Orbit.....                             | 11          |
| 4             | SSTO Wing L.E. Temperature Reduction with Heat Pipes.....                  | 12          |
| 5             | Deflected Control Surface - Shuttle Body Flap.....                         | 13          |
| 6             | Typical Entry Heating Rate History for Deflected Shuttle<br>Body Flap..... | 15          |
| 7             | Shuttle Body Flap Temperature Reduction with Heat Pipes.....               | 16          |
| 8             | Control Surface Hinge Seals - Shuttle Body Flap.....                       | 17          |
| 9             | Base Heat Shield - Shuttle Aft Propulsion System .....                     | 18          |
| 10            | Fin/Body Shock Interaction - Hypersonic Aircraft.....                      | 20          |
| 11            | Engine Cowl Lip - Hypersonic Tactical Missile.....                         | 22          |
| 12            | Fin/Body Shock Interaction - Hypersonic Cruise Missile.....                | 23          |
| 13            | Peak Skin Temperatures Resulting From Deflected Missile Fins..             | 24          |
| 14            | Fin Leading Edge - Hypersonic Cruise Missile.....                          | 26          |
| 15            | Nose Cap - Hypersonic Cruise Missile.....                                  | 27          |
| 16            | Strake Leading Edge - MRRV.....  | 28          |
| 17            | Nose Cap - MRRV.....   | 30          |
| 18            | Vertical Fin Leading Edge - MRRV.....                                      | 31          |
| 19            | SSTO Wing L.E. Heat Pipe Design Layout.....                                | 35          |
| 20            | SSTO Wing L.E. Stagnation Line Temperature Histories.....                  | 37          |
| 21            | SSTO Wing L.E. Stagnation Line Static Pressures During Entry..             | 39          |
| 22            | SSTO Wing L.E. Local Heat Flux and Pressure Distributions.....             | 40          |
| 23            | Basic Heat Pipe Operation.....   | 41          |
| 24            | SSTO Wing L.E. Maximum Integrated Heat Transfer Rates.....                 | 43          |
| 25            | Determination of Required Heat Pipe Length.....                            | 44          |
| 26            | Transient Temperatures of Heat Pipe Leading Edge During Entry.             | 46          |
| 27            | Leading Edge Temperature Profiles During Entry.....                        | 47          |
| 28            | Heat Pipe Internal Pressures During Entry.....                             | 48          |
| 29            | Heat Pipe Radial Heat Flux During Entry.....                               | 50          |
| 30            | Heat Pipe Axial Heat Transfer Rates During Entry.....                      | 51          |
| 31            | Wing L.E. Elevations vs. Distance From Geometric Centerline...             | 52          |
| 32            | Heat Pipe Requirements Summary for SSTO Wing L.E.....                      | 53          |
| 33            | SSTO Wing L.E. Heat Pipe Vapor Limits.....                                 | 55          |
| 34            | SSTO Wing L.E. Heat Pipe Wick Limits.....                                  | 56          |
| 35            | Summary of Candidate Heat Pipe Configurations.....                         | 59          |
| 36            | Trade Study - Circular Tube with Single Face Sheet.....                    | 65          |
| 37            | Trade Study - Square Tube Configuration.....                               | 66          |
| 38            | Trade Study - D Tube Configuration.....                                    | 67          |
| 39            | SSTO Wing Leading Edge Structural Model.....                               | 69          |
| 40            | Heat Pipe Bending Moment.....  | 70          |
| 41            | SSTO Wing Leading Edge Weight Breakdown.....                               | 72          |



LIST OF ILLUSTRATIONS (CONT.)

| <u>Figure</u> | <u>Title</u>  | <u>Page</u> |
|---------------|---|-------------|
| 42            | Heat Pipe Working Fluid Transition Temperatures.....                          | 77          |
| 43            | Maximum Reference Stagnation Heat Flux.....                                   | 80          |
| 44            | Cylindrical Leading Edge Stagnation Line Heat Flux.....                       | 81          |
| 45            | Leading Edge Peak Stagnation Line Temperatures.....                           | 82          |
| 46            | Local Heating Rate Distribution.....  | 83          |
| 47            | Ratio of Average to Stagnation Line Heating Rate.....                         | 84          |
| 48            | Leading Edge Heat Pipe Axial Load VS. $W/SC_L$ .....                          | 86          |
| 40            | Leading Edge Heat Pipe Length Required VS. $W/SC_L$ .....                     | 87          |
| 50            | Leading Edge Heat Pipe Axial Load VS. Angle of Attack.....                    | 88          |
| 51            | Leading Edge Heat Pipe Length Required VS. Angle of Attack....                | 89          |
| 52            | Leading Edge Radial Heat Transfer Rates For Zero Angle of<br>Attack.....      | 90          |
| 53            | Leading Edge Radial Heat Transfer Rates For 30° Angle of<br>Attack.....       | 91          |
| 54            | Heat Pipe Lower Surface Adverse Elevation.....                                | 92          |
| 55            | Heat Pipe Lower Surface Heat Transfer Rates.....                              | 93          |
| 56            | Heat Pipe Upper Surface Heat Transfer Rates.....                              | 94          |
| 57            | Heat Pipe Wick Requirements For $R_{L,E}=10.16$ CM(4 In).....                 | 96          |
| 58            | Heat Pipe Wick Requirements For $R_{L,E}=20.32$ CM(8 In).....                 | 97          |
| 59            | Heat Pipe Wick Requirements For $R_{L,E}=30.48$ CM(12 In).....                | 98          |
| 60            | Effect Of Adverse Head On Potassium Wicking Performance<br>Parameter.....     | 100         |
| 61            | Effect of Adverse Head on Sodium Wicking Performance<br>Parameter.....        | 101         |
| 62            | Effect of Adverse Head on Lithium Wicking Performance<br>Parameter.....       | 102         |
| 63            | Heat Pipe Vapor Limits - Potassium.....                                       | 104         |
| 64            | Heat Pipe Vapor Limits - Sodium.....  | 105         |
| 65            | Heat Pipe Vapor Limits - Lithium.....   | 106         |
| 66            | Heat Pipe Application in Honeycomb Panel for Low Temperature<br>Gradient..... | 107         |

## LIST OF ABBREVIATIONS AND SYMBOLS

### ABBREVIATIONS

APS  
F.S.  
HWADM  
HYTAM  
H/C  
I.D.  
L.E.  
MRRV  
n.m  
O.D.  
OME  
RSI  
SLRV  
SSTO

### DEFINITIONS

Aft Propulsion System  
Factor of Safety  
Hypersonic Wide Area Defense Missile  
Hypersonic Tactical Missile  
Honeycomb  
Inner Diameter  
Leading Edge  
Maneuvering Re-entry Research Vehicle  
Nautical Mile  
Outer Diameter  
Orbital Maneuvering Engine  
Reuseable Surface Insulation  
Shuttle Launch Research Vehicle  
Single Stage-to-Orbit

### SYMBOLS

A  
Btu  
D, d  
D<sub>h</sub>  
°F  
ft  
FOM<sub>1</sub>  
FOM<sub>0</sub>  
g  
h  
hr  
in  
k  
K<sub>p</sub>  
K<sub>1</sub>  
  
L  
lb  
ṁ  
min  
M  
P  
psf  
psia  
psid  
q  
q̇  
Q<sub>b,m</sub>

Area  
British Thermal Unit  
Diameter  
Hydraulic Diameter  
Degrees Fahrenheit  
Feet  
One g Figure of Merit  
Zero g Figure of Merit  
Acceleration due to gravity  
Heat transfer coefficient, height  
Hour  
Inch  
Thermal conductivity  
Wick permeability  
Constant = 1.234 for laminar flow and  
2.2 for turbulent flow  
  
Length  
Pounds, force or mass  
Mass flow rate  
Minute  
Molecular weight, mesh number  
Pressure  
Pounds per square foot  
Pounds per square inch, absolute  
Pounds per square inch, differential  
Heat transfer rate  
Heat transfer rate per unit area  
Boiling heat transfer limit

## LIST OF ABBREVIATIONS AND SYMBOLS ( CONT. )

### SYMBOLS

|           |                                  |
|-----------|----------------------------------|
| $Q_{d,m}$ | Axial dry-out limit              |
| $Q_{s,m}$ | Entrainment limit                |
| $Q_S$     | Sonic Limit                      |
| $Q^w$     | Wicking Limit                    |
| $R^w$     | Radius, Universal gas constant   |
| $r_c$     | Capillary pore radius            |
| $r_n$     | Nucleation site radius           |
| $S$       | Surface distance                 |
| sec       | Second                           |
| $T$       | Temperature                      |
| $T^*$     | Continuum transition temperature |
| $T_F$     | Wall thickness                   |
| $w$       | Span                             |
| $W/SC_L$  | Glide parameter                  |
| $X$       | Distance, length or width        |
| $\zeta$   | Centerline                       |
| $\perp$   | Perpendicular                    |

### GREEK SYMBOLS

|            |                             |
|------------|-----------------------------|
| $\alpha$   | Angle of attack             |
| $\gamma$   | Specific heat ratio         |
| $\delta$   | Flap deflection angle       |
| $\Delta$   | Difference                  |
| $\epsilon$ | Emissivity                  |
| $\lambda$  | Latent heat of vaporization |
| $\Lambda$  | Wing sweep angle            |
| $\mu$      | Viscosity, absolute         |
| $\nu$      | Viscosity, dynamic          |
| $\psi$     | Molecular mean free path    |
| $\rho$     | Density                     |
| $\sigma$   | Surface tension             |

### SI UNITS

|       |                      |
|-------|----------------------|
| g     | Gram (Mass)          |
| J     | Joule (Heat)         |
| K     | Kelvin (Temperature) |
| m     | Meter (Length)       |
| N     | Newton (Force)       |
| $P_a$ | Pascal (Pressure)    |
| W     | Watt (Power)         |
| s     | Second (Time)        |

## LIST OF ABBREVIATIONS AND SYMBOLS (CONT.)

### SI PREFIXES

|   |                     |
|---|---------------------|
| m | Milli ( $10^{-3}$ ) |
| c | Centi ( $10^{-2}$ ) |
| k | Kilo ( $10^3$ )     |
| M | Mega ( $10^6$ )     |

### DEFINITIONS

### SUBSCRIPTS

|          |                       |
|----------|-----------------------|
| Avg      | Average               |
| ax       | Axial                 |
| c        | Capillary             |
| cond     | Condenser             |
| e, evap  | Evaporator            |
| eff      | Effective             |
| g        | Gravity               |
| L        | Liquid, local, lower  |
| L.E.     | Leading edge          |
| o        | Reference, stagnation |
| rad      | Radial                |
| SL       | Stagnation line       |
| t        | Tube                  |
| u        | Upper                 |
| v        | vapor                 |
| W        | Wick                  |
| $\infty$ | Freestream condition  |

## 1.0 SUMMARY

The feasibility of integrating heat pipes in high temperature structure to reduce local "hot spot" temperature was evaluated for a variety of hypersonic aerospace vehicles. These include: advanced space transportation systems, hypersonic missiles and hypersonic flight test vehicles. An initial list of twenty-two potential applications was screened in a two stage process to identify structural concepts most likely to benefit from the isothermalizing characteristics of heat pipes. Five applications remained after the screening: 1) Space Shuttle Body Flap, 2) Single Stage to Orbit (SSTO) wing leading edge, 3) structure adjacent to the hypersonic cruise aircraft vertical fin, 4) structure between missile fins, and 5) leading edge of the maneuvering reentry research vehicle (MRRV). From this group the SSTO wing leading edge was selected for preliminary design of an integrated heat pipe thermostructural system.

The SSTO wing leading edge heat pipe design consisted of a Hastelloy-X double-walled panel, comprised of a smooth outer skin and a corrugated inner skin. The two skins would be pre-formed to the contour of the leading edge, lined with screen wicking, and then longitudinally seam-welded together; resulting in D-shaped heat pipe channels two meters in length and aligned normal to the leading edge. Sodium was selected as the heat pipe working fluid since it has the best characteristics in the 1256K (1800°F) operational range and has demonstrated long-term compatibility with Hastelloy-X. The D-shaped heat pipe cross-section was determined to be optimum from the standpoint of structural weight. Use of standard gage materials and a 1.27 cm (0.5 in) D-tube diameter results in a panel unit weight of 11.3 kg/m<sup>2</sup> (2.23 lb/ft<sup>2</sup>) - approximately 35% lower than a circular cross-section. Optimization studies showed that the panel unit weight could be reduced to 9.5 kg/m<sup>2</sup> (1.94 lb/ft<sup>2</sup>) by using 1.0 cm (0.4 in) diameter D-tubes and non-standard material gages.

A potential thermostructural heat pipe concept supplied by NASA was evaluated from the standpoint of performance and fabricability. The concept used potassium working fluid in a honeycomb panel to reduce transient temperature gradients between face sheets. No performance constraints were found, but fabrication and servicing of a honeycomb assembly with heat pipe working fluid is the major concern. Fabrication and filling approaches were investigated, but insufficient fabrication experience is available to verify their feasibility.



## 2.0 INTRODUCTION

The tests reported in References 1 and 2 demonstrated the durability of heat-pipe-cooled leading edge structures for withstanding earth-entry thermal and mechanical loads and indicated the reliability of the concept for fully reusable hypersonic cruise and space transportation systems. Hence, a study was initiated to review potential thermostructural applications of heat pipes and analytically evaluate the feasibility of selected concepts. Hypersonic vehicles considered were: advanced space transportation, entry research and advanced missiles. The investigation was limited to applications where the isothermalizing characteristics of heat pipes could reduce structural temperatures at local "hot spots" and allow replacement of refractory metal structure with superalloy construction or superalloy structure with titanium. It was anticipated that such applications could result in cost or weight advantages relative to competing reusable thermostructural systems. This study consisted primarily of two tasks:

Task I - Survey and Screening of Candidate Concepts

Task II - Design of a Selected Concept

The results of these two tasks are presented in Sections 3 and 4, respectively.

An appendix is included in this report which provides parametric data for use in assessing the feasibility of heat pipe cooling of leading edges for vehicles not specifically considered in this study. The appendix also includes a cursory evaluation of a NASA supplied concept which employs heat pipes for minimizing temperature gradients within a honeycomb sandwich panel of an airframe-integrated scramjet engine.





## 3.0 SURVEY OF POTENTIAL APPLICATIONS

The purpose of this task was to identify specific problem areas on advanced space transportation systems, future high speed missiles, and research vehicles for which heat pipe cooling is promising. The high effective thermal conductivity provided by heat pipe systems suggests their use in reducing structural temperatures and temperature gradients often encountered on high speed flight vehicles; e.g. stagnation locations, regions of flowfield shock interactions, and regions of impinging combustion gases. More generally, any area which is subjected to localized high heating rates and is located adjacent to a cooler region that might be used as a heat sink could be considered as a potential application for the isothermalizing capability of heat pipes. Whether or not this potential can be realized depends on more specific design factors such as the actual magnitude of the heating rates, g levels and directions, and dimensional constraints unique to the particular application.

### 3.1 CANDIDATE VEHICLES

Examples of relevant vehicle configurations where heat pipes might be applied are shown in Figure 1. These include representative advanced space transportation systems such as Space Shuttle and Single Stage-to-Orbit (SSTO); research vehicles such as Manned Maneuvering Reentry Vehicle (MRRV) and Shuttle Launch Research Vehicle (SLRV); and other hypersonic applications such as Hypersonic Airbreathing Missile, Hypersonic Tactical Missile (HYTAM), and Hypersonic Wide Area Defense Missile (HWADM). Candidate locations were selected for further evaluation and screening to determine the potential use of heat pipes for reducing structural temperatures and gradients in areas subjected to intense heating rates. The initial list of potential applications is presented in Figure 2. Subsequent screening analyses determined the most promising applications for further study. The primary criteria utilized for these analyses was whether or not heat pipes could be expected to result in a structural material change which would be beneficial in terms of cost, weight, reuseability, or other relevant factors compared to more conventional baseline designs.

Based on previous studies (Reference 3), it was felt that the most promising applications were those where the thermal environment would ordinarily dictate the use of refractory materials. Refractories are not only expensive but also are subject to damage from either oxidation or handling and thus require protective coatings which are generally susceptible to damage and are life-limited. Substitution of a thermostructural design incorporating liquid metal heat pipes and superalloy material would be more durable, have longer life capability, and for reusable applications possible be cheaper. Likewise, areas which normally would require the use of superalloy materials might be lighter if constructed of a titanium thermostructural heat pipe design. The study was therefore constrained to evaluate vehicle locations where temperatures and temperature gradients can be reduced sufficiently to allow the use of titanium or superalloys. For this range of temperatures, 900K to 1300K (1160°F to 1800°F), the most likely heat pipe working fluids are potassium and sodium.

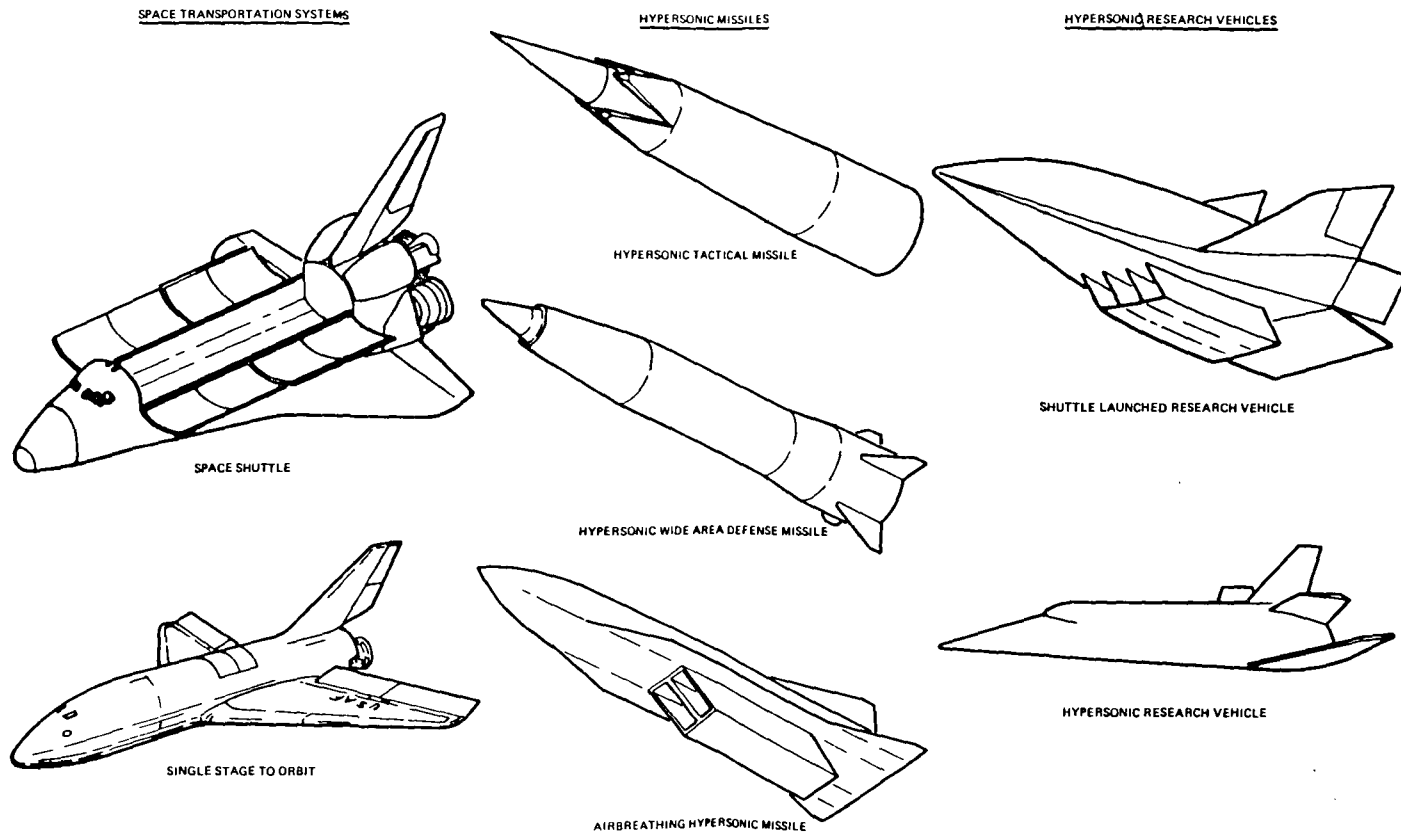


Figure 1. - Representative vehicle configurations.

## 3.2 CANDIDATE SCREENING

The candidate vehicles and locations initially postulated were analyzed and screened via a two-stage screening process, which determined the most promising application for more detailed evaluation. Results of the screening analyses are summarized in the following paragraphs.

### 3.2.1 First Screening

During the first screening process, some of the applications listed in Figure 2 were eliminated based on either a judgemental assessment, lack of design information required to adequately determine a pay-off, or similarity to another candidate location which was retained. Due to the preliminary design status of some of the candidate vehicles postulated, a clear definition of the baseline designs was not always available, nor were the specific environments known to the degree required for complete assessment of heat pipe potential. Therefore, for many applications, cursory evaluation of the environments was required before being able to determine general heat pipe requirements. It was found that in a number of cases, the objective of using superalloy materials for heat pipe applications in lieu of refractory construction or titanium in lieu of superalloys could not be met--simply because the heating rates were so high that an excessively long heat pipe would be required to reduce temperature levels to within the allowable temperature range - i.e. <1256K (1800°F) for superalloys and <1033K (1400°F) for titanium. The concepts eliminated during the first screening are discussed below.

#### 3.2.1.1 Advanced Space Transportation Systems

The Shuttle nose cap was evaluated during a previous study (Reference 3) and was found to offer little potential as a viable location for heat pipes because of dimensional complexity and the requirement for a cascaded heat pipe design. Therefore, the nose Cap (A2) was eliminated in the first screening.

High localized heating rates resulting from upper-body shock impingement (A5) are somewhat similar to localized heating of fuselage structure caused by shocks generated by adjacent fins (A9). Because of this similarity and the higher degree of difficulty in defining design heating rate distributions, upper body shock impingement areas (A5) were not considered beyond the first screening.

Fin leading edge heat protection for space transportation systems (A8) will generally be determined by ascent heating rather than entry because of the high angles of attack flown during the descent trajectory and resultant lower heating rates. However, during ascent, the high axial g forces (typically up to approximately 3 g's) will tend to drive the heat pipe working fluid aft and away from the regions of highest heating. It was deemed unlikely that adequate wick capacity could be provided for a fin leading edge heat pipe design during ascent because of the high adverse g levels, and thus this concept was eliminated from further consideration.

The remaining concepts after this first screening were: the SSTO wing leading edge, shuttle body flap, control surface gaps, shuttle base heat shield and structure adjacent fins.



| A - <u>Advanced Space Transportation Systems</u>  | <u>1st Screening</u>   | <u>2nd Screening</u>   |
|---|--|--|
| 1. Leading Edge<br>2. Nose Cap<br>3. Flaps<br>4. Control Surfaces<br>5. Upper Body Shock Impingement<br>6. Control Surface Gaps<br>7. Base Heat Shield<br>8. Fin Leading Edge<br>9. Structure Adjacent Fins | SSTO Wing Leading Edge<br>Shuttle Body Flap<br>Control Surface Gaps<br>Base Heat Shield<br>Structure Adjacent Fins | SSTO Wing Leading Edge <br>Shuttle Body Flap<br>Structure Adjacent Fins |
| B - <u>Hypersonic Missiles</u>  | Cowl Lip<br>Combustor Flame Holder<br>Structure Between Fins<br>Fin Leading Edge<br>Nose Cap                       | Structure Between Fins   |
| C - <u>Research Vehicles</u>  | Leading Edge<br>Nose Cap<br>Fin Leading Edge   | MRRV Fin Leading Edge  |
| 1. Leading Edge<br>2. Nose Cap<br>3. Fin Leading Edge<br>4. Flow Field Probes<br>5. Control Surface Gaps<br>6. Scramjet Components  |  |  Selected for<br>further evaluation                                   |

Figure 2. - Potential thermostructural applications for heat pipes.

### 3.2.1.2 Hypersonic Missiles

The combustor structure for scramjets (B3) as well as exhaust nozzle throats (B6) were judged to be unsuitable candidates for heat pipes. Environments in these locations are highly transient and will most likely result in heat pipe start-up problems. In addition, the temperature levels encountered, 2400K to 3600K (3860°F to 6020°F), are higher than can be tolerated by superalloy materials. Missiles in general have several other drawbacks with regard to possible heat pipe cooling. They are single use applications where initial low cost is the primary factor and reuse is not a requirement. Also, heat pipe locations on missiles should be limited to those having either favorable or no g force effects (i.e. with g forces either assisting the return of condensate within the heat pipe from the condenser to the evaporator or else having minimal influence). These locations are expected to be at some leading edge areas and portions of the fuselage. The concepts chosen for additional investigation were: Inlet cowl lips, combustor flame holder, structure between fins, fin leading edge, and nose cap.

### 3.2.1.3 Research Vehicles

As indicated in Figure 2, hypersonic research vehicles have thermostructural problems similar to advanced space transportation systems and hypersonic missiles plus some additions. Experiments may require local protuberances or pods, with resulting local heating rate increases. One example is flow field probes which are not only subjected to stagnation heating and need to be cooled, but also generate impinging shocks which cause large temperature gradients and high temperatures on adjacent vehicle surfaces. However, further evaluation of flow field probes (C4) was ruled out for this study because their uses are for limited application. Furthermore, specific probe configuration definition and design requirements needed for evaluation were not readily available, and efforts required to attain them were believed beyond the scope of this study.

Problems caused by control surface gaps (C5) and resultant hot boundary layer air flow over internal components due to seal leakage were assumed to be generally the same type associated with advanced transportation system control surfaces and eliminated in this first screening. Scramjet components (C6) as applied to the possible integration of heat pipes in honeycomb structure for minimizing thermal gradients between the inner and outer face sheets are considered in a separate area (Appendix B) and thus not considered further in this task. The remaining concepts were: wing leading edge, nose cap, and fin leading edge.

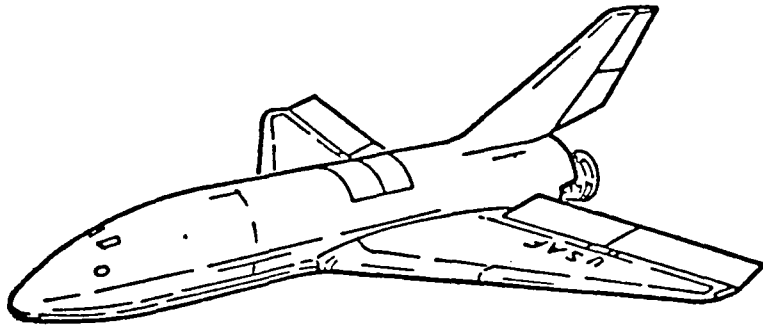
### 3.2.2 Second Screening

The candidate applications remaining after the first screening process are identified on Figure 2 and described briefly in the following paragraphs. In general, the most promising applications at this point appeared to be related to either leading edges, deflected control surfaces, or fuselage areas subjected to shock impingement due to adjacent protuberances.

- o SSTO Wing Leading Edge - The currently postulated wing leading edge of the SSTO vehicle (Figure 3) is columbium (Reference 4). Peak stagnation

line temperatures in excess of 1478K (2200°F) will be encountered during entry. The primary disadvantage of columbium for the leading edge material is the requirement for an oxidation resistant coating, hence, the possibility of frequent refurbishment due to coating damage, with resultant high life cycle costs. Since the inner surfaces of the columbium will also be subjected to oxidation effects and will have to be coated, inspection is likely to be difficult. As shown on Figure 4, utilization of a heat pipe cooled leading edge could reduce stagnation temperatures from 1494K (2230°F) to below 1256K (1800°F), thus permitting the use of a superalloy material which is less susceptible to damage from oxidation and does not require a protective coating. Previous design studies and scale model tests on the Shuttle wing leading edge showed adequate performance of a Hastelloy X heat pipe cooled leading edge design utilizing sodium as the working fluid. Even though the design was relatively straightforward and demonstrated adequate performance, its main drawback was its considerably higher weight than competing designs employing either columbium, carbon-carbon, or ablative material. Alternate heat pipe designs employing different construction methods than those used in the Shuttle wing leading edge design studies offer the potential for reduced weight.

- o Shuttle Body Flap - The Shuttle body flap is typical of deflected control surfaces on advanced space transportation systems, Either attached or separated flow conditions can occur on the flap, depending on flight parameters and flap deflection angle. The surface of the flap which is deflected into the airstream is subjected to intense heating rates because of compression shock waves, while the opposite surface remains relatively cool. For example, the peak radiation equilibrium temperature of the lower surface of the Shuttle body flap during entry is approximately 1756K (2700°F) while the upper surface remains below around 757K (900°F). This temperature difference suggests the use of heat pipes for isothermalizing the two surfaces, and perhaps allowing a change to lower temperature materials. The Shuttle baseline design, depicted on Figure 5, utilizes high temperature RSI tiles (reusable surface insulation) on the lower surface for thermal protection of the aluminum primary structure during entry. The flap upper surface, subjected to lower heating rates, employs a lighter weight low temperature RSI. Potential problems or disadvantages of RSI for the Shuttle body flap are cited on Figure 5. Peak temperatures are very close to the RSI temperature limit, leaving little margin for error in the predicted heating rates or operational flight conditions. In addition, the tiles are inherently fragile and frequent refurbishment may be required due to damage either in flight or during ground handling. Installation or refurbishment of the tiles has been shown to be a time consuming and expensive operation. Although the Shuttle body flap primary structure is a relatively lightweight state of the art design utilizing aluminum honeycomb, the thickness and weight of the RSI required for adequate thermal protection results in a sizeable weight increment.



PRESENT PROPOSED CONSTRUCTION:

- o INTEGRALLY STIFFENED COATED COLUMBIUM SKIN SUPPORTED BY DETERMINATE TRUSS

PEAK TEMPERATURES DURING ENTRY > 1478K (2200°F)

POTENTIAL PROBLEMS WITH PROPOSED CONFIGURATION

- o DAMAGE TO COLUMBIUM COATING MAY DICTATE FREQUENT REFURBISHMENT
- o DIFFICULT INSPECTION OF COLUMBIUM INBOARD SURFACES

HEAT PIPE POTENTIAL:

- o ISOTHERMALIZATION OF LEADING EDGE WILL REDUCE PEAK TEMPERATURES TO 1256K (1800°F), PERMITTING USE OF SUPERALLOY MATERIALS
- o LESS POSSIBILITY OF DAMAGE SINCE NO EXTERNAL COATING WOULD BE REQUIRED
- o POSSIBLE LIFE-CYCLE COST REDUCTION DUE TO LOWER MAINTENANCE EXPENSE

Figure 3. - Wing leading edge - single stage to orbit.

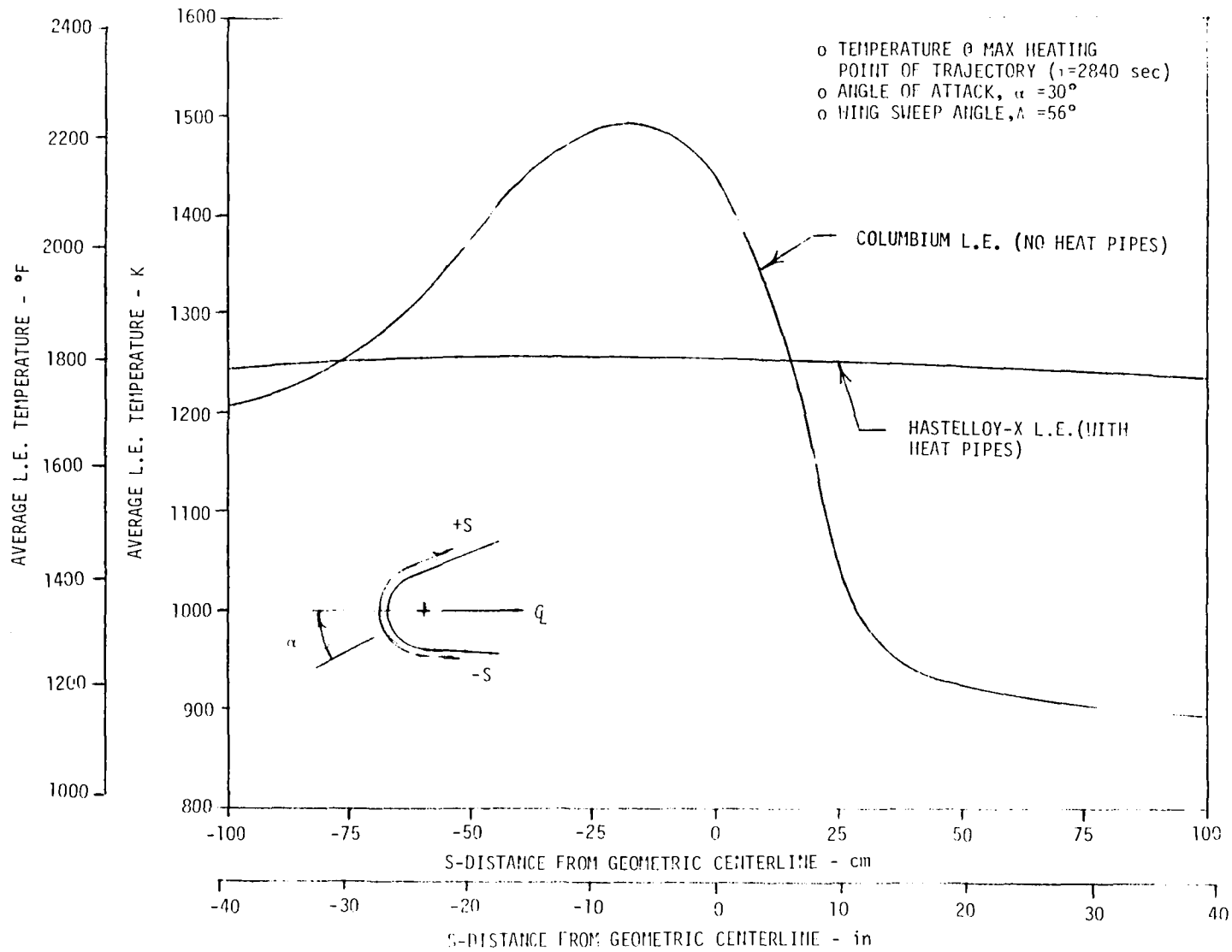
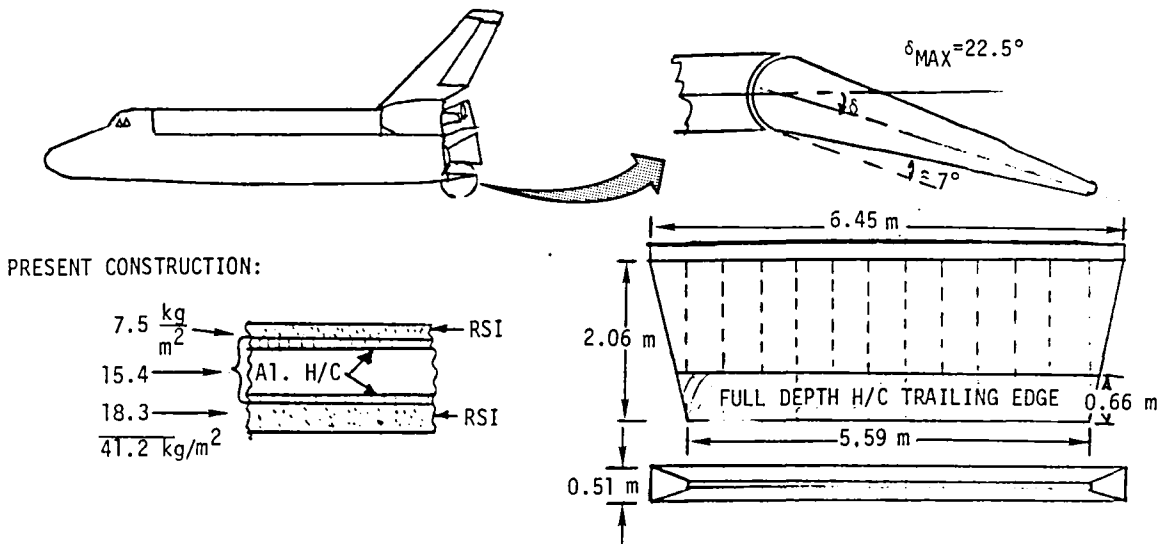
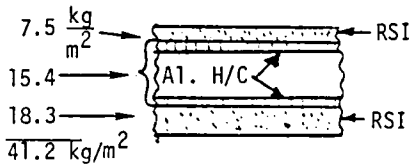


Figure 4. - SSTO wing L.E. temperature reduction with heat pipes.





PRESENT CONSTRUCTION:



PEAK HEATING RATES AND RADIATION EQUILIBRIUM TEMPS DURING ENTRY:

- o UPPER SURFACE - 14.8 kW/m<sup>2</sup> (1.3 Btu/Sec-ft<sup>2</sup>), 756K (900°F)
- o LOWER SURFACE - 431 kW/m<sup>2</sup> (38 Btu/Sec-ft<sup>2</sup>), 1756K (2700°F)

POTENTIAL PROBLEMS WITH CURRENT CONFIGURATION:

- o PEAK TEMPERATURE ON LOWER SURFACE CLOSE TO RSI LIMIT
- o RSI TILES ARE FRAGILE AND MAY REQUIRE FREQUENT REFURBISHMENT
- o RELATIVELY HIGH WEIGHT

HEAT PIPE POTENTIAL:

- o ISOTHERMALIZING UPPER AND LOWER SURFACES MAY PERMIT THE USE OF SUPERALLOY CONSTRUCTION (e.g. HASTELLOY X) WITH POTENTIAL ADVANTAGES OF:
  - LOWER WEIGHT
  - MORE DURABLE BY ELIMINATION OF RSI
  - LOWER REFURBISHMENT COSTS
- o PRELIMINARY THERMAL ANALYSES WITH HEAT PIPE BODY FLAP CONFIGURATION SHOW:
  - PEAK SKIN TEMP OF 1367K (2000°F) WHICH IS EXCESSIVE FOR SUPERALLOYS
  - HEAT PIPE START-UP TRANSIENT IS ACCEPTABLE

Figure 5. - Deflected control surface - shuttle body flap.

The utilization of heat pipes to reduce the lower surface temperature to within the range of superalloy construction would have the potential for minimizing the disadvantages cited for the current baseline configuration. The heat pipe concept would consist of thermally connecting the upper and lower surfaces by means of U-shaped heat pipes, thus providing for conduction of a portion of the aerodynamic heat absorbed by the lower surface to the upper surface for rejection by radiation. Transient thermal analyses were conducted on the flap and determined the extent of temperature reduction achievable for an uninsulated Hastelloy X structural configuration, with sodium filled tubular heat pipes connecting the upper and lower surfaces. Heat pipe limits assumed for the analyses were based on sonic velocity limits and a transition of the sodium vapor within the heat pipes from free molecular to continuum flow at approximately 700K (800°F). Since the heat pipe evaporator will in general be below the condenser with respect to g loads, it was assumed that refluxing heat pipe operation could be provided, resulting in minimal wick requirements. The heating rate profile of Figure 6 was used in the calculations. Results of the analyses are shown on Figure 7 and indicate a peak skin temperature of approximately 1367K (2000°F), which is above the 1256K (1800°F) re-use limit assumed for superalloy materials. The analyses neglected any variation in body flap heating rates in either a spanwise or chordwise direction. If a pronounced heating gradient exists on the flap lower surfaces, (e.g. due to separation and re-attachment), the isothermalizing capability of a heat pipe could further reduce flap temperatures. The Shuttle design data of Reference 5 shows detailed heating rate distributions but did not indicate large gradients. It was therefore concluded that an uninsulated thermostructural heat pipe design would not reduce flap temperatures to a level permitting the use of superalloy materials if based on the existing Shuttle design heating rates and distributions. Additional analyses defined the benefits of a Rokide Z flame sprayed coating on the lower surface and also a thin refractory radiation shield to reduce the flap structure to 1256K (1800°F) and below. Although both of these methods would achieve the desired result, the additional complexity, weight and potential coating problems of the shield approach for multi-mission operations make them unattractive alternates. Therefore, the Shuttle body flap was rejected in this second screening.

- o Control Surface Hinge Seal Gaps - Shuttle Body Flap - Areas on advanced space transportation systems where hinges are provided for the deflection and actuation of control surfaces are vulnerable to high localized heating rates. Hinge seals (Figure 8) are therefore provided to prevent or minimize the inboard flow of hot boundary layer air. Should a malfunction occur which results in seal leakage, the flow of hot air and impingement on internal components such as the aluminum primary structure employed on Shuttle, overheating could occur very rapidly. The potential of heat pipes for minimizing the consequences of hinge seal failure was assessed. It was concluded that heat pipes for this application have little or no benefits since the complexity of the

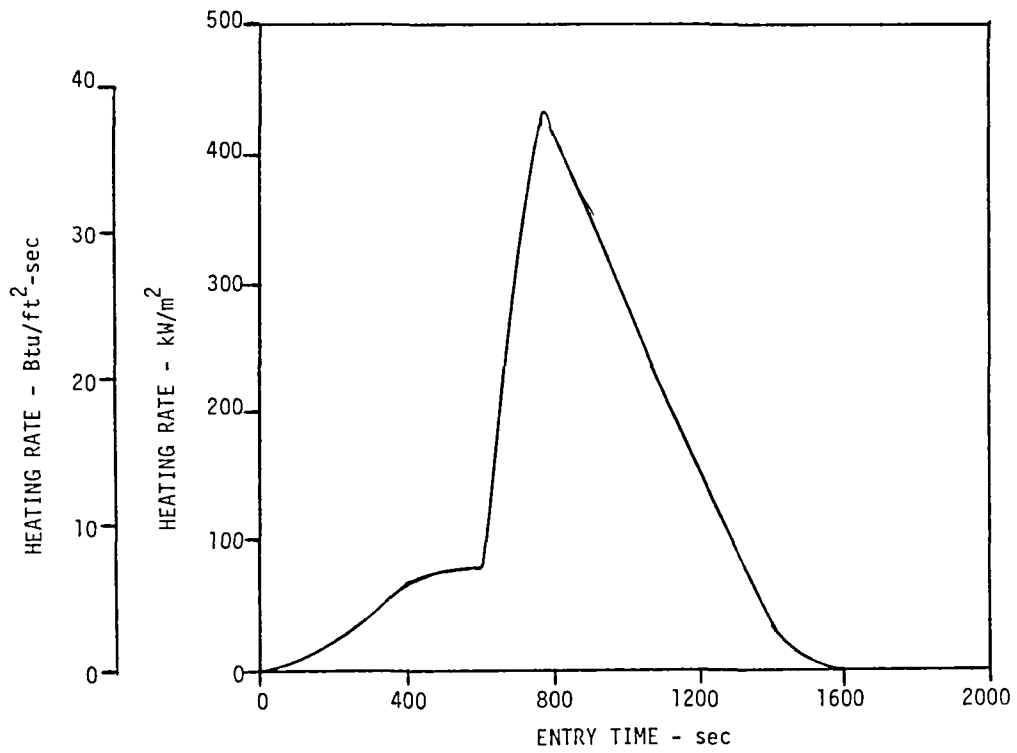


Figure 6. - Typical entry heating rate history for deflected shuttle body flap.

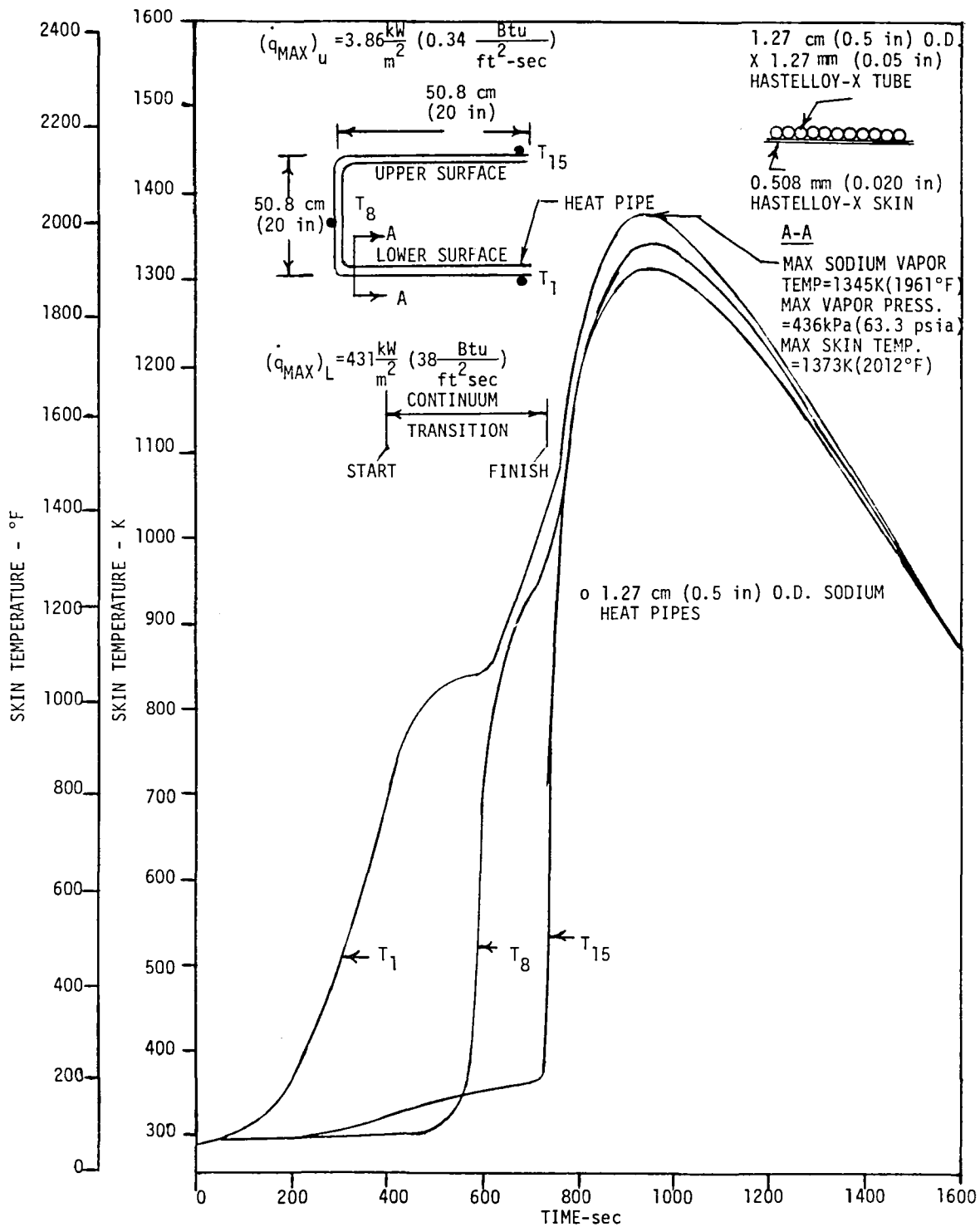
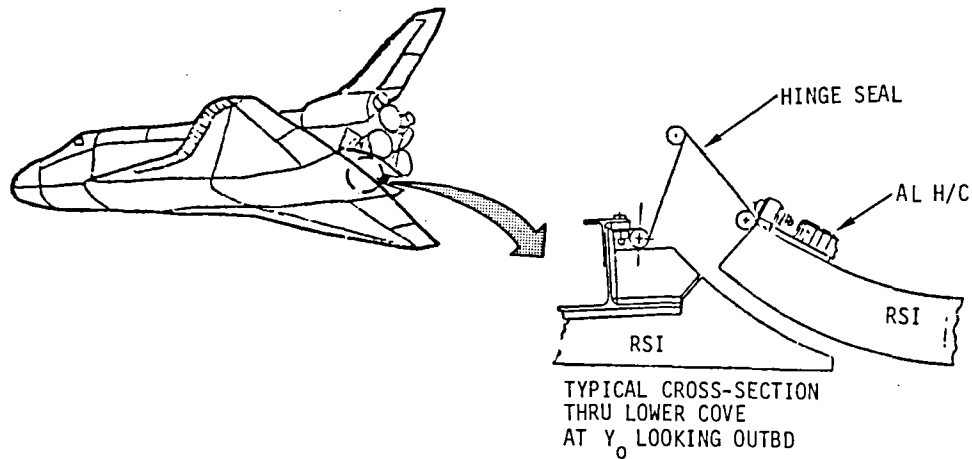


Figure 7. - Shuttle body flap temperature reduction with heat pipes.

underlying structural geometry and lack of an adequate heat sink would make it difficult to effectively utilize heat pipes.



POTENTIAL PROBLEM:

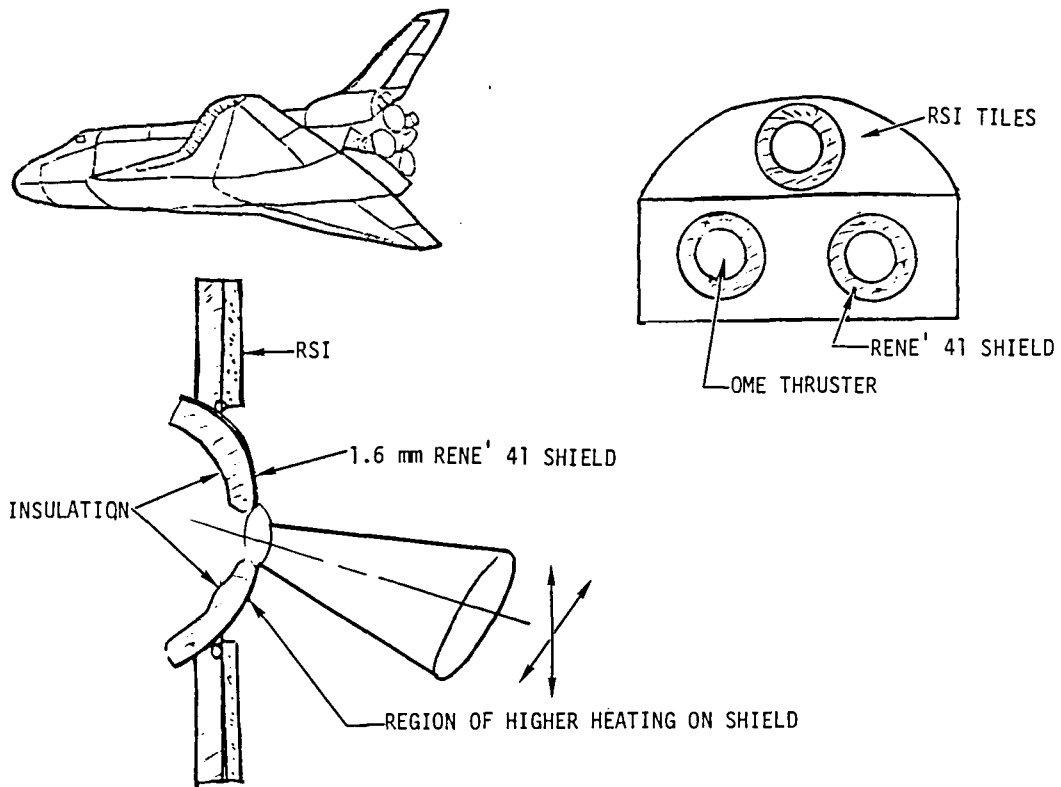
- o IN CASE OF SEAL LEAKAGE, HOT BOUNDARY LAYER AIR FLOWS OVER INTERNAL ALUMINUM STRUCTURE, RESULTING IN OVER HEATING.

HEAT PIPE POTENTIAL:

- o LITTLE IF ANY--COMPLEXITY OF STRUCTURE GEOMETRY AND LACK OF A GOOD HEAT SINK WOULD MAKE IT DIFFICULT TO EFFECTIVELY UTILIZE HEAT PIPES.

Figure 8. - Control surface hinge seals - shuttle body flap.

- o Base heat Shield - Shuttle Aft Propulsion System (APS) - The Shuttle APS base heat shield is illustrated in Figure 9. Peak temperatures of approximately 1060K (1450°F) will exist on portions of the shield during Orbital Maneuvering Engine (OME) thruster firing because of localized high radiant heating and reduced view factors to space due to nozzle cant. These local hot spots resulted in modifying the initial shield design of thin titanium to 1.6 mm (0.063 inch) thick Rene' 41. The use of circumferential heat pipes around the shield to reduce locally high temperatures was considered as a possible means of weight savings. It was concluded however that no weight savings would be provided with a heat pipe design and that the present Rene' 41 shield configuration is an adequate design solution. Thus no further effort is recommended for this application.



PROBLEM:

- o LOCAL REGIONS OF HIGHER SHIELD TEMPERATURES
  - INCREASED HEATING DUE TO NOZZLE CANT
  - REDUCED RADIATION VIEW FACTOR TO SPACE
- o HIGHER TEMPERATURES RESULTED IN CHANGING SHIELD FROM THIN TITANIUM TO RENE' 41. (CURRENT PEAK TEMPERATURE IS 1061K (1450°F) WITH 1.6 mm (0.063 in) RENE' 41)

HEAT PIPE POTENTIAL:

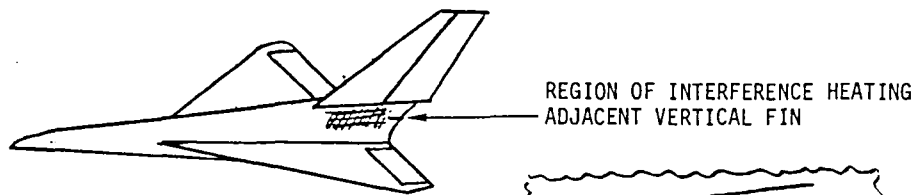
- o PEAK TEMPERATURES CAN BE REDUCED BY INSTALLING CIRCUMFERENTIAL HEAT PIPES ON INTERIOR OF SHIELD
  - HOWEVER--
  - LITTLE OR NO WEIGHT SAVING LIKELY WITH HEAT PIPES (PROBABLY WOULD BE HEAVIER SINCE SHIELD DIAMETER IS ONLY  $\sim 20.32$  cm (8 in))
  - PRESENT CONFIGURATION IS ADEQUATE

Figure 9. - Base heat shield - shuttle AFT propulsion system.

- o Fin/Body Shock Interaction - Hypersonic Cruise Aircraft - Shock impingement on fuselage structure near protuberances such as vertical fins can result in local heating rates considerably higher than those on undisturbed adjacent skin areas. The magnitude of the increased heating rate or amplification factor will depend on the strength of the impinging shock and other flight conditions and geometries, but will typically range from two to five times the undisturbed surface heating rate. Heating rate amplification factors are illustrated on Figure 10 for a typical hypersonic cruise aircraft representative of the configuration described in References 6 and 7. Since the location of peak heating on the fuselage structure for this example is near the base of the fin, the local view factor to space is also reduced, resulting in even higher local temperatures and gradients for a passive radiation cooled structure. The net effect could be thermal stress problems and/or the requirement for a change to a material capable of higher temperatures in the areas of high heating.

The application of heat pipes integrated in the skin could have the potential for reducing peak temperatures and gradients, thus avoiding the requirement for a local material change if the baseline configuration were radiation cooled. Figure 10 shows the effect of various length isothermalizing heat pipes for reducing skin temperatures from the indicated peak values assumed for the four typical heating profiles. For conditions (1) and (2), a heat pipe 1.52m (5.0 ft) long would permit the use of advanced titanium in areas of interference heating whereas a superalloy material would otherwise be required without heat pipes. Likewise for conditions (3) and (4), a superalloy heat pipe configuration could be substituted for a localized refractory construction.

There are several potential problems or disadvantages to heat pipes for this particular application. It is apparent that the heat pipes would have to operate against an adverse gravity head during level flight since the evaporator would be near the base of the fin and therefore above the condenser. Whether or not sufficient heat pipe wicking capability could be provided to overcome this gravity head would require additional detailed study with specific knowledge of the aircraft mold line geometry. The main drawback to heat pipe use for this application, however, is the fact that active structural cooling will be baselined. The aircraft is fueled with liquid hydrogen which will serve as a heat sink for a methanol/water mixture of coolant circulated for cooling the external skin. Areas of interference heating were studied in Reference 7, where it was shown that adequate thermal protection could be provided by the actively cooled panels. Therefore, liquid metal heat pipes would only have merit for this application if it was subsequently decided that a radiation cooled structure should be used. No further activity was recommended for this application.

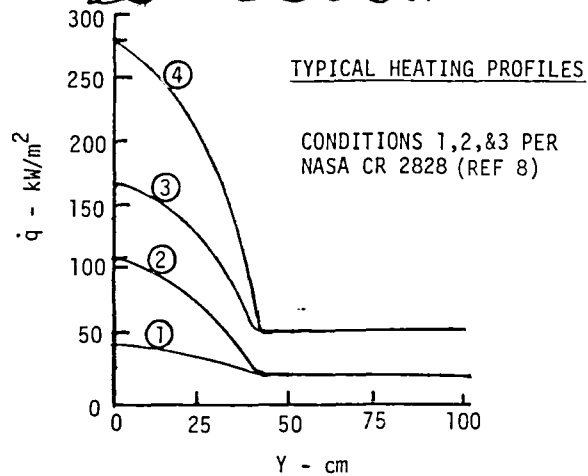
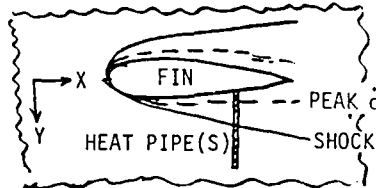
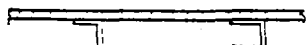


TYPICAL CONSTRUCTION

ACTIVELY  
COOLED



RADIATION  
COOLED



| CONDITION | UNDISTURBED<br>SKIN<br>TEMP | HEATING<br>AMPLIFICATION<br>$\dot{q}_{PEAK}/\dot{q}_{UNDISTURBED}$ | PEAK<br>SKIN<br>TEMP | AVG SKIN TEMP WITH<br>HEAT PIPES OF VARIOUS LENGTHS |       |        |        |
|-----------|-----------------------------|--|----------------------|---|-------|--------|--------|
|           |                             |  |                      | 61 cm   | 91 cm | 122 cm | 152 cm |
| 1         | 841K                        | 2  | 1058K                | 998K  | 969K  | 950K   | 938K   |
| 2         | 841                         | 5  | 1288                 | 1144  | 1079  | 1041   | 1015   |
| 3         | 1058                        | 3  | 1447                 | 1325  | 1270  | 1236   | 1215   |
| 4         | 1058                        | 5  | 1619                 | 1438  | 1358  | 1309   | 1277   |

PROBLEMS WITH PRESENT CONSTRUCTION:

- o LOCALIZED HIGH TEMP ADJACENT FIN MAY EXCEED MATERIAL LIMITS
- o LARGE TEMPERATURE GRADIENTS CAUSE THERMAL STRESS PROBLEMS

HEAT PIPE POTENTIAL:

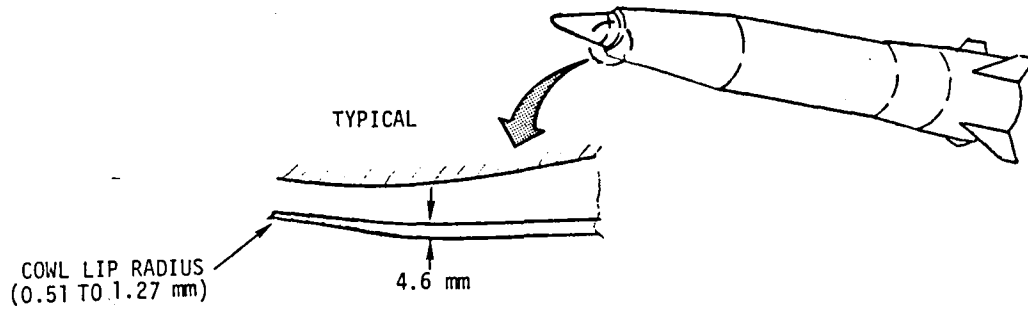
- o REDUCES PEAK TEMPERATURES
- o REDUCES THERMAL STRESSES
- o ELIMINATES REQUIREMENT FOR LOCAL MATERIAL CHANGE

Figure 10. - Fin/body shock interaction - hypersonic cruise aircraft.



- o Engine Cowl Lip - Hypersonic Tactical Missile - Hypersonic missile cowl lip leading edges (Figure 11) will be subjected to very high heating rates and require special high temperature materials. In order to attain good aerodynamic inlet efficiency, the leading edge radii must be extremely small. Radii as small as 0.51 - 1.27mm (0.02 - 0.05 in) have been proposed. The small leading edge radii required will make heat pipe fabrication and operation difficult, if not impossible. In addition, adverse g forces during forward acceleration would present problems with wick design. Even if an adequate heat pipe design could be devised, little or no weight advantage would seem likely. Thus heat pipes do not appear to be a viable solution for these areas.
  
- o Fin/Body Shock Interaction - Hypersonic Cruise Missile - A region of interference heating will occur on hypersonic missile fuselage structure near the base of control fins (Figure 12). The heating phenomena and local view factor blockage is similar to that for hypersonic cruise aircraft vertical fins, but in some respects even more severe because of fin deflection and stronger shocks. Figure 13 illustrates peak skin temperatures that could result from fin interference heating as a function of fin deflection angle and Mach number for level cruise at 24.4 km (80,000 ft). For the missile configuration shown on Figure 12, typical fuselage structure could be of advanced titanium (Ti-11) monocoque for those areas not subjected to interference heating effects. Equilibrium temperatures in these regions are around 922K (1200°F). However, near the base of the fin, it is seen that peak skin temperature of almost 1256K (1800°F) will occur, with rather sharp temperature gradients. The increased heating rates and distributions were calculated from the method of Scuderi (Reference 8). These temperatures exceed the limit for titanium, resulting in the requirement for localized superalloy construction or some form of superalloy radiation shield.

Use of heat pipes to isothermize the skin between fins has the potential of providing an average skin temperature of approximately 1033K (1400°F). This may be marginally acceptable for advanced titanium alloys, assuming further development. Titanium heat pipes for this application might provide a weight reduction below a superalloy construction. Probable incompatibility between titanium and liquid metals for heat pipe operation has been cited in the literature (e.g. Reference 9). However, the corrosion resistance of titanium in contact with liquid potassium or sodium looks more promising according to NASA Lewis, who is presently engaged in a test program which will provide additional compatibility data. Due to skin curvature, adverse g forces will be present at certain locations where the evaporator is above the condenser. The specific design requirements would have to be evaluated further to determine the magnitude of this problem, and influence on heat pipe wick requirements. In general, it would seem that utilization of heat pipes for this application may have merit, but potential problems with material compatibility and effects of adverse g forces must be addressed.



CANDIDATE MATERIALS:

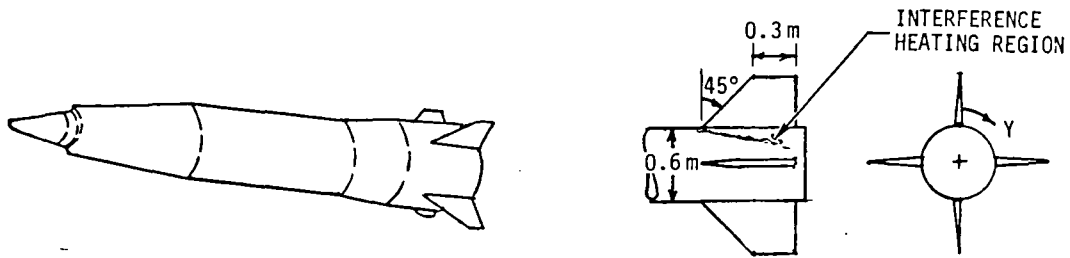
- o TANTALUM 222 WITH HAFNIA COATING

STAGNATION TEMPERATURE  $\sim 2478\text{K}$  ( $4000^\circ\text{F}$ )

HEAT PIPE POTENTIAL:

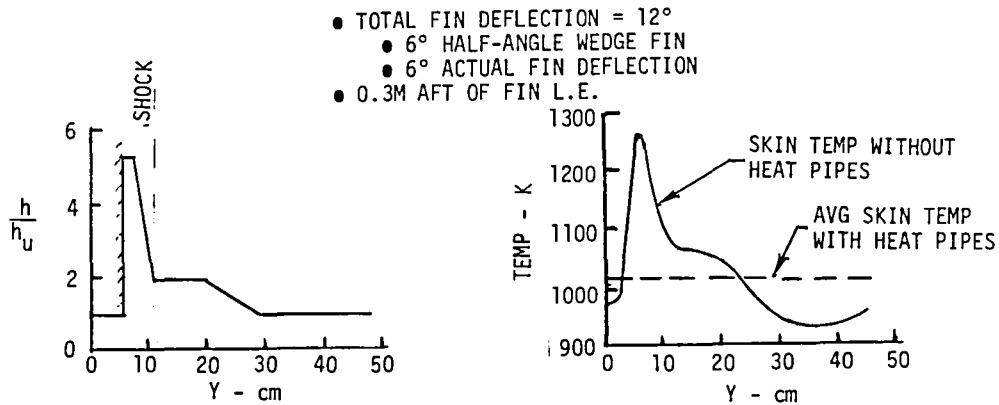
- o SMALL NOSE RADIUS WILL MAKE HEAT PIPE FABRICATION AND OPERATION DIFFICULT IF NOT IMPOSSIBLE
- o ADVERSE  $g$  GRADIENT DURING FORWARD ACCELERATION
- o LITTLE OR NO WEIGHT ADVANTAGE

Figure 11. - Engine cowl lip - hypersonic tactical missile.



TYPICAL HEATING DISTRIBUTION

TYPICAL TEMP PROFILE



TYPICAL FUSELAGE STRUCTURE:

- o ADVANCED TITANIUM (Ti-11) MONOCOQUE

PROBLEMS WITH PRESENT CONSTRUCTION:

- o LOCALIZED HIGH TEMP ADJACENT FINS EXCEEDS MATERIAL LIMIT
- o LARGE TEMP GRADIENTS CAUSE HIGH THERMAL STRESSES

HEAT PIPE POTENTIAL:

- o REDUCES PEAK TEMPERATURES
- o REDUCES THERMAL STRESSES
- o MAY ELIMINATE REQUIREMENT FOR LOCAL MATERIAL CHANGE

Figure 12. - Fin/body interaction - hypersonic cruise missile.

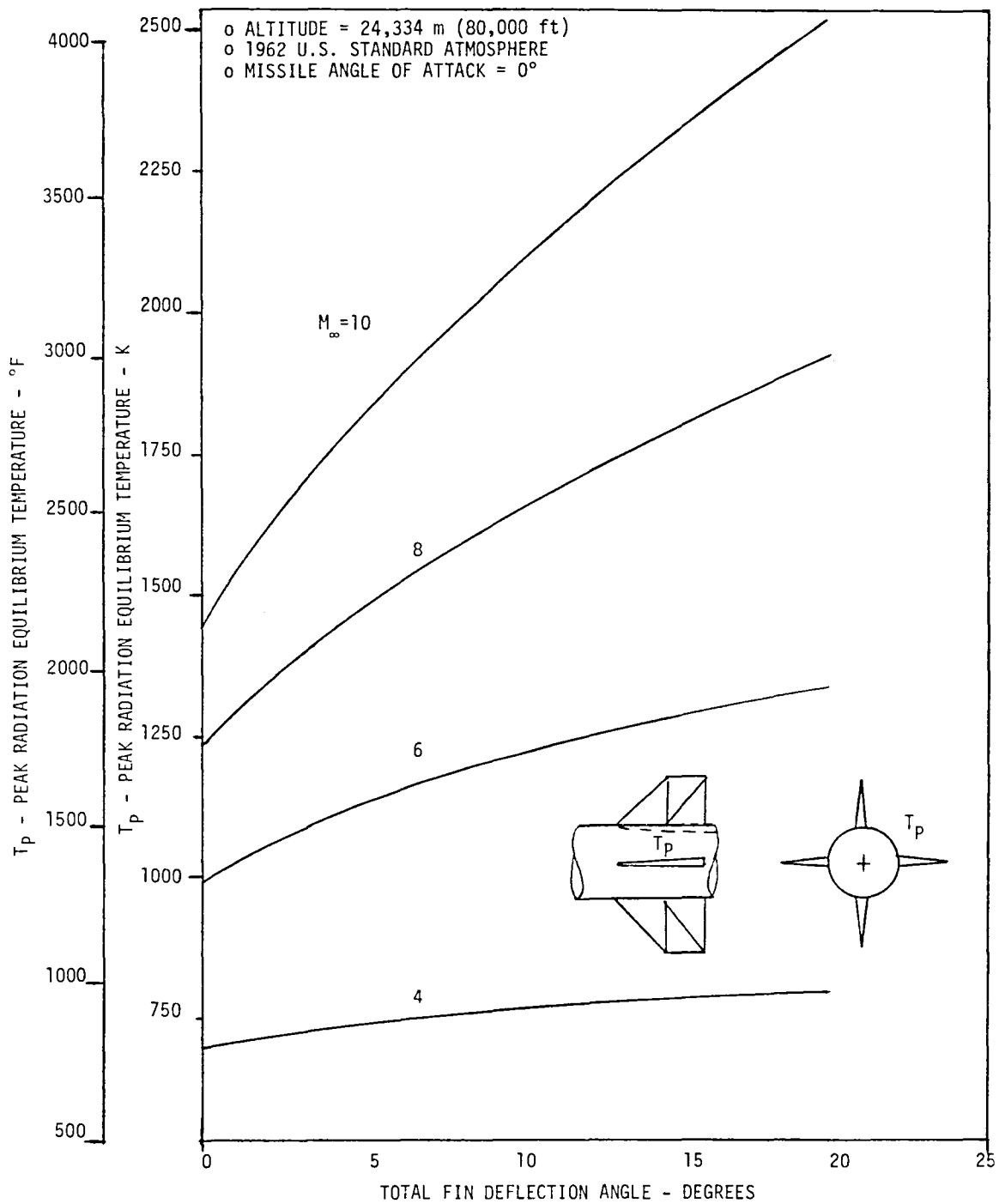
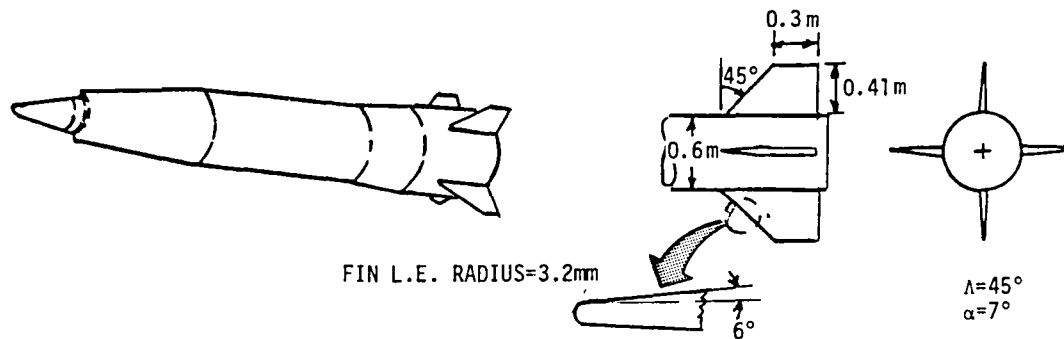


Figure 13. - Peak skin temperatures resulting from deflected missile fins.

- o Fin Leading Edge - Hypersonic Cruise Missile - Typical stagnation line temperature at the leading edge of a Mach 6 hypersonic cruise missile control fin are shown on Figure 14, as well as temperatures of adjacent surfaces aft of the leading edge and on the fin tip. Candidate materials suitable for withstanding these temperatures include refractories for the leading edge and superalloys for the other locations. Use of heat pipes for isothermalizing the leading edge via conduction to the aft skin or fin tip would permit constructing the fin entirely of superalloy material. An average temperature of 1256K (1800°F) could be provided over the leading edge by applying heat pipes encompassing the leading edge and approximately 3.81 cm (1.5 in) of the aft adjacent surface. This would suggest the use of a vapor chamber type heat pipe design similar to that described in Reference 10. Design problems associated with wick installation might be encountered, however, due to the small leading edge radius and the magnitude of the wick requirements. Adverse g effects could be minimized by segmenting the heat pipe to reduce vertical elevation heads. But, from the standpoint of comparative weights and costs, it is doubtful that heat pipes for this application could compete with the candidate baseline materials listed on Figure 14 and no further work was conducted on this concept.
  
- o Nose Cap - Hypersonic Cruise Missiles - High stagnation heating rates to nose caps of future hypersonic cruise missiles will generally dictate the use of materials capable of withstanding temperatures in excess of superalloy limits. This is illustrated on Figure 15, which shows the typical magnitude of expected nose cap temperatures and possible material candidates. Isothermalization of the nose cap via a vapor chamber type heat pipe design could be employed for reduction of stagnation temperatures to levels compatible with superalloy materials. However, since no significant payoff in terms of weight or cost reduction seemed apparent, this concept was not considered further.
  
- o Strake Leading Edge - MRRV Hypersonic Research Vehicle - The leading edge of the MRRV strake (Figure 16) was evaluated on a preliminary basis as a potential application for heat pipes. Although this vehicle is still in the early stages of investigation, some details of configuration and flight conditions were made available by the Air Force Flight Dynamics Laboratory (AFFDL) to assist in the evaluation. The leading edge construction of the strake is currently postulated by AFFDL to be reinforced carbon-carbon. Stagnation heating rate histories were determined for the strake leading edge for two types of trajectories: (1) a synergetic maneuver for orbital plane change and (2) a long range entry. As indicated on Figure 16, peak stagnation temperature will exceed 1922K (3000°F) for the postulated baseline configuration. Investigation of heat pipe requirements to isothermalize the strake leading edge to 1256K (1800°F) where superalloy construction could be used indicated that extensive heat pipe coverage relative to the total surface area available would be necessary. Required heat pipe lengths were determined to be approximately 1.09 m (43 in) and 1.8 m (71 in) respectively, for a long range descent trajectory and a synergetic maneuver. Therefore, heat pipes would have to be applied to most of



TYPICAL LOWER FIN TEMPERATURES:

- o FIN LEADING EDGE - 1608K (2434°F)
- o AFT SKIN - 1144K (1600°F)
- o FIN TIP - 1161K (1630°F)

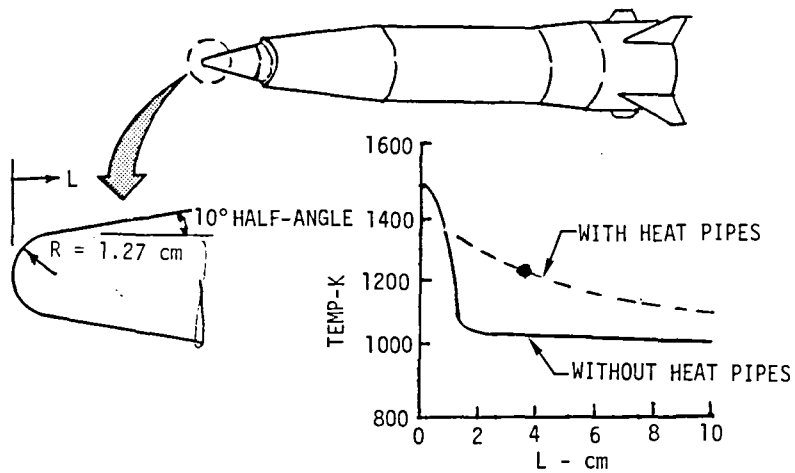
CANDIDATE MATERIALS:

- o LEADING EDGE - COLUMBIUM F85, CARBON/CARBON
- o SKIN - RENE' 41, L605, COLUMBIUM F85

HEAT PIPE POTENTIAL:

- o ISOTHERMALIZATION OF LEADING EDGE VIA CONDUCTION TO AFT SKIN OR FIN TIP PERMITS USE OF SUPERALLOY CONSTRUCTION
- o ADVERSE g's ON LOWER FIN REDUCES CAPILLARY PUMPING

Figure 14. - Fin leading edge - hypersonic cruise missile.



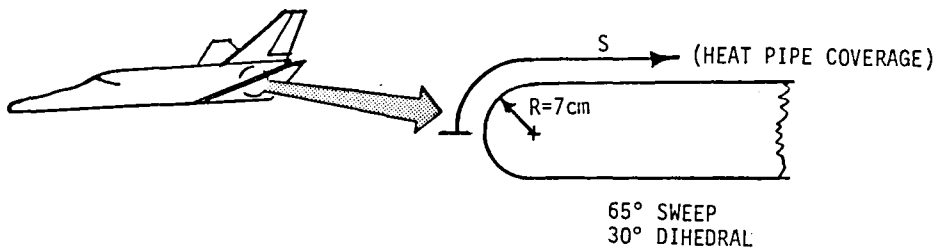
CURRENT MATERIAL CANDIDATES AND TEMPERATURES:

- o NOSE CAP TEMP: 1506K (2251°F) @ STAGNATION POINT  
1042K (1416°F) @ SHOULDER OF NOSE
- o MATERIAL CANDIDATES: COLUMBIUM, MOLYBDENUM, TANTALUM, CARBON, ETC.

HEAT PIPE POTENTIAL:

- o AVG. TEMP CAN BE REDUCED TO 1256K (1800°F) BY HEAT PIPE INTEGRATED INTO NOSE AND EXTENDING 3.8 cm (1.5 in) AFT OF STAGNATION POINT
- o SUPERALLOY MATERIALS COULD BE USED
- o INSIGNIFICANT OR NO WEIGHT SAVINGS LIKELY

Figure 15. - Nose cap - hypersonic cruise missile.



POSTULATED LEADING EDGE BASELINE CONSTRUCTION:

- o REINFORCED CARBON/CARBON (PER AFFDL)

PEAK STAGNATION HEATING RATES & EQUILIBRIUM TEMPS:

- o SYNERGETIC MANEUVER -  $944 \text{ kW/m}^2$  ( $83 \text{ Btu/Sec-ft}^2$ ), 2136K (3385°F)
- o LONG RANGE DESCENT -  $659 \text{ kW/m}^2$  ( $58 \text{ Btu/Sec-ft}^2$ ), 1952K (3054°F)

POTENTIAL PROBLEMS WITH POSTULATED BASELINE CONSTRUCTION:

- o REQUIRES OXIDATION RESISTANT COATING
- o COST
- o WEIGHT

HEAT PIPE POTENTIAL:

- o ISOTHERMALIZATION OF STRAKE LEADING EDGE AND AFT SKIN MAY PERMIT USE OF SUPERALLOY CONSTRUCTION
- o PRELIMINARY THERMAL ANALYSES SHOW TO ISOTHERMALIZE LEADING EDGE TO 1256K:
  - S/R REQUIRED DURING SYNERGETIC MANEUVER = 13  
 $\therefore S = 0.91\text{m}$  (35.8 in)
  - S/R REQUIRED DURING LONG RANGE DESCENT = 7.9  
 $\therefore S = 0.55\text{m}$  (21.7 in)

LEADING EDGE HEAT PIPE ON MRRV DOESN'T LOOK PROMISING

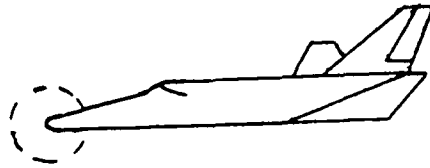
- o HEAT PIPE SURFACE COVERAGE REQUIREMENT EXCESSIVE
- o UNLIKELY TO BE COMPETITIVE WITH CARBON LEADING EDGE ON EITHER A WEIGHT OR COST BASIS

Figure 16. - Strake leading edge - MRRV.



the strake surface area. Specific effects of maneuvers and resultant g levels on heat pipe wick requirements could not be addressed because of insufficient data, but they are expected to be significant. More detailed studies are required to fully evaluate these effects. In addition to the extensive heat pipe surface coverage requirement and possible adverse g effects, it would seem unlikely that heat pipes could be competitive with the proposed baseline carbon-carbon leading edge on either a weight or cost basis. Therefore, no additional work was conducted on this concept.

- o Nose Cap - MRRV Hypersonic Research Vehicle - As indicated on Figure 17, the MRRV nose cap is not a viable candidate for a superalloy heat pipe design because of excessive stagnation heating rates.
- o Vertical Fin Leading Edge - MRRV Hypersonic Research Vehicle - Leading edge heat pipes on the MRRV vertical fin (Figure 18) appear to be a workable application for the long range descent trajectory insofar as thermal feasibility is concerned. However, almost the entire fin surface area would have to be utilized to limit peak temperatures to 1256K (1800°F). For the synergetic maneuver, the heat pipe coverage required on the upper portion of the fin is greater than the available fin chord. Therefore, vertical heat pipe operation would be required to take advantage of the larger surface area below for isothermalization. The possibility of excessive wick requirements would result, however, assuming downward acting gravity forces.



CONFIGURATION: ELLIPSOIDAL , 7.9 cm (3.1 in) X 6.0 cm (2.4 in)

POSTULATED NOST CAP MATERIAL

- o GRAPHITE COMPOSITE (PER AFFDL)

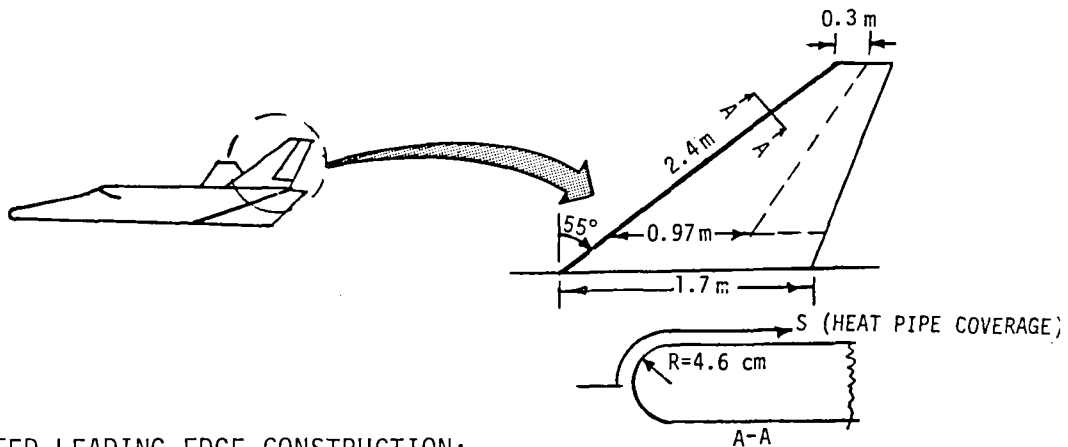
PEAK STAGNATION HEATING RATES AND EQUILIBRIUM TEMP:

- o SYNERGETIC MANEUVER -  $3257 \text{ kW/m}^2$  ( $287 \text{ Btu/Sec-ft}^2$ ), 2911K (4780°F)
- o LONG RANGE DESCENT -  $2145 \text{ kW/m}^2$  ( $189 \text{ Btu/Sec-ft}^2$ ), 2822K (4620°F)

HEAT PIPE POTENTIAL:

- o TEMPERATURES TOO HIGH FOR HEAT PIPE SUPERALLOY ENVELOPES WITH RADIATION COOLING
- o A DESIGN WHICH INCORPORATES HEAT PIPES INTERFACING WITH A SEPARATE HEAT SINK (e.g. LITHIUM) MIGHT REDUCE TEMPERATURES COMPATIBLE WITH SUPER ALLOYS

Figure 17. - Nose cap - MRRV.



POSTULATED LEADING EDGE CONSTRUCTION:

- o REINFORCED CARBON/CARBON (PER AFFDL)

PEAK STAGNATION HEATING RATES AND EQUILIBRIUM TEMPS:

- o SYNERGETIC MANEUVER -  $806 \text{ kW/m}^2$  (71 Btu/Sec-ft<sup>2</sup>), 2053K (3235°F)
- o LONG RANGE DESCENT -  $659 \text{ kW/m}^2$  (58 Btu/Sec-ft<sup>2</sup>), 1796K (2773°F)

POTENTIAL PROBLEMS WITH POSTULATED CONSTRUCTION:

- o REQUIRES OXIDATION RESISTANT COATING
- o COST
- o WEIGHT

HEAT PIPE POTENTIAL:

- o ISOTHERMALIZATION OF FIN LEADING EDGE AND AFT SKIN MAY PERMIT USE OF SUPERALLOY CONSTRUCTION
- o PRELIMINARY THERMAL ANALYSES SHOW TO ISOTHERMALIZE LEADING EDGE TO 1256K (1800°F):
  - S/R REQUIRED DURING SYNERGETIC MANEUVER = 10.4  
 ∴ S = 48 cm (18.9 in)
  - S/R REQUIRED DURING LONG RANGE DESCENT = 5.3  
 ∴ S = 24.6 cm (9.7 in)

LEADING EDGE HEAT PIPE ON MRRV VERTICAL FIN APPEARS TO BE A CANDIDATE APPLICATION INSOFAR AS THERMAL FEASIBILITY IS CONCERNED. FOR SYNERGETIC MANEUVER, VERTICAL HEAT PIPE OPERATION IS REQUIRED DUE TO INSUFFICIENT CHORD @ TOP, WHICH RESULTS IN ADVERSE g OPERATION.

Figure 18. - Vertical fin leading edge - MRRV.

### 3.3 APPLICATION SELECTED FOR FURTHER STUDY

Based on the results of the preceding screening evaluations, the most promising application which would benefit from the use of heat pipes was judged to be the SSTO wing leading edge. In general, leading edges as a class appear more suitable for utilizing heat pipes for cooling high heat flux regions to temperatures compatible with superalloy materials. Less uncertainties on heating rate levels and gradients exist in these areas than at shock impingement regions or on deflected control surfaces. Potential areas for leading edge heat pipe application on hypersonic missiles and re-entry research vehicles are more likely to be subjected to higher stagnation heat fluxes, be more vulnerable to g forces encountered during maneuvers, and be subjected to higher transient heating rates which will make heat pipe start-up more difficult.

One of the main advantages of using superalloy materials as opposed to higher temperature refractory or ablative materials is their reuse capability, because they are not as susceptible to damage from either oxidation or ground handling. Advanced space transportation systems will be designed for multi-mission use, whereas missiles will not, and research aircraft will in general have higher priority in other areas. Therefore, greater benefits will be derived from an advanced space transportation system design application which requires little or no refurbishment.

As pointed out earlier, the design studies and tests conducted on a Space Shuttle wing leading edge heat pipe configuration showed positive performance results, but its weight was not competitive with alternate leading edge thermal protection methods. In selection of the SSTO leading edge configuration for further evaluation, it was anticipated that a lighter weight heat pipe system design could be devised which would be competitive with a columbium or carbon-carbon design.

## 4.0 SSTO WING LEADING EDGE HEAT PIPE DESIGN

Approaches for efficiently integrating heat pipes into the wing leading edge of the SSTO vehicle are defined in this section. Pertinent elements of the baseline vehicle are briefly described, followed by a thermal and structural design analysis of the selected heat pipe leading edge configuration. Fabrication techniques and heat pipe servicing are addressed, as well as relative weight and cost factors.

The purpose for applying heat pipe technology to the SSTO wing leading edge is to provide an alternative to the proposed refractory metal thermal protection system. Heat pipes have the capability of redistributing net heat inputs and lowering thermal gradients so that superalloys can be used in place of the coated refractory metals. Replacement of refractory metals with heat pipe cooled superalloy construction would minimize refurbishment cost of the leading edge between launches. The heat pipes would also operate closed-loop so other vehicle systems are not affected and flight operations complexity is not increased by their application.

For trajectories and heating rates of the SSTO vehicle, a heat pipe thermostructural system can be successfully applied to the wing leading edge. The system as shown on Figure 19 would use Hastelloy-X heat pipe tubes and face sheet, stainless steel mesh screen for the wicking material, and sodium as the working fluid. The heat pipe assemblies would consist of integrally stiffened segments supported by trusses similar to those currently baselined for the coated columbium leading edge. A detailed description of the segment design and fabrication techniques is presented in the following paragraphs.

Based on the trajectories and wing geometry cited in Reference 4, the SSTO wing leading edge stagnation line heating rates were calculated for both ascent and descent flight conditions. Resultant stagnation line temperature histories with and without heat pipes are shown in Figure 20. Peak temperature during entry is 1494K (2230°F) for the columbium design and 1254K (1797°F) for the Hastelloy-X heat pipe design.

### 4.1 SSTO BASELINE DESCRIPTION

A dual mode propulsion SSTO vehicle, as described in Reference 4 utilizes a delta planform wet wing with an overall span of 49.81m (163.43 ft), sweep angle of 56 degrees, thickness to chord ratio of 8.5 percent, and a leading edge radius of 30.48 cm (12 in). The wing contains liquid oxygen located to provide load relief from the aerodynamic lift and reduce wing bending loads.

A single all metallic structural system is used throughout the vehicle. It consists of titanium and Rene'41 honeycomb structure panels stiffened and supported by beams, frames and trusses. The multi-function panels serve to provide thermal protection, load carrying structure, cryogenic tankage, and cryogenic insulation.









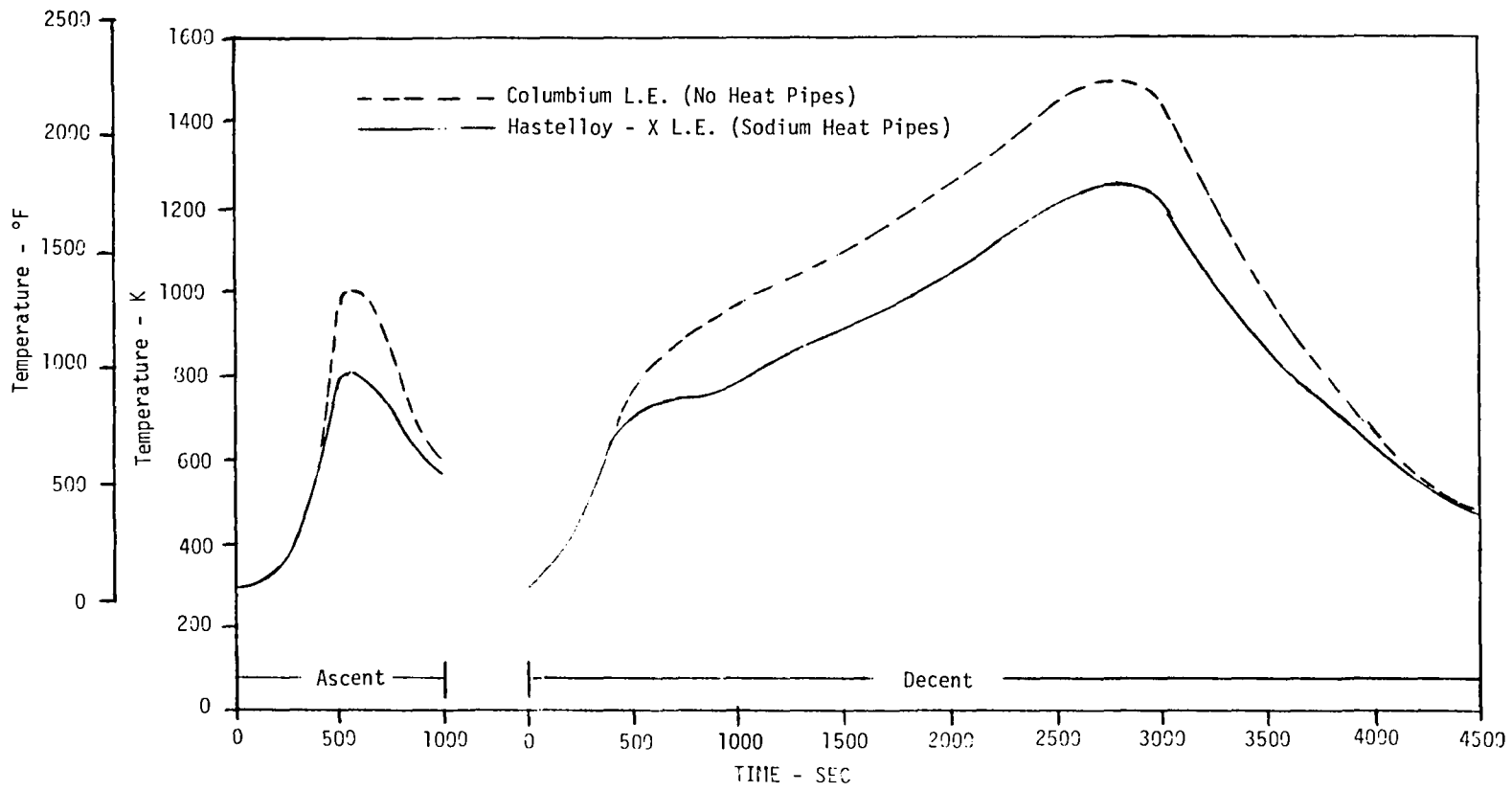


Figure 20. - SSTO wing L.E. stagnation line temperature histories.

The wing upper surface uses titanium panels. In areas where added thermal protection is required because of plume induced flow separation, an additional single faced honeycomb panel of Rene'41 is bonded to the titanium surface. Wing lower surface panels are all Rene'41 honeycomb material with the outer face sheet slotted chordwise to relieve thermal stress. The wing panels are stiffened by internal titanium spar chords using padded attachments to handle load distributions. Wing bending loads are carried by a series of spanwise spar trusses spaced every 76.2 cm (30 in) and located at the same fuselage station as the body frames. The trusses are boron-aluminum tubes with titanium end fittings which tie into the spar chords. Since wing leading edge temperatures will exceed the capability of Rene'41, a refractory metal structure is used. The leading edge construction consists of integrally stiffened coated columbium alloy segments supported by a determinate truss system.

## 4.2 DESIGN ENVIRONMENTS

Preliminary estimates of launch and descent design trajectories are defined in Reference 4. The vehicle is sled-launched from the Eastern Test Range to a Reference Energy Orbit having a 93 km (50 n.m.) perigee and 185 km (100 n.m.) apogee. Mission duration is 12 hours from lift-off to landing. The entry trajectory is initiated from a 185 km (100 n.m.) circular orbit with an east entry and 28.5° orbit inclination. An initial angle of attack of 50° is maintained until the flight path first levels off (i.e. flight path angle = 0°), followed by a decrease in angle of attack to 30° to provide a high cross range. A bank angle of 45° is also initiated at this time. This trajectory was reported in Reference 4 to achieve a cross range slightly in excess of 2222 km (1200 n.m.). Entry wing loading is about 1.3 kPa (24 psf) and at 30° angle of attack, equilibrium glide ( $W/SC_L$ ) is 317 kg/m<sup>2</sup> (65 psf).

Wing leading edge stagnation line static pressures are depicted in Figure 21. Heating and pressure distributions over the wing leading edge which were used for subsequent thermal and structural design analyses are described on Figure 22. The data assume a vehicle angle of attack of 30° which is typical for practically all of the entry trajectory where significant heating is encountered.

A complete load factor history for the SSTO was not available. However, peak g levels during ascent are expected to be around 3 g's along the vehicle body axis. Load factors during entry are anticipated to be moderately low and similar to those experienced by Space Shuttle. For this study, it was assumed that entry g forces are directed normal to the plane of the SSTO wing with maximum values not exceeding one g until after the time of peak heating. The typical g force used for the Shuttle design studies of Reference 3 was approximately 0.6 g at peak heating.

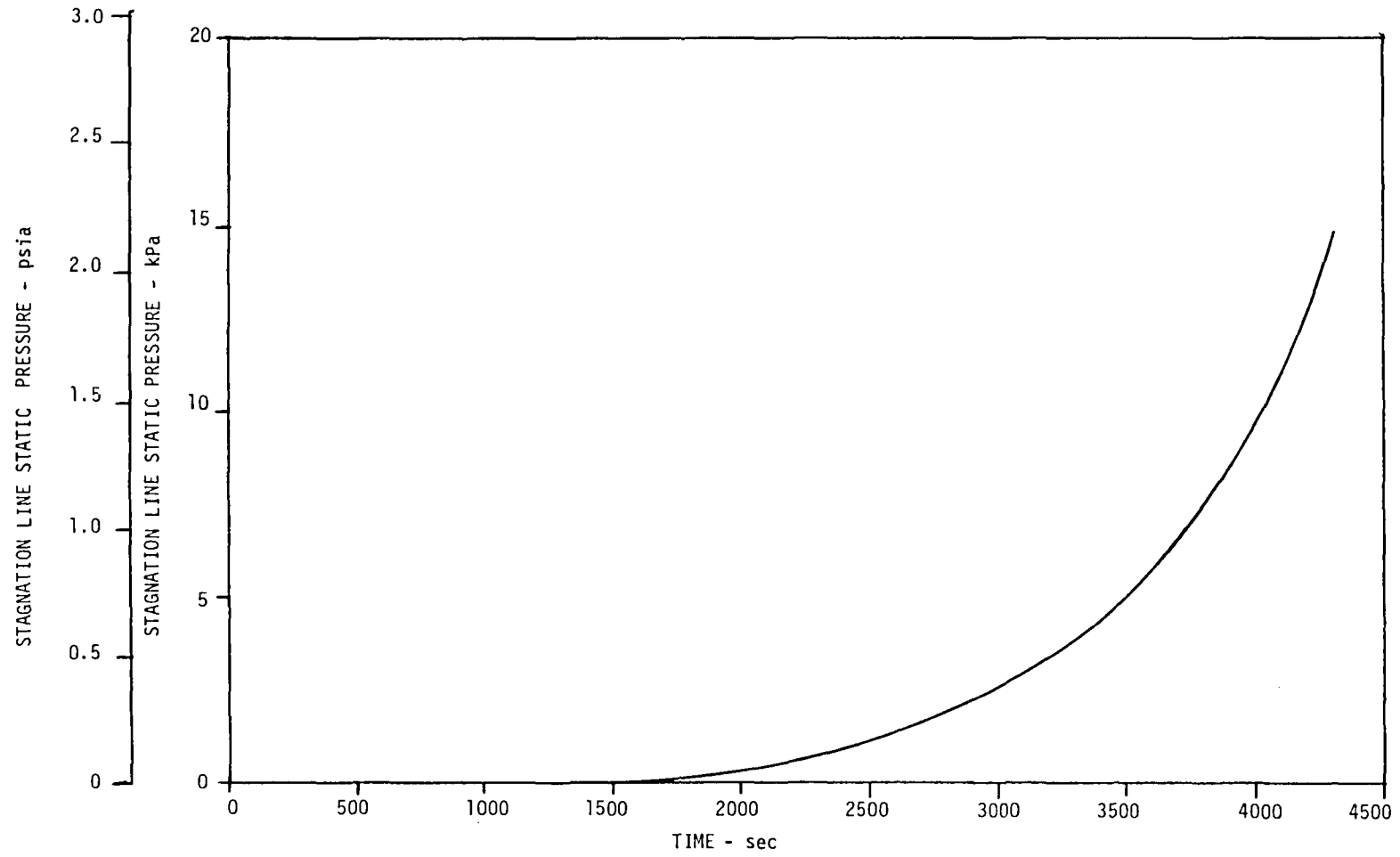


Figure 21. - SSTO wing L.E. stagnation line static pressures during entry.

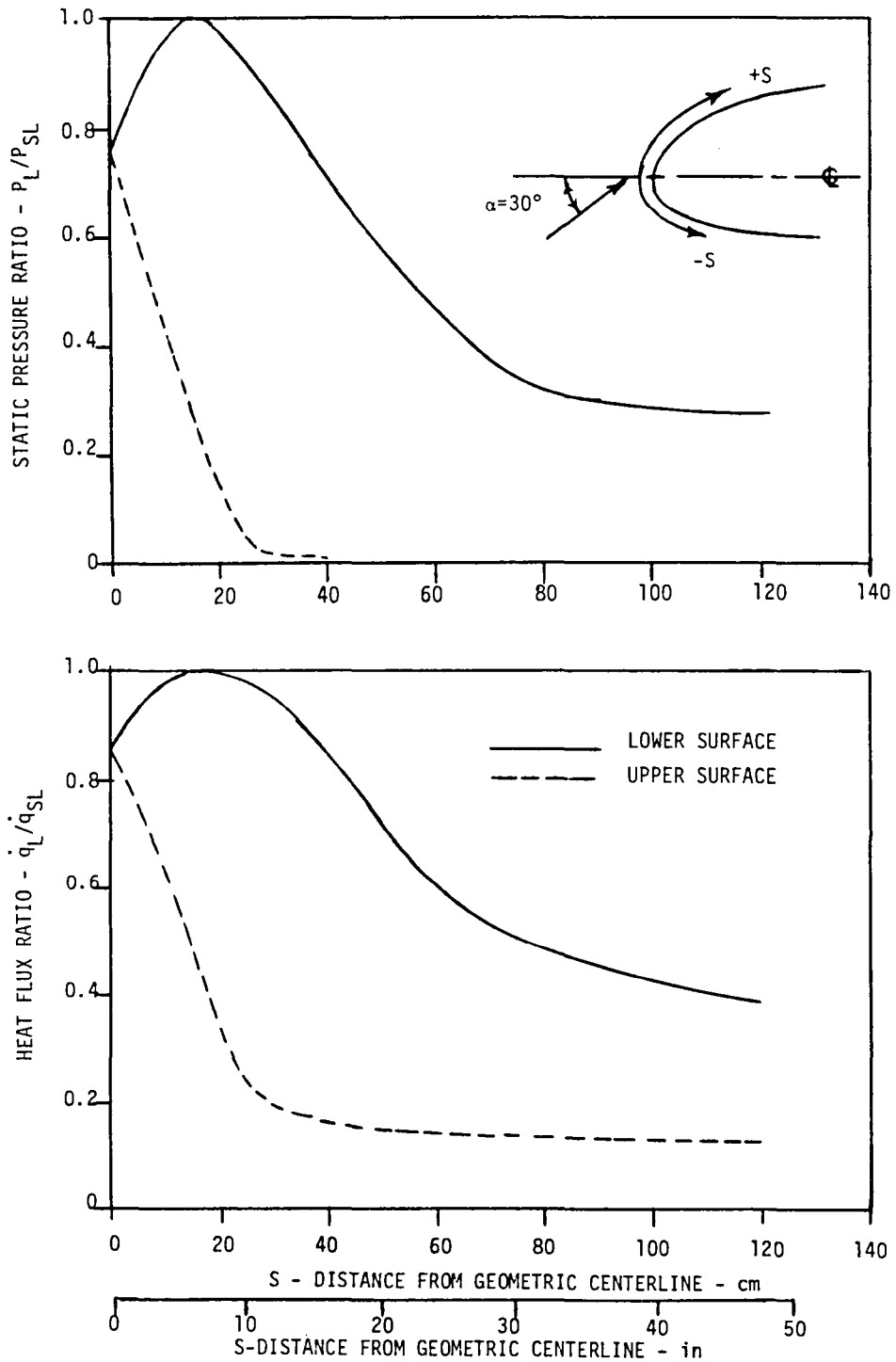


Figure 22. - SSTO wing L.E. local heat flux and pressure distributions.

### 4.3 HEAT PIPE DESIGN

Integration of heat pipes into the leading edge structure requires an understanding of heat pipe operation and quantitative evaluation of various operational limits which will be encountered. General performance limits are summarized in Appendix A, including consideration of working fluid properties, heat transport limits, and the influence of gravitational effects on heat pipe operation.

The elements comprising a heat pipe and a brief review of its operation are indicated in Figure 23. When heat is added to a region of the pipe, the following processes take place: (a) the temperature in the heated region rises slightly, (b) liquid is vaporized and vapor pressure increases in this region, (c) vapor flows to the lower pressure/low temperature areas and condenses, giving up its latent heat of vaporization, and (d) liquid is returned to the evaporator area by a wick structure using capillary pumping or a combination of capillary pumping and gravity forces. The maximum heat transfer capability of the system is limited by: (a) the thermal flux which can be transported across the tube wall and liquid-wick layer (nucleate boiling limit), (b) maximum vapor flow before liquid entrainment in the vapor occurs (entrainment limit), (c) the ability of the wick structure to supply liquid to the heated evaporator region (pumping limit), and (d) adequate vapor flow area to prevent sonic flow at the evaporator exit (sonic limit). In addition to the performance limiting considerations, the working fluid must be compatible with the wick and container material. This is particularly true for high temperature systems which use liquid metal working fluids and are highly corrosive. Compatibility and each of the limiting conditions have been treated in detail for the leading edge Hastelloy-X heat pipe designs and are reported in Reference 3.

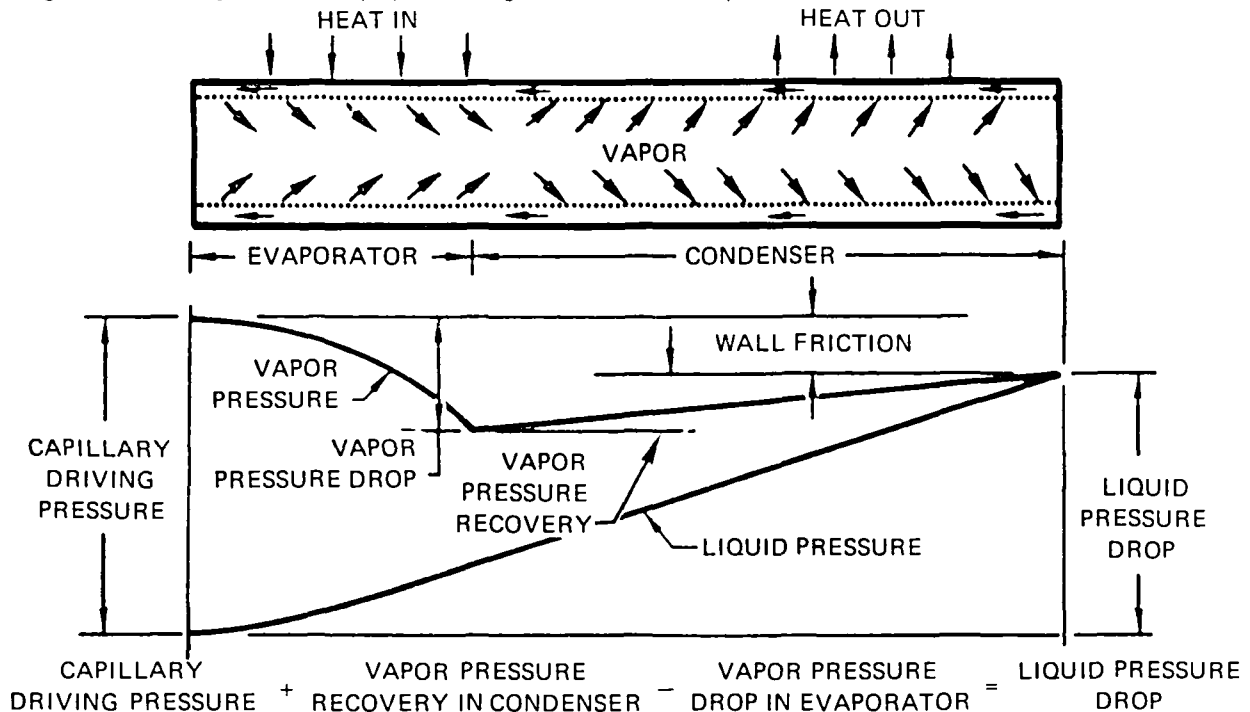


Figure 23. - Basic heat pipe operation.

The heat pipe design process for the SSTO wing leading edge, which is similar to that described in Reference 3, was as follows:

1. Based on the thermal design environments, heat pipe surface coverage required to isothermalize the leading edge to 1256K (1800°F) at the point of peak heating during entry was determined.
2. A baseline heat pipe configuration was selected, modeled, and analyzed to define heat pipe temperature profiles, pressure, start-up characteristics, and transient heat loads.
3. Heat pipe radial and axial heat transfer rates were calculated to define the magnitude of required heat transfer and the location of the heat pipe evaporation and condensation transition zones.
4. The wing leading edge elevation relationships at different heat pipe axial stations were calculated from the geometry of the leading edge to assist in definition of adverse or favorable gravity heads, assuming vehicle g levels normal to the plane of the wing.
5. Heat pipe requirements were summarized in terms of radial and axial heat transfer rates, evaporator and condenser lengths, and elevation heads due to g levels and evaporator/condenser transition locations.
6. Heat pipe vapor and liquid limits were calculated for the initially selected heat pipe configuration and compared with actual requirements during entry.

#### 4.3.1 Definition of Heat Pipe Length

The normalized local heat transfer distribution shown on Figure 22 was combined with the peak stagnation line heat fluxes integrated over the leading edge. The approximate heat pipe length required to limit leading edge temperature to 1256K (1800°F) was then determined based on a radiation thermal balance. Figure 24 shows the integrated heat flux as a function of heat pipe length at the time of peak heating. The corresponding average heat pipe skin temperature as a function of heat pipe length is shown on Figure 25, assuming equal upper and lower surface distances from the geometric centerline. It is seen that for a surface emissivity of 0.85 the heat pipe length would have to be approximately 200 cm (78.7 in) long, in order to limit equilibrium skin temperature to 1256K (1800°F) during entry. Heat pipe overall length could be reduced in an additional iteration by terminating it at the lower surface where 1256K (1800°F) occurs, and extending it further aft on the upper surface where heating rates are lower.

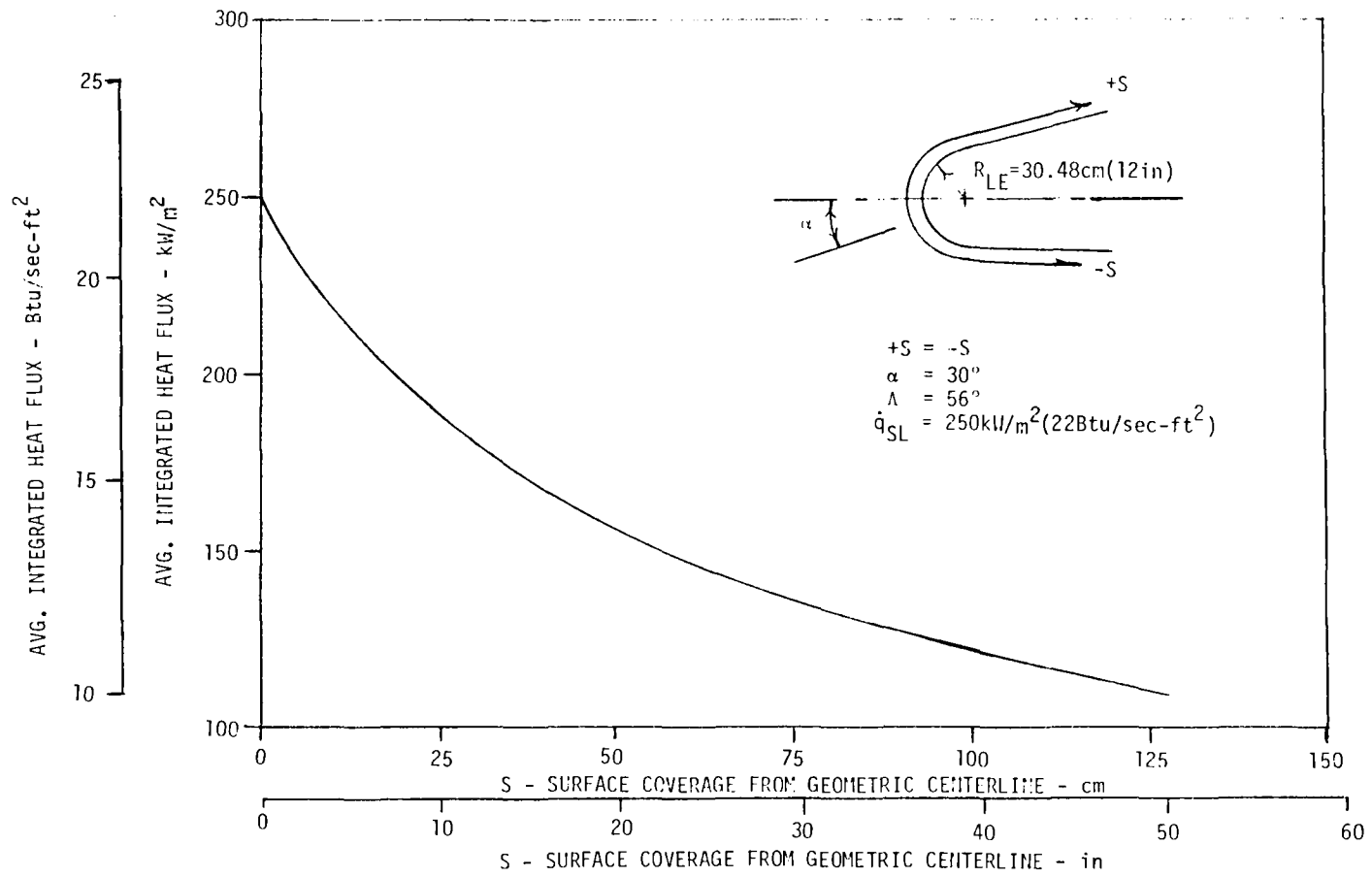


Figure 24. - SSTO wing L.E. maximum integrated heat transfer rates.

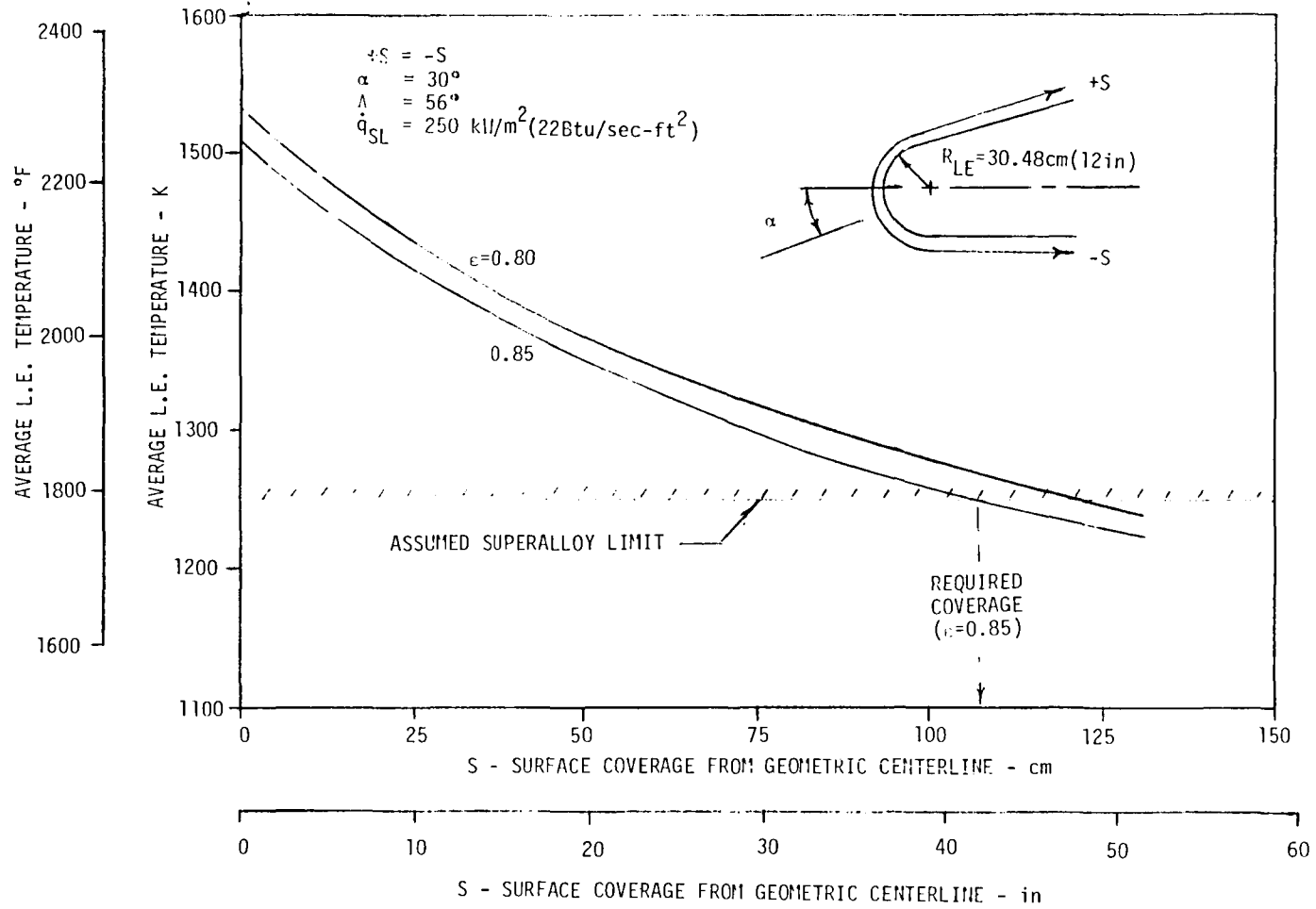


Figure 25. - Determination of required heat pipe length.



### 4.3.2 Transient Analysis

A thermal model of the heat pipe leading edge was constructed to define transient behavior and performance requirements. The analyses employed the McDonnell Douglas general heat transfer program, HEATRAN, which is programmed on the CDC-CYBER 175 computer. The thermal model sub-divided the heat pipe into 24 longitudinal segments and incorporated 72 nodes representing various elements of the heat pipe (i.e. working fluid, wick, envelope and skin). Both temperature and time dependent heat fluxes and material properties were included. The assumed heat pipe configuration consisted of a Hastelloy-X double-walled corrugated panel, comprised of a smooth 0.51mm (0.02 in) outer skin and a corrugated 0.41mm (0.016 in) inner skin (Figure 19). The two skins would be pre-formed to the contour of the leading edge, lined with screen wicking, and then longitudinally seam welded together, resulting in 1.27 cm (0.5 in) diameter D-shaped channels running in a chordwise direction. The wick-lined channels would be closed off at the ends, filled with sodium working fluid, and serve as longitudinal heat pipes. The total length of the heat pipe channels was 200 cm (78.7 in). Overall design studies showed this configuration to be a light-weight design, as described in Section 4.4. Sodium was selected as the working fluid since it has the best characteristics in the 1256K (1800°F) range and has demonstrated long-term compatibility with Hastelloy-X. A simple homogeneous wick structure, consisting of a single layer of 100 mesh stainless steel screen was assumed in the model.

The results of the transient analysis are depicted on Figure 26. The peak external skin temperature adjacent the wick is 1254K (1797°F) and occurs at approximately 2840 seconds. Although not shown on the figure, the skin temperature in the seam-weld area (i.e. between D-tubes) is approximately 33K (60°F) higher at the time of peak heating. Heat pipe axial heat transfer rates were assumed to be negligible for working fluid vapor temperatures below 700K (800°F) because of free molecular flow of the vapor and by sonic velocity limitations at higher temperatures. It is seen that the entire heat pipe is fully operational at around 800 seconds, well before the time at which peak heating occurs. Although it is not expected that any significant problems with start-up should be encountered, detailed assessment of the transient fluid wicking behavior was not incorporated in the analysis. This assessment should be made during more detailed design studies to validate the adequacy of the wick system during the starting transient.

Wing leading edge temperature profile histories during entry are further illustrated by Figure 27, which depicts the movement of the continuum regime into the condenser regions, and the eventual isothermalization of the leading edge. The working fluid pressure history is shown on Figure 28 and was used for structural analyses for candidate heat pipe container designs. Peak internal fluid pressure coincides with peak temperature and is approximately 221 kPa (32 psia) at 2840 seconds into the entry trajectory. At temperatures below approximately 800K (980°F), internal fluid pressures are essentially zero.

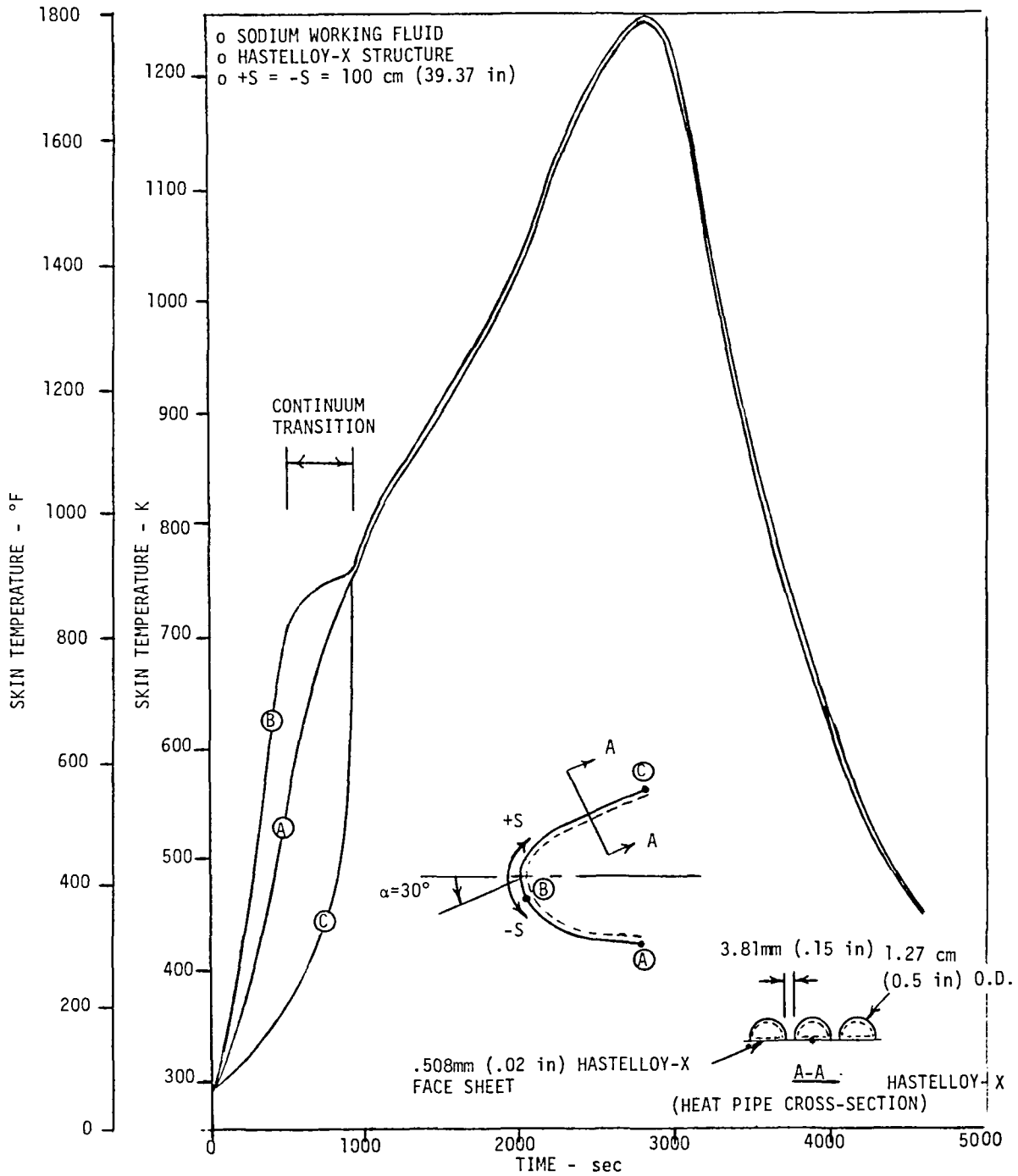


Figure 26. - Transient temperatures of heat pipe leading edge during entry.

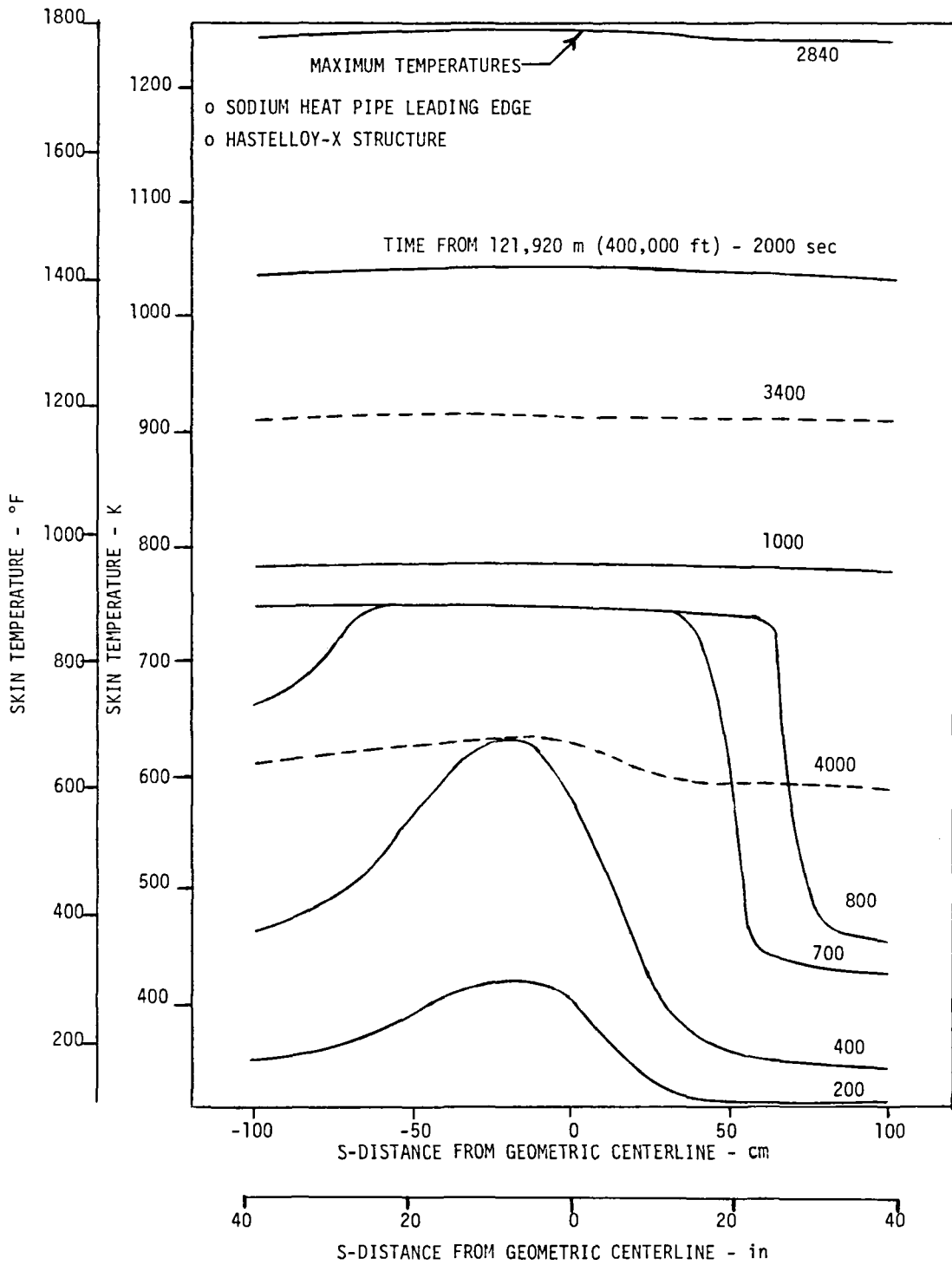


Figure 27. - Leading edge temperature profiles during entry.

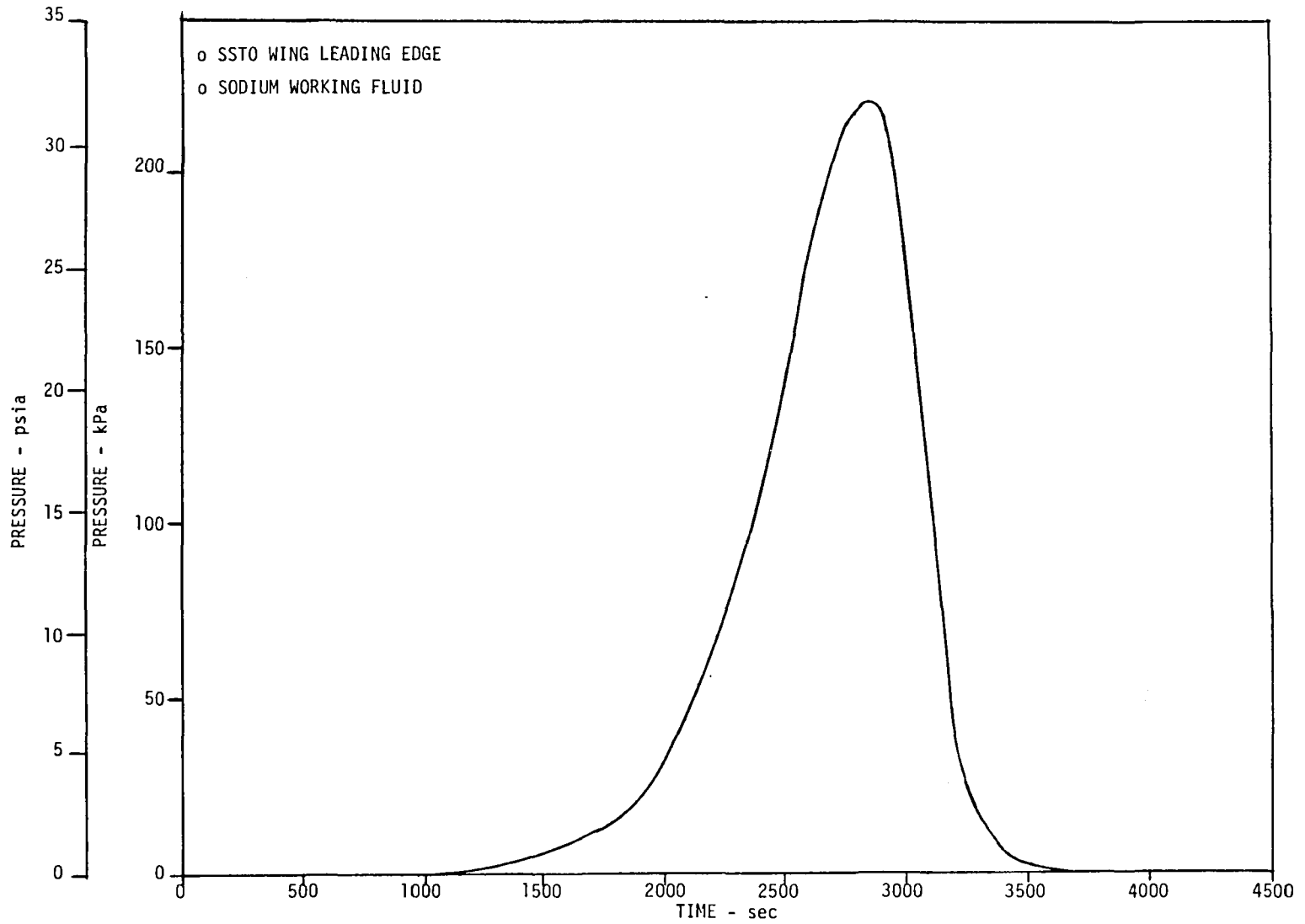


Figure 28. - Heat pipe internal pressures during entry.

### 4.3.3 Radial and Axial Heat Transfer Rates

Radial heat transfer rates to the heat pipe leading edge at various times during the descent trajectory are depicted on Figure 29 as a function of surface distance from the geometric centerline. The curves are for three times in the trajectory during isothermal operation: 2840 seconds, (peak heating), 1200 seconds, and 3200 seconds. Positive values of radial heat flux signify net heating into the system at that particular location (i.e. the local aerodynamic heat flux exceeds heat transferred away from the surface by radiation). Conversely, negative radial heat fluxes indicate higher radiation cooling capability than local aerodynamic heat flux. Points on Figure 29 where the radial heat flux is zero represent a transition point between a condenser and evaporator region in the heat pipe. These transition points occur at values of  $S$  equal to  $-81$  cm ( $-31.9$  in) and  $+16$  cm ( $+6.3$  in). Therefore, the heat pipe condensers are approximately  $19$  cm ( $7.5$  in) long on the lower aft surface and  $84$  cm ( $33.1$  in) on the upper aft surface, with the evaporator region in between. Peak heat fluxes are  $15.6$   $\text{w/cm}^2$  ( $13.7$   $\text{Btu/sec-ft}^2$ ) to the evaporator and  $10.8$   $\text{w/cm}^2$  ( $9.5$   $\text{Btu/sec-ft}^2$ ) from the condenser.

Total axial heat transfer rates required to be transferred by the heat pipe per unit span at a specific time in the trajectory can be calculated from Figure 29 as the integral below the portion of the curves defining the evaporator region. Axial heat transfer rates proportioned to the lower and upper surface condensation regions are represented in a like manner by the integral above the curves applicable to the respective condensation zones. Figure 30 depicts axial heat transfer rate histories during the descent trajectory for heat pipe D-tube diameters of  $1.27$  cm ( $0.5$  in) and  $1.91$  cm ( $0.75$  in). For the  $1.27$  cm ( $0.5$  in) diameter configuration, it is seen that the peak axial heat transfer rate is approximately  $1030$   $\text{W}$  ( $3515$   $\text{Btu/hr}$ ) to the upper surface and only around  $23$   $\text{W}$  ( $79$   $\text{Btu/hr}$ ) to the lower surface.

Assuming that gravity forces act downward and normal to the plane of the wing, most of the heat pipe will operate in a reflux mode (i.e. where the condenser is above the evaporator and condensate return to the evaporator is by gravity). This is illustrated on Figure 31, which shows the wing leading edge elevation relationships as a function of distance from the geometric centerline. As indicated by this figure, approximately  $165$  cm ( $65$  in) of the heat pipe total length will operate in a reflux mode, while the remaining  $35$  cm ( $13.8$  in) on the lower surface will require wicking and the accompanying surface tension forces for condensate return.

Heat pipe design parameters applicable to the SST0 wing leading edge are summarized on Figure 32. Upper and lower surface parameters are presented in terms of required radial and axial peak heat transfer rates, condenser and evaporator lengths, elevation heads, and maximum temperature and internal pressures.

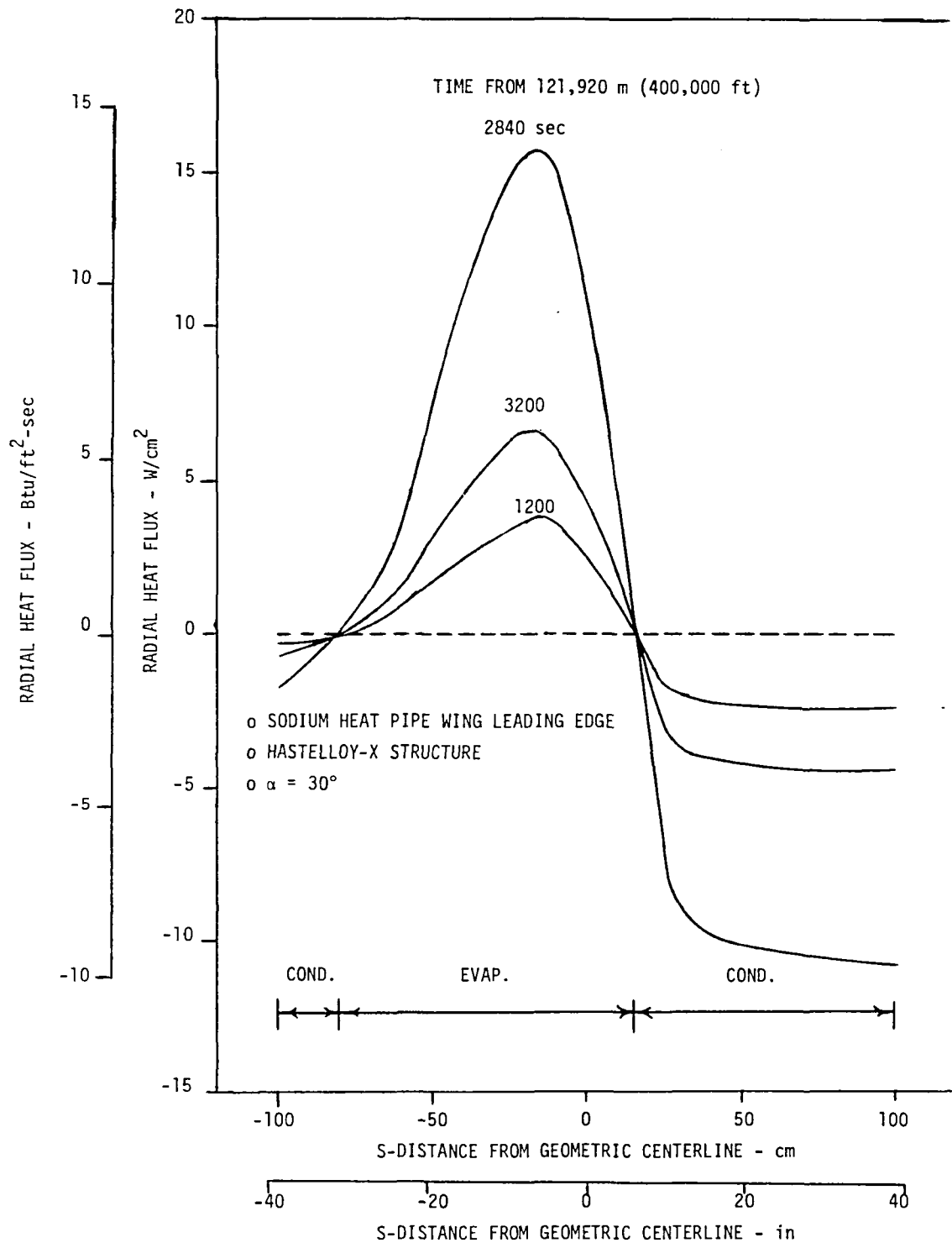


Figure 29. - Heat pipe radial heat flux during entry.

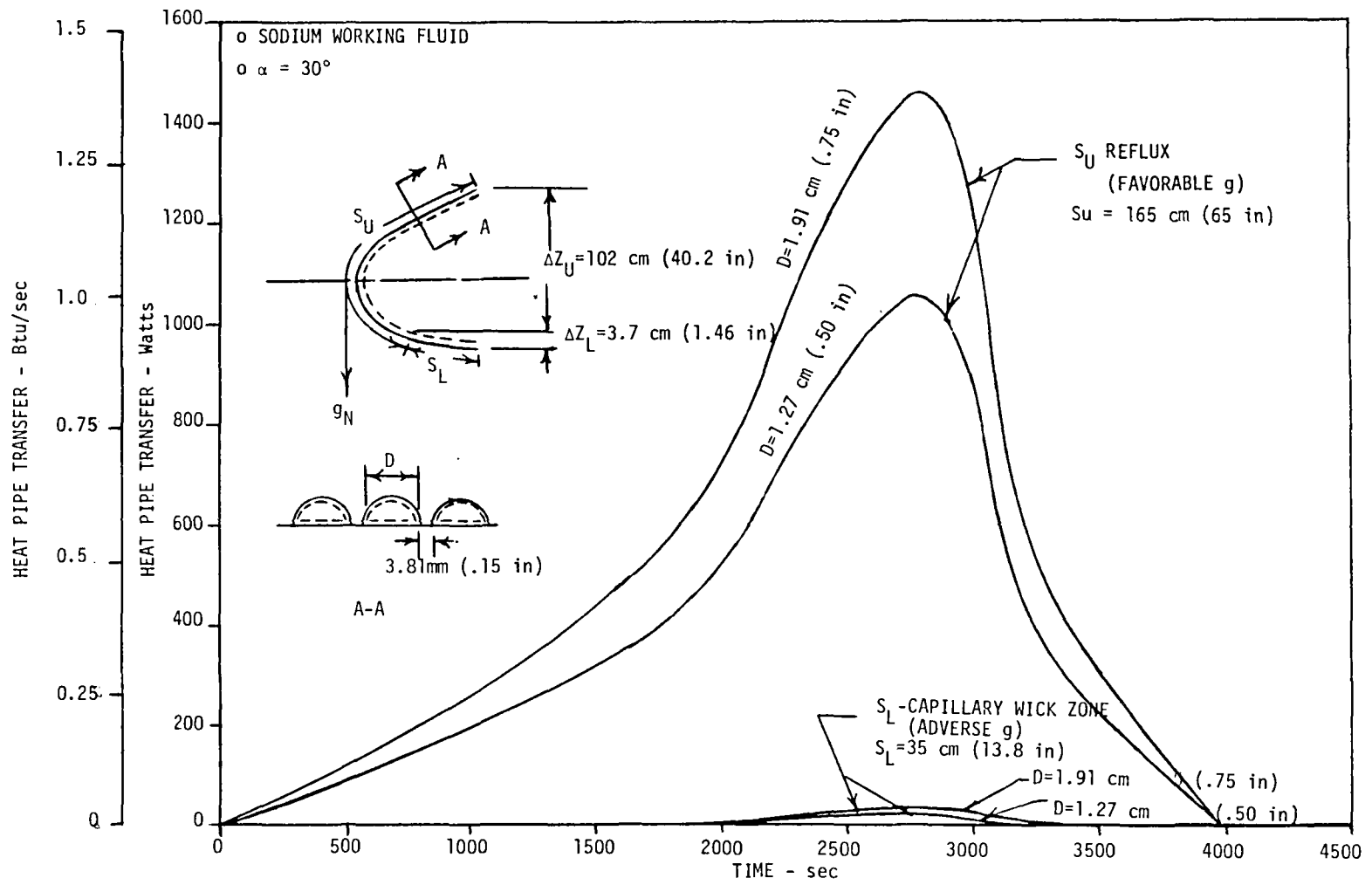


Figure 30. - Heat pipe axial heat transfer rates during entry.

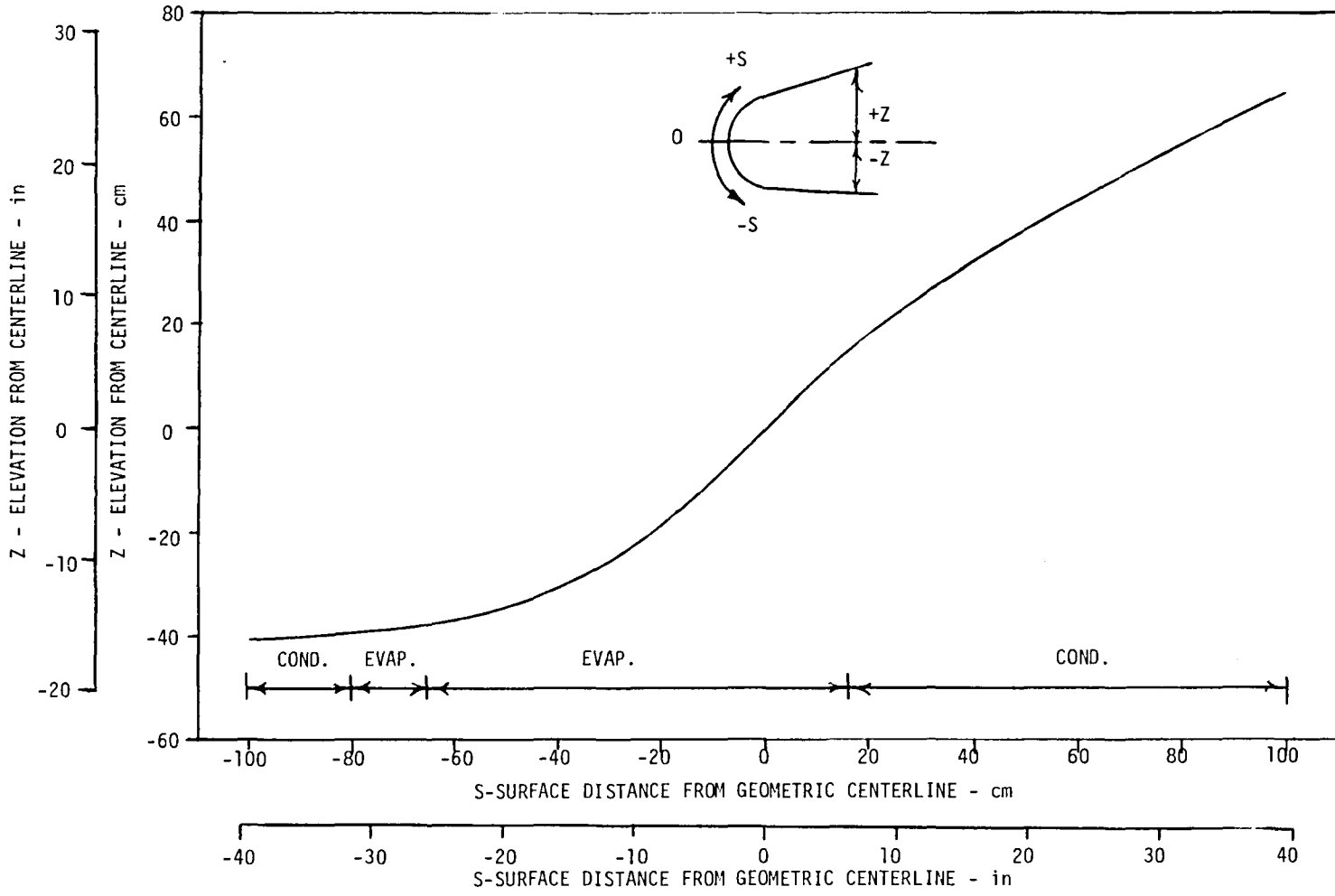
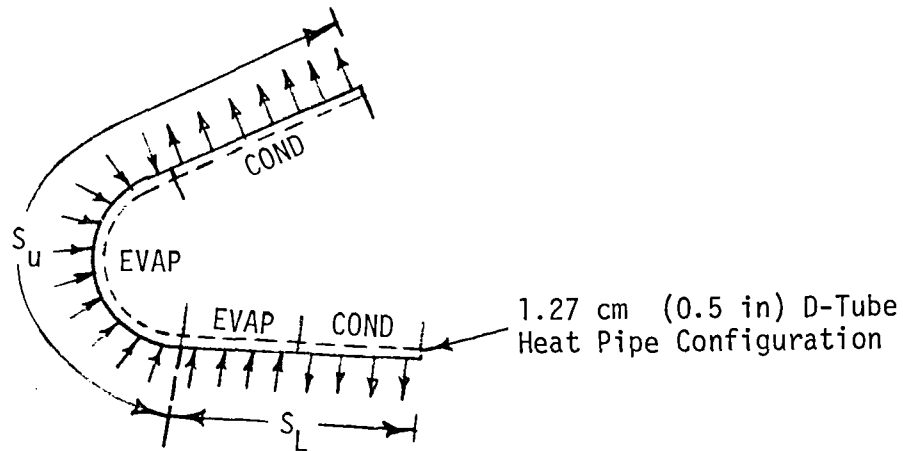


Figure 31. - Wing L.E. elevations vs. distance from geometric centerline.





S<sub>u</sub> - Gravity Assist Zone

S<sub>L</sub> - Adverse Gravity Zone

|                      |  |  |
|----------------------|--|--|
| ( $\dot{q}$ rad) max | 15.6 W/cm <sup>2</sup> (13.7 Btu/sec-ft <sup>2</sup> ) | 2.0 W/cm <sup>2</sup> (1.8 Btu/sec-ft <sup>2</sup> ) |
| ( $\dot{q}$ ax) max  | 1030 W (3515 Btu/hr)                                   | 23 W (78 Btu/hr)                                     |
| L <sub>evap</sub>    | 81 cm (31.9 in)  | 16 cm (6.3 in)                                       |
| L <sub>cond</sub>    | 84 cm (33.1 in)  | 19 cm (7.5 in)                                       |
| $\Delta Z$           | -103.6 cm (-40.8 in)                                   | +3.7 cm (1.5 in)                                     |

Max. Hastelloy X Skin Temp = 1253K (1795°F) @  $\phi$  of D-tube  
 = 1286K(1855°F) between D-tubes

Max. Sodium Vapor Pressure = 221 kPa (32 psia)

Figure 32. - Heat pipe requirements summary for SSTO wing L.E.

#### 4.3.4 Heat Pipe Limits

Heat pipe vapor limits applicable to the upper portion of the SST0 wing leading edge are shown on Figure 33 and compared with actual axial heat transfer rates encountered during entry. Minimal wick requirements are needed in this portion of the heat pipe because the favorable gravity forces permit reflux operation. The only wick structure required is to provide for local fluid distribution to the outboard heated surface. A single layer of 100 mesh screen in contact with the heat pipe inner surface is sufficient for this purpose.

The first limit encountered during start-up after continuum flow is established is the sonic velocity limit. Below 700K (800°F), the heat pipe vapor will be in a free molecular state and essentially no heat pipe action will be provided. Axial heat transfer is thus limited to that indicated by the sonic velocity curve until the heat pipe reaches approximately 810K (998°F). Beyond this temperature level, no limits are encountered since the actual axial heat transfer required is less than the entrainment and axial dry-out limits.

Wicking limits for the lower portion of the leading edge where an adverse gravity situation exists are shown on Figure 34 as a function of normal g loading. It can be seen that there is a substantial margin between the wicking requirements for 23 W (78 Btu/hr) and the pumping capability of either a single layer of 100 or 200 mesh screen.

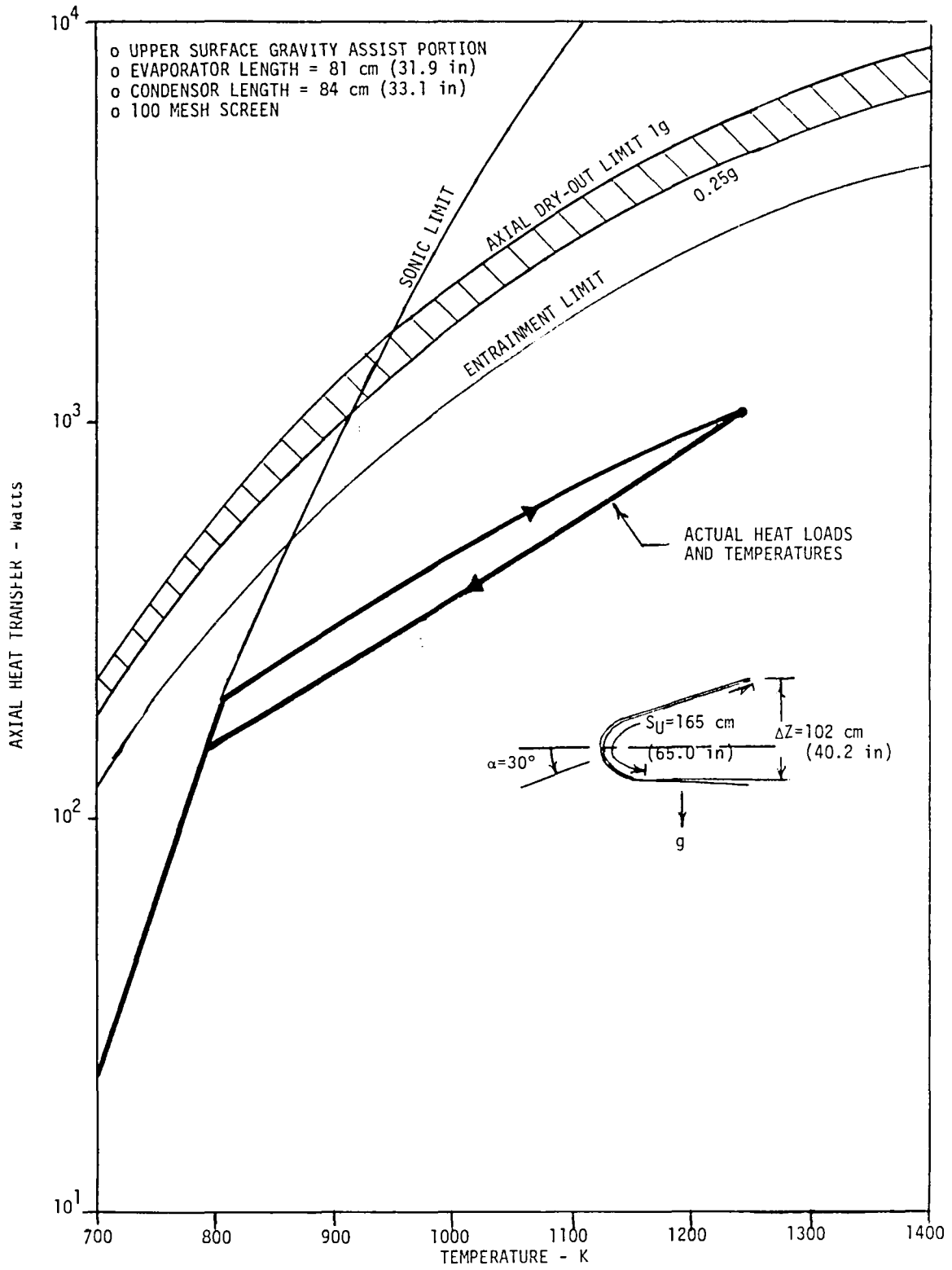


Figure 33. - SSTO wing L.E. heat pipe vapor limits.

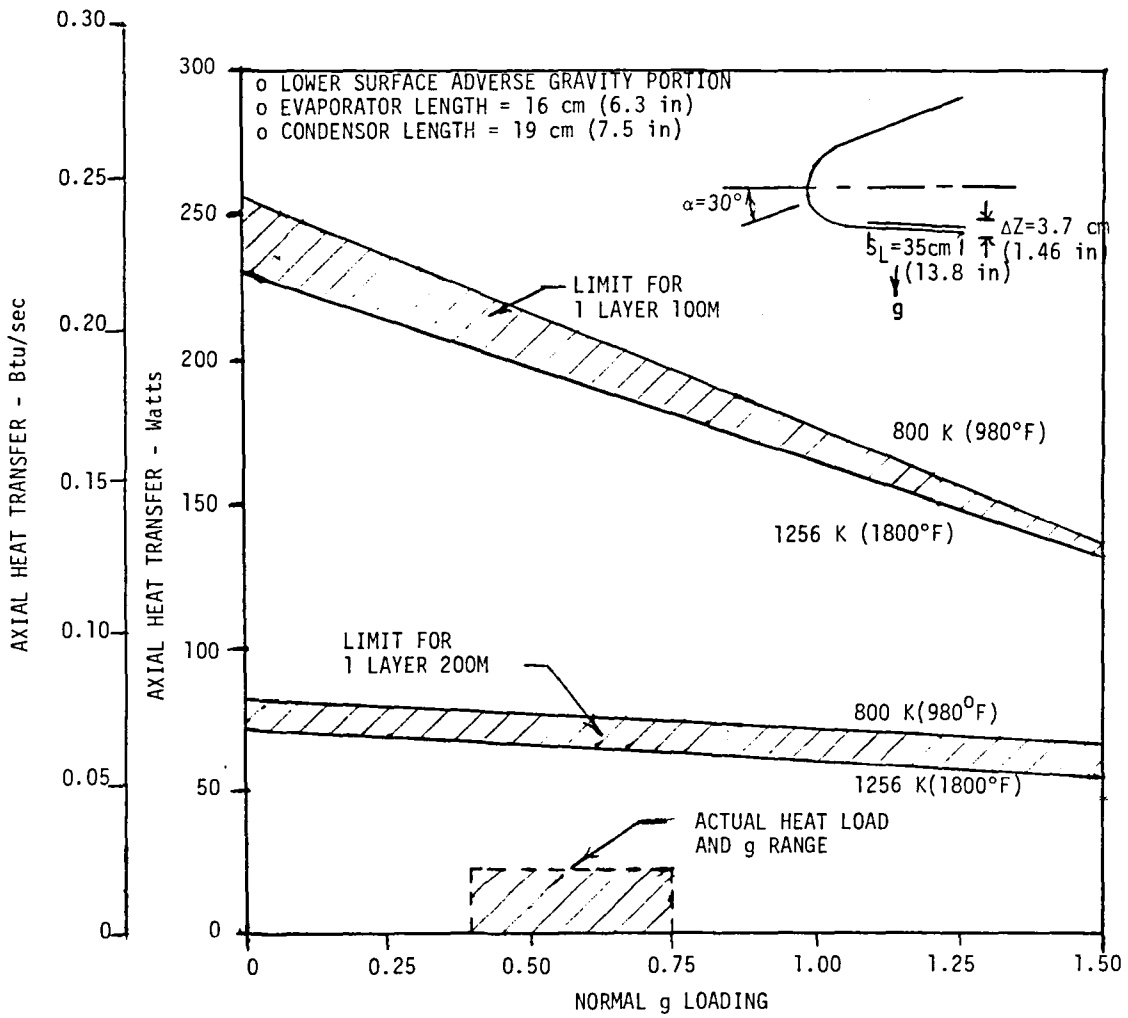


Figure 34. - SST0 wing L.E. heat pipe wick limits.

#### 4.4 LEADING EDGE DESIGN

It became apparent early in the study that the simplest and most efficient leading edge segment design would also be the most economical to produce. This is a segment where all elements are normal to the wing leading edge sweep angle. When compared to a chordwise designed segment, design advantages of the normal segment are shorter heat pipe and wicking lengths, less complex thermal expansion joints, reduced joint sealing requirements, and shorter load paths resulting from a more direct interface with supporting trusses and wing main structure. Advantages which facilitate fabrication are simplified tooling and forming methods required, smaller overall segment size, and less complex assembly procedure. A disadvantage of the normal segment is that the overlapping expansion joints are not parallel to the airstream and additional cant is required to minimize discontinuities at the segment edges.

The leading edge envelope was defined by the length of heat pipe required to maintain acceptable peak heating temperatures. This length is 100 cm (39.4 in) aft from the leading edge radius along both the upper and lower mold-line surfaces. The SSTO leading edge airfoil shape causes the lower section of heat pipe to terminate 9.1 cm (3.6 in) further aft than the upper section. Since the wing leading edge closure web acts as the forward pressure bulkhead of the liquid oxygen tank, a forward canted configuration is optimum for obtaining maximum wing tank volume and minimum bulkhead depth. The offset terminations of the heat pipe produce a 12.25 degree forward cant angle on the closure web.

Supporting truss spacing and leading edge segment width was determined by location of the main wing spar chord and truss primary structural system. The main wing trusses have a chordwise spacing of 76.2 cm (30 in). This results in a span between truss tie-ins at the leading edge closure web of 92 cm (36.2 in) when projected normal to the leading edge. Leading edge segment support trusses were positioned normal to the leading edge closure web and located at the main wing truss tie-ins for load carry-through continuity, and intermediate to the tie-ins to provide adequate structural support for the segments. A segment width of 46 cm (18.1 in) was the result of this arrangement. The segment support trusses are bolted to closure web stiffeners to facilitate assembly or removal and are fixed in position by diagonal drag struts to accommodate aerodynamic loads induced by the leading edge sweep angle. The resulting leading edge heat pipe configuration is depicted on Figure 19.

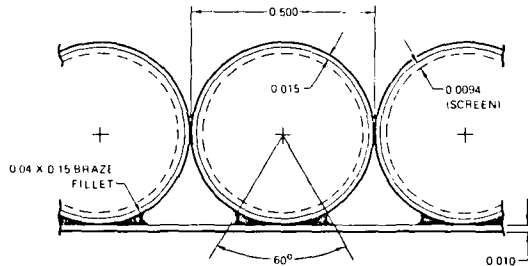
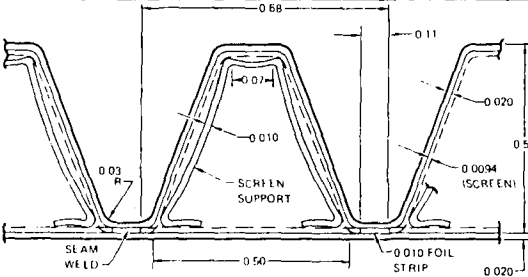
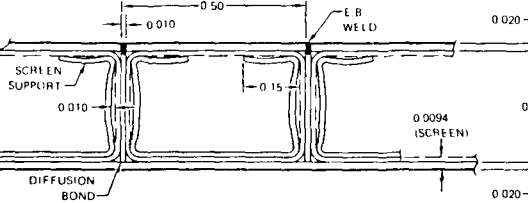
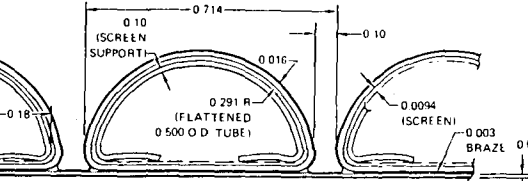
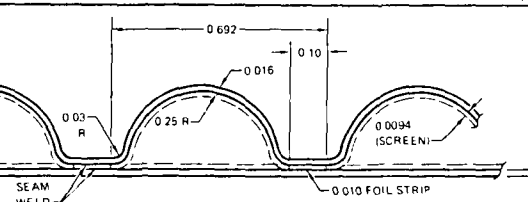
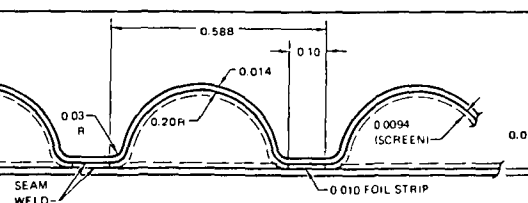
#### 4.4.1 Heat Pipe Cross-Section Design

A primary consideration of leading edge segment design was integrating the heat pipes into the design such that the segment presented a smooth airfoil shape to the airstream. Second, for most effective heat pipe operation, it is desirable that the heat input be conducted to the heat pipe via the shortest practical route. Finally, the heat pipes are to serve as load carrying structure, providing depth of section and stiffness to accommodate bending moments from aerodynamic pressures. Six configurations were investigated and compared on the basis of fabrication feasibility, operational suitability, cost, and weight. They are illustrated on Figure 35 and a summarized description of each design follows.

- o Circular Heat Pipe (Tube) - Configuration I of Figure 35 was the first concept investigated and served as the baseline for comparison with other configurations; primarily because of the experience and data accumulated on other circular containment chamber heat pipe applications. (Reference 3).

Based on the SSTO flight environments, heat pipe operating parameters and weight trade studies, a 1.27 cm (0.5 in) O.D. tube was selected as being near to optimum size for this application. The fabrication procedures would be similar to those used in the assembly of the leading edge segment described in Reference 1. A wire mesh wicking material is formed on a cylindrical mandrel and inserted into the individual tubes. The tube is filled with glass beads to retain the screen against the tube I.D. and the tube is then formed into the airfoil leading edge shape. End caps and fill tubes are welded to the ends of the heat pipe and normal heat pipe filling procedures are conducted. The leading edge segment is then assembled by brazing the tubes to the face sheet.

This concept is considered to offer the least development risk and lowest fabrication costs, and results in taking advantage of minimum gage materials because of the inherent pressure and load carrying capabilities of circular cross sections. However, one serious disadvantage does exist. Each heat pipe tube only makes line contact with the face sheet surface which does not provide an adequate path to conduct heat from the portion of the face sheet which is not in contact with the heat pipe. Sufficient fillets of braze material must be added so that at least 60 degrees of the tube circumference is covered and can make thermal contact with the face sheet. This excess braze material imposes a significant weight penalty. Since gross lift-off weight is a critical design constraint for the SSTO vehicle, alternate heat pipe design concepts were investigated.

| CONFIGURATION <sup>1</sup> |   | RELATIVE DEVELOPMENT RISK | RELATIVE PROTECTION PROVIDED <sup>3</sup> | RELATIVE FABRICATION COST <sup>3</sup> | UNIT WEIGHT - kg/m <sup>2</sup> (lb/ft <sup>2</sup> ) | TOTAL WEIGHT kg(lb) <sup>2</sup> | RELATIVE TOTAL WEIGHT DIFFERENCE - kg(lb) |
|----------------------------|---|---------------------------|---|--|---|----------------------------------|---|
| I                          | CIRCULAR TUBE<br>                           | 1                         | 5   | 1                                      | 16.60 (3.400)   | 2692 (5935)                      | 1153 (2543)                               |
| II                         | TRAPEZOIDAL CORRUGATION<br>                 | 4                         | 3   | 5                                      | 17.74 (3.634)   | 2877 (6343)                      | 1339 (2951)                               |
| III                        | RECTANGULAR BUILDUP<br>                    | 5                         | 1   | 6                                      | 16.27 (3.333)   | 2639 (5818)                      | 1100 (2426)                               |
| IV                         | SEMICIRCULAR TUBE<br>                     | 2                         | 2   | 2                                      | 13.74 (2.815)   | 2229 (4914)                      | 690 (1522)                                |
| V                          | STANDARDIZED SEMICIRCULAR CORRUGATION<br> | 3                         | 3   | 3                                      | 10.89 (2.230)   | 1765 (3892)                      | 227 (500)                                 |
| VI                         | OPTIMIZED SEMICIRCULAR CORRUGATION<br>    | 3                         | 4   | 4                                      | 9.49 (1.943)  | 1538 (3392)                      | 0 (0)                                     |

<sup>1</sup> DIMENSIONS IN INCHES (1 IN = 2.54 cm)  
<sup>2</sup> BASED ON L.E. SURFACE AREA = 162.2m<sup>2</sup> (1746 ft<sup>2</sup>).  
<sup>3</sup> ONE IS MOST DESIRABLE SIX IS LEAST DESIRABLE

Figure 35. — Summary of candidate heat pipe configurations.





- o Trapezoidal Heat Pipe (Corrugation) - This design (configuration II of Figure 35) consisted of a backup sheet corrugated to form trapezoidal shapes each having a 1.27 cm (0.5 in) wide base opening, 0.46 cm (0.18 in) wide cap, and a height of 1.27 cm (0.5 in). Both corrugated sheets and face sheets are formed longitudinally into the leading edge airfoil shape and then lined with strips of wire mesh wicking material electron beam welded to alternating strips of foil. Shaped perforated sheet spring supports are inserted in the corrugations to assure conformance of the wicking material to the walls and corners of the trapezoidal shaped containment chamber. When brought together, foil strips on the wicking are aligned with bearing corrugation caps and sandwiched between the corrugated backup sheet and face sheet. The assembly is then joined by seam welding along each bearing corrugation cap. Trapezoid shaped corrugation end closures and servicing tubing are welded in place to complete the assembly. Conventional heat pipe filling procedures would be performed and the servicing tubing welded shut.

This configuration provides direct thermal conduction paths into the heat pipes but the increased tooling complexity, more elaborate wick subassembly, and the need for internal wicking support make it a more expensive configuration to produce. In addition, this concept is heavier than the circular tube design. The flat sides of the trapezoidal containment chamber and inclusion of the face sheet as a containment wall requires that thick gage material be used to withstand heat pipe pressures. This increase and the addition of wicking supports results in greater unit weight than the circular heat pipe concepts, thus precluding it from further consideration.

- o Rectangular Heat Pipe (Built-Up)- In a continuing effort to improve unit weight, a rectangular heat pipe concept was investigated (configuration III of Figure 35). In this concept, a single wall acts as a common membrane between adjacent containment chambers. The configuration consists of diffusion bonded 0.76 cm (0.3 in) deep airfoil shaped ribs at 1.27 cm (0.5 in) intervals on the back side of an airfoil shaped face sheet. Wire mesh wicking material, formed into rectangular shaped tubes and electron beam welded, are internally supported with shaped perforated sheet spring supports then inserted into the channels formed by the face sheet ribs. A channel closure sheet is then electron beam welded to the upper edges of the ribs to complete the containment chamber. The ends of the ribs are tapered to form end closures and servicing tubing is inserted and welded in place.

The rectangular heat pipe arrangement provides direct thermal conduction paths to the containment chambers and offers the most complete coverage. Over 95 percent of the leading edge surface area is backed by heat pipes. However, it also represents the most expensive configuration to produce at the greatest development risk. The unit is lighter than the trapezoidal concept and approximately the same as the preceding circular tube concept.

- o Semicircular Heat Pipe (Tube) - In order to take advantage of the pressure capabilities yet eliminate the weight penalty associated with braze fillet conductive paths of the circular heat pipe, a semicircular or "D" shaped heat pipe configuration was investigated (Configuration IV of Figure 35). Semicircular tubes with an initial O.D. of 1.27 cm (0.5 in) are formed into leading edge airfoil shape with the flat surfaces conforming to the convex side of curvature. The flat sides of the tubes are then brazed to an airfoil shaped face sheet. Wick installation and heat pipe servicing would be the same as for the circular tube concept.

Elimination of excess braze material is achieved using this concept with only moderate increase in tooling cost and slightly higher development risk. Close spacing of the tubes also provides a high percentage of surface area protection, second only to the rectangular heat pipe concept. Despite the slightly thicker gage material, brazed assembly, and the requirement for internal wicking supports, the weight advantage gained by elimination of excess braze fillets makes the unit weight of this concept less than the circular heat pipes.

- o Semicircular Heat Pipe (Corrugation) - Encouraged by the results of the semicircular tube study, a variation in construction of the same basic cross section was investigated. The configuration (Configuration V of Figure 35) consists of a backup sheet formed into corrugations resulting in a series of 1.27 cm (0.5 in) I.D. semicircles and 0.41 cm (0.16 in) wide flats. Both face sheet and corrugated sheet are formed longitudinally into the leading edge airfoil shape. The corrugated sheet is formed so that only the corrugation flats mate with the formed face sheet. Strips of wire mesh wicking material are pre-formed and electron beam welded to alternating strips of foil and flat wire mesh. The result is a series of semicircular shaped wicking tubes joined laterally by thin strips of foil. This subassembly is then tack welded to the back side of the face sheet. When brought together, the foil strips on the wicking are sandwiched between the flats of the corrugations and the face sheet. The assembly is then joined by seam welding along the corrugation flats. Fabricated to be slightly oversize, the semicircular shaped wicking tubes are compressed during the joining operation forcing the wicking against the inner surface of the containment chamber; thereby eliminating the need for internal supports. Formed ends of the semicircular corrugations are tapered to blend into the flat portion and servicing tubing are inserted and welded in place. Standard filling procedures would be used to service the individual heat pipes and subsequently seal the service tubes.

Increased tooling complexity and more elaborate wick subassembly make this concept more expensive to produce. It also represents slightly greater development risk. However, the efficient use of shape, material and joining technique make this configuration the lightest of any investigated, despite thicker gage material requirements for both corrugation and face sheets. The shape and corrugated construction

method are also readily adaptable to technological advances under development which could make it cheaper and lighter. For example, super plastic forming techniques and the use of etched or embossed surfaces for wicking might be used to provide more efficient fabrication. It is for these reasons, particularly the existing and potential weight advantages, that this type configuration was selected.

- o Optimized Semicircular Heat Pipe (Corrugation) - Sizing of the preceding semicircular heat pipe configuration was based on the maximum corrugation radius obtainable using industry standard sheet metal gage thicknesses. An even lighter heat pipe design can be obtained by selecting a corrugation size which is based on minimum wall thicknesses required to accommodate bending moments and burst pressure. This concept (Configuration VI of Figure 35) would be identical to the preceding configuration except the semicircular corrugations would have an I.D. of 1.0 cm (0.4 in) and both corrugated and face sheets would be fabricated from thinner, non-standard sheet metal thicknesses. The resulting weight reduction from the larger corrugation design is approximately  $1.0\text{kg/m}^2$  ( $0.2\text{ lb/ft}^2$ ) of surface area, 227kg (500 lb) per vehicle. Because the width of the weld flats on the optimized corrugation design remain the same as for the larger corrugations, the weight advantage realized is also accompanied by a decrease in heat pipe protected surface area of approximately 2.5 percent. However, this reduction is well within the capabilities of the overall design and would not significantly affect the SSTO wing leading edge temperature control system.

The methods and procedures for fabricating the optimized corrugated heat pipe configuration would be the same as for the larger standardized corrugation design. Tooling costs would not increase appreciably but non-standard material gage thicknesses would require special mill runs or chemical machining at greatly increased cost. The most significant production cost increases would result during fabrication and assembly. The optimized corrugation design contains approximately 15 percent more heat pipe containment chambers and results in a corresponding increase in the number of wicking subassemblies, seam welds, and servicing and inspection operations required. Although the larger standardized configuration was selected for more detailed analyses in this study because of lower anticipated production costs, the weight-optimized configuration may actually be shown to be more cost-effective during SSTO development should equivalent costs of launch weight reduction be less than production costs.

#### 4.4.2 Strength Analysis

The structural design criteria used in the study requires that there be no detrimental deformation at limit load or proof pressure and no failure at ultimate load or burst pressure, considering proof and burst pressurization as singular conditions. The design factors used in the study are:

- o Factor of Safety 1.4
- o Proof Pressure Factor 1.67
- o Burst Pressure Factor 2.22

Thermal stresses are treated as limit stress and conservatively added directly to the limit stresses from other sources.

The heat pipe structure is loaded by aerodynamic pressure and by thermal gradients. The aerodynamic pressure is derived from Figure 21 and Figure 22 by multiplying the static pressure ratio on Figure 22 by the static pressure from Figure 21. The thermal gradient between the face sheet and the heat pipe was a function of the configuration, but did not exceed 33K (60°F). This occurs for the maximum temperature of 1256K (1800°F). The heat pipes must also withstand a maximum internal operating pressure of 221 kPa (32 psig) per paragraph 4.4.2, and an external collapsing pressure of 102 kPa (14.7 psig).

Structural trade studies were performed for three heat pipe leading edge configurations subjected to the same load. They are shown on Figures 36, 37, and 38. Deriving the bending moment from aerodynamic pressure and thermal gradients is an iterative process depending upon the final structural stiffness. The stiffness cannot be calculated before the tube and face sheet thicknesses are explicitly defined. Therefore, an initial estimate was required and an ultimate value of 1.308 N.m (11.58 in-lbs) per 2.54 cm (1.0 in) of width from Reference 3 was selected for the trade studies.

If designed to withstand a given bending moment, a configuration made up of large diameter tubes weighs less than one with smaller diameter tubes. Conversely, if internal pressure causes the most severe loading, a configuration made up of smaller diameter tubes weighs less than one with larger tubes.

Small computer routines were written to determine the required face sheet and tube wall thickness for various size tubes. The subroutines, which contain an iteration loop, were used to check the tube and face sheet for local crippling due to axial and tangential compressive stresses resulting from the pressures and bending moment and also to check the flat sections for bending stresses resulting from pressure loads. Thicknesses were iterated in small increments starting at minimum gage until the strength requirements were satisfied. The required thicknesses and resulting weights per unit area were printed out as a function of tube size.

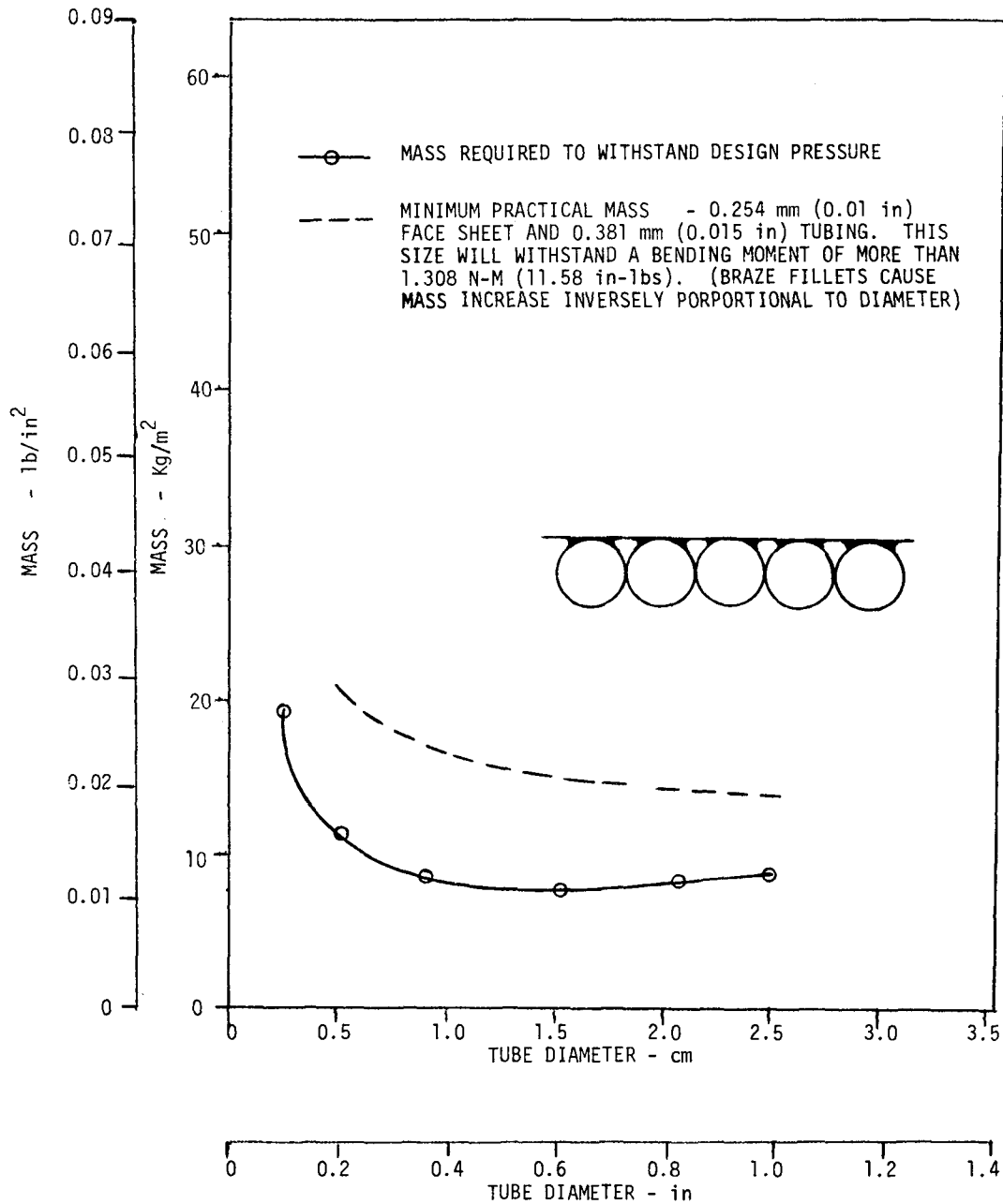


Figure 36. - Trade study - circular tube with single face sheet.

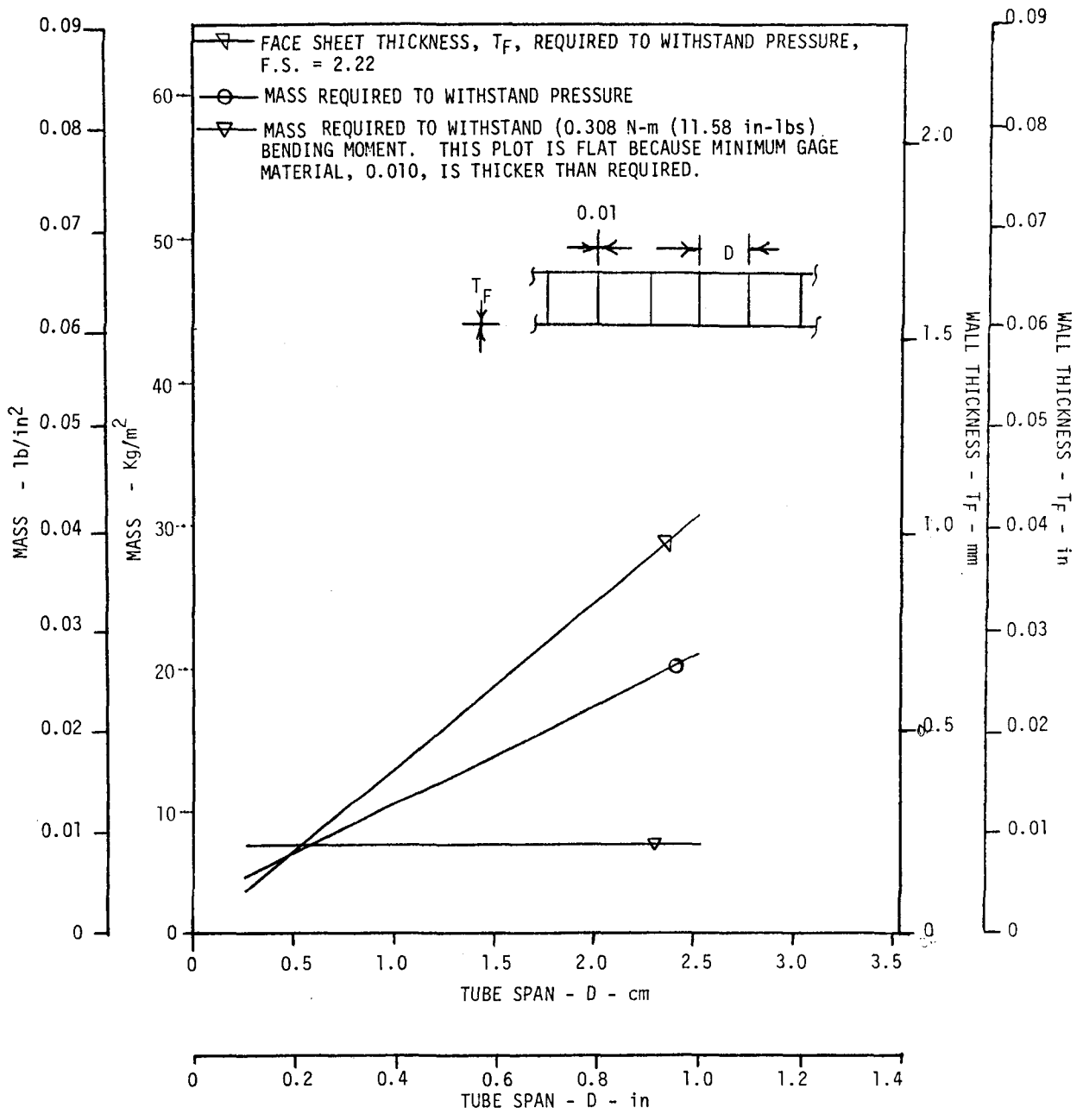


Figure 37. - Trade study - square tube configuration.

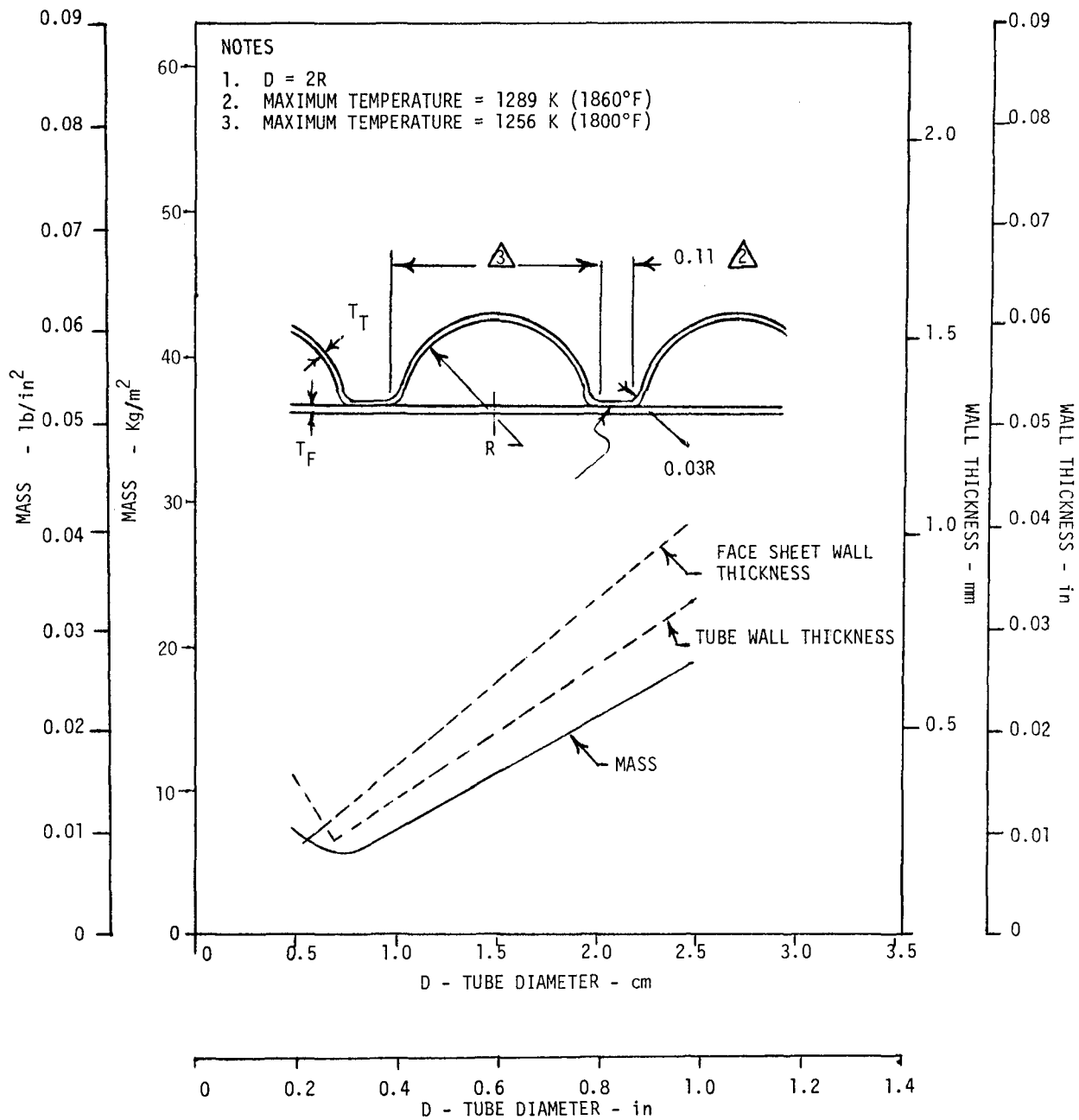


Figure 38. - Trade study - D tube configuration.

Analytical relationships used for the strength analyses were obtained from the following references:

- o Flat sections subjected to normal pressure - Reference 11
- o Circular sections subjected to internal pressure - Reference 11
- o Circular sections subjected to external pressure - Reference 12
- o Allowable crippling stresses - Reference 13

Figure 36 shows the results for a face sheet and circular tube configuration (Configuration I of Figure 35). The lower curve was derived on the basis of structural considerations only and did not reflect minimum gage limitations or the weight of braze fillets required for augmenting thermal conduction. The upper curve reflects the unit weight when the braze fillets are needed to transfer heat from the face sheet to the circular tube and minimum gage constraints are applied.

Figure 37 shows equivalent parametric results for a square tube design (Configuration III of Figure 35). The weight of the system is directly proportional to tube size. Since a square tube does not efficiently carry pressure, the pressure loads are critical for realistic tube sizes. The optimum tube size for minimum weight is 0.58 cm (0.23 in).

Figure 38 shows the parametric results for a face sheet and hemi-cylindrical tube or "D tube" (Configuration V of Figure 35). This configuration was chosen for the baseline design. The D tubes are formed by seam welding a corrugated sheet to a simply curved face sheet to form what is sometimes called a single faced corrugation structure. It is relatively easy to manufacture and is often used in applications involving this type of loading. When used as a heat pipe, the flat side of the D tube carries the heat pipe pressure in bending and becomes heavier than round tubing. However, this configuration has maximum heat pipe contact with the hot face sheet and is efficient in that respect. The figure indicates that the minimum weight occurs for a tube diameter of 0.76 cm (0.3 in).

A 1.27 cm (0.50 in) diameter D-tube was used for structural analysis of the wing leading edge. This size was used rather than the optimum of Figure 38 since it is close to the practical lower limit, based on minimum gage limitations and fabricability. The structure shown on Figure 19 was modeled as shown on Figure 39 and internal loads found using the NASTRAN finite element computer program. Bending moment vs arc length around the leading edge is plotted for the aerodynamic pressure load, thermal gradient, and the sum of the two, (Reference Figure 40). The maximum limit moment is 0.73 N·m (6.48 in-lbs) per heat pipe. The corresponding ultimate load is 1.02 N·m (9.07 in-lbs) per heat pipe or 1.55 N·m (13.7 in-lbs) per 2.54 cm (1.0 in) of width. This compares favorably with the 11.58 in-lbs used in the trade studies and the conclusions drawn are therefore valid without additional iterations.

The heat pipes are supported at 5 places in this design as shown on Figure 19. The NASTRAN program was re-run using 4 heat pipe supports to check the possibility of reducing the support structure. Results of this analysis indicated that the heat pipe bending moment due to air load increased appreciably for the 4 support configuration. It was therefore concluded that the 5 point support configuration is preferable.



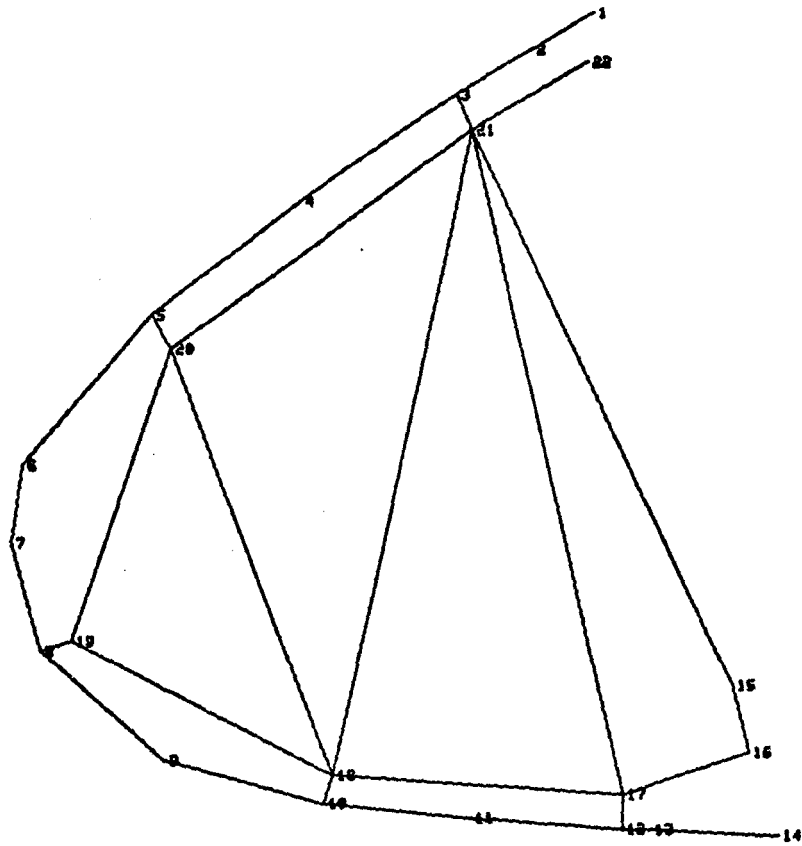


Figure 39. - SSTO wing leading edge structural model.

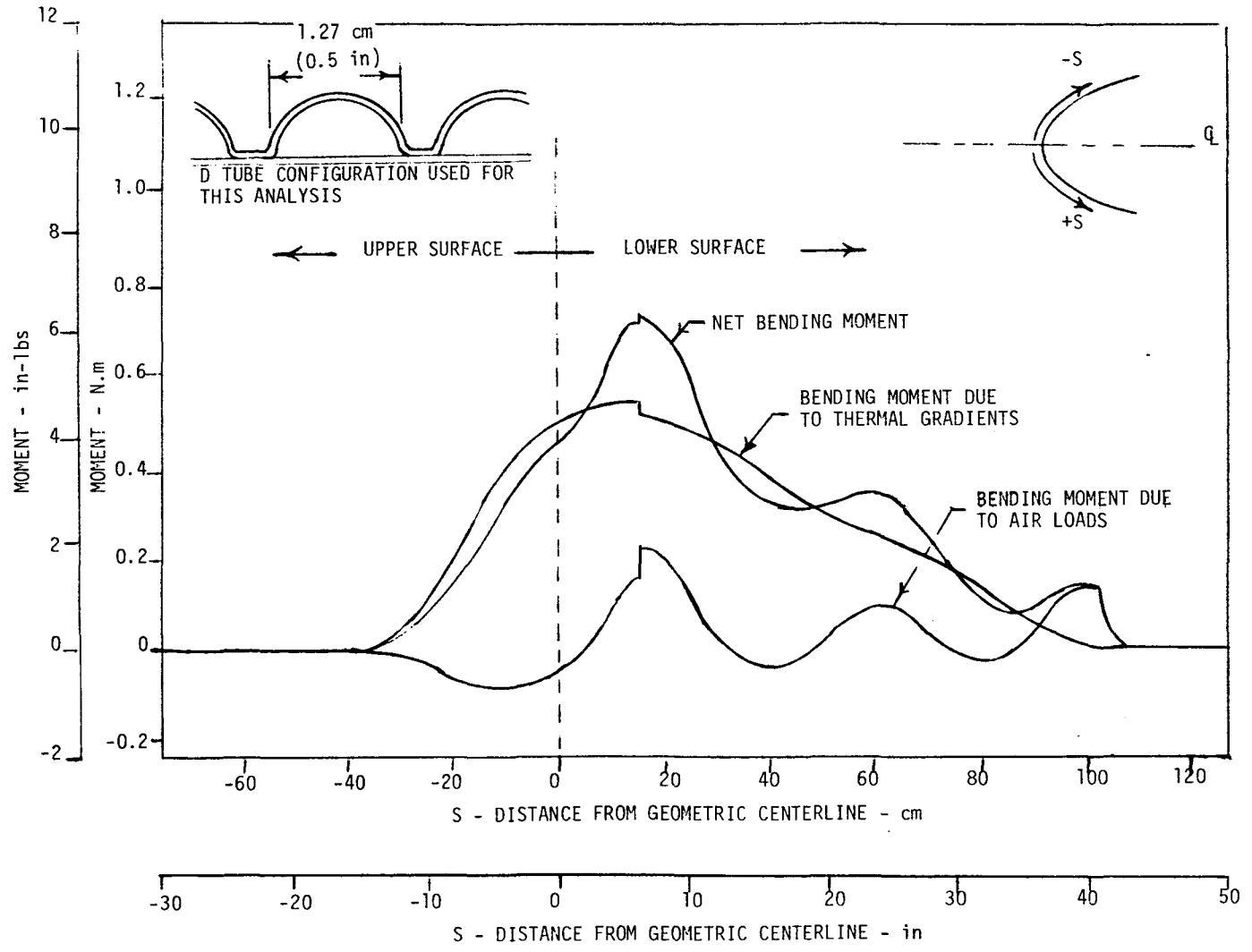


Figure 40. - Heat pipe bending moment.

#### 4.4.3 System Weight

The heat pipe leading edge total and component weights are summarized on Figure 41, assuming the D-tube heat pipe panel design utilizing standard gage materials (configuration V of Figure 35). As shown by Figure 41, the heat pipe panels represent approximately 37% of the total leading edge weight, with the remainder being chargeable to leading edge support and backup structure. No detailed weight breakdown was available from Reference 4 for the baseline columbium leading edge configuration. However, the total heat pipe design weight compares favorably with leading edge weight allocations, being only slightly heavier - 115 kg (255 lbs). All structural materials used for the weight derivations of Figure 41 were assumed to be Hastelloy-X. Since the backup structure will be cooler or can be made to run cooler by isolation from the leading edge with insulation, it is probable that a lighter material (e.g. titanium) could be used in certain locations, thus reducing total weight below the allocation.

The results of this study show that the unit weight of the heat pipe leading edge design can be reduced considerably from the circular tube configuration determined for the shuttle wing leading edge studies of Reference 3 - i.e., 10.89 kg/m<sup>2</sup> (2.23 lb/ft<sup>2</sup>) for the standardized D-tube design (configuration V of Figure 35) vs. 16.8 kg/m<sup>2</sup> (3.44 lb/ft<sup>2</sup>) for the circular tube design (configuration I of Figure 35).

As described in Section 4.4.1, the heat pipe panel unit weight could be further reduced to 9.49 kg/m<sup>2</sup> (1.94 lb/ft<sup>2</sup>) by using smaller diameter D-tubes and non-standard gages (configuration VI of Figure 35), but at a higher production cost. This change would result in a total weight reduction for the SSTO wing leading edge of 227 kg (500 lb), which is substantial when actual launch weight cost factors are considered. For example, current Space Shuttle launch weight costs are estimated at around \$66,000/kg (\$30,000/lb). Therefore, the higher production costs associated with the lighter optimized design would have to be traded off against the lower launch weight costs to define the most cost-effective design.

| ITEM  | UNIT WEIGHT       |                    | TOTAL WEIGHT |        |    |
|---|-------------------|--------------------|--------------|--------|----|
|   | kg/m <sup>2</sup> | lb/ft <sup>2</sup> | kg           | lb     |    |
| HEAT PIPES:   | 10.89             | 2.23               | 1765         | 3892   | △1 |
| o FACESHEETS  | (8.85)            | (1.813)            | (1435)       | (3165) |    |
| o WICK  | (1.76)            | (0.36)             | (285)        | (628)  |    |
| o WORKING FLUID   | (0.28)            | (0.057)            | (45)         | (99)   |    |
| LEADING EDGE SUPPORT STRUCTURE:   | 3.79              | 0.776              | 739          | 1629   | △2 |
| o TRUSS LINKS   | (1.52)            | (0.311)            | (296)        | (653)  |    |
| o TRUSS FITTINGS  | (0.57)            | (0.116)            | (110)        | (243)  |    |
| o LATERAL SUPPORTS  | (0.79)            | (0.349)            | (333)        | (733)  |    |
| BACKUP STRUCTURE:   | -                 | -                  | 2261         | 4984   |    |
| o FACESHEET EXTENSION & STIFFENERS  | -                 | -                  | (1549)       | (3415) |    |
| o EXPANSION JOINT SPRING SEALS  | -                 | -                  | (37)         | (81)   |    |
| o ATTACHMENT BRACKETS & FASTENERS   | -                 | -                  | (76)         | (168)  |    |
| o ACCESS DOORS & SILLS  | -                 | -                  | (599)        | (1320) |    |
| TOTAL   |                   |                    | 4765         | 10505  |    |
| WING LEADING EDGE WEIGHT ALLOCATION (REF. 4)  |                   |                    | 4649         | 10250  |    |
| △1 BASED ON TOTAL HEAT PIPE SURFACE AREA OF 162 m <sup>2</sup> (1746 ft <sup>2</sup> )    |                   |                    |              |        |    |
| △2 BASED ON TOTAL LEADING EDGE SURFACE AREA OF 195 m <sup>2</sup> (2100 ft <sup>2</sup> ) |                   |                    |              |        |    |

Figure 41. - SST0 wing leading edge weight breakdown

## 5.0 CONCLUSIONS

In performing the study, locations on advanced space transportation and missile systems which will be subjected to high localized heating rates were analyzed to identify areas where an integrated heat pipe thermostructural approach could potentially result in reduced weight or cost. The main attraction of heat pipes for high temperature thermostructural applications is their potential to reduce temperatures low enough to effect a material change which may be beneficial in terms of weight or cost reduction. For example, titanium may be substituted for superalloy construction, thus realizing a weight savings. Also, superalloy materials might be used where refractories would otherwise be required. The greater durability of superalloys provides potentially higher re-use capability, which in turn reduces maintenance and life-cycle costs.

The following general conclusions are drawn from this study.

- a) Design Environments are Important for Feasible Heat Pipe Operation - The feasibility of utilizing heat pipes for elimination of localized hot spots requires a fairly detailed knowledge of the heating rate histories and distributions in addition to the magnitude and direction of gravity forces relative to the heat pipe.
- b) Space Transportation System Wing Leading Edges are Attractive Applications for Heat Pipes - Of the applications examined where heat pipes might be used for advanced space transportation systems, hypersonic missiles, and entry research vehicles, the Single Stage-to-Orbit wing leading edge showed the greatest promise. Missiles do not benefit from the advantages of the re-use capability offered by liquid metal/superalloy heat pipes and in general impose adverse gravity forces, thereby placing more stringent design requirements on the heat pipe wick system. The high thermal environments encountered by entry research vehicles such as the MRRV make it difficult to cool high temperature regions to levels compatible with superalloys - i.e., <math>1256\text{K}</math> (1800°F).
- c) SSTO Wing Leading Edge is a Feasible Design Application - The design analyses conducted for the SSTO show it to be a viable heat pipe application. The Hastelloy X double-wall corrugated heat pipe panel designs (D-tube) are approximately 35% to 45% lighter than a previous circular-tube heat pipe panel design for the Shuttle wing leading edge. This weight reduction makes the heat pipe cooled leading edge configuration more weight-competitive with the columbium leading edge baselined for the SSTO, in addition to being more durable.

Although the D-tube heat pipe panel design which uses standardized material gages would result in lower production costs than the weight-optimized design which uses non-standard material gages, its unit weight is approximately 15% higher - i.e.  $10.89\text{ kg/m}^2$  (2.23 lb/ft<sup>2</sup>) vs.  $9.49\text{ kg/m}^2$  (1.94 lb/ft<sup>2</sup>). This weight difference is equivalent to a 227 kg (500 lb) difference in SSTO launch weight. Therefore, the lower production cost of the standardized configuration

would have to be traded off against the lower weight (and resultant lower launch weight cost) of the optimized configuration to determine the most cost-effective design.

The following general observations are also provided relative to wing leading edge heat pipe applications similar to the SSTO:

- o Sodium is the preferred working fluid
  - o Hastelloy x is the preferred heat pipe container material
  - o Wick requirements are minimal and can be satisfied with a simple homogeneous screen wick, particularly for the planned high angle of attack entries, which permit predominantly gravity assist heat pipe operation.
  - o Transient start-up during initial heat pipe operation does not appear to be a significant problem, but more detailed modeling of the working fluid mass transport behavior is recommended.
- d) Heat Pipe Cooled Honeycomb Sandwich Panel Evaluation - From a thermal performance standpoint, the basic approach seems reasonable. The biggest uncertainty in the honeycomb sandwich panel design is whether a suitable fabrication and servicing technique can be devised. Manufacture of a superalloy honeycomb core which incorporates a capillary wick structure has not yet been attempted. One promising concept, however, would utilize a tack welding operation for joining the core material to itself and to the face sheets, after initially forming capillary grooves in the cell walls.

## 6.0 APPENDIX A - LEADING EDGE PARAMETRIC STUDIES

In order to provide additional insight to the utilization of heat pipes for space transportation system leading edge applications and establish design trends, some generalized parametric analyses were conducted. Emphasis of these analyses was placed on defining heat pipe requirements and configurations which would lend themselves to using a heat pipe of superalloy construction in lieu of higher temperature refractory materials. The latter materials generally require coatings for oxidation resistance and are thus more susceptible to damage; resulting in the need for more rigorous inspection and possibly more frequent refurbishment.

This appendix describes basic analytical relationships used for defining heat pipe performance limits, a general evaluation of the thermal environments encountered by a hemi-cylindrical shaped wing leading edge during earth entry and a definition of heat pipe configurations required to limit temperatures to 1256K (1800°F).

A1. Heat Pipe Limits and Analytical Methods - The design and performance of heat pipes are governed by phenomena which limit the liquid and vapor flow and consequently the maximum heat transfer rates that can be sustained. Operational failures will generally be caused by exceeding one of several performance limits, resulting in a deficiency of liquid working fluid available for evaporation at the heated surfaces of the evaporator. Specific limits which will affect heat pipe maximum performance include the following:

- o Sonic velocity limit
- o Entrainment limit
- o Axial dry-out limit
- o Wick limit or capillary pumping limit
- o Nucleate boiling limit

A full description of these limits are available in the heat pipe literature (e.g. References 9, 10, and 14-18) and therefore will not be repeated herein, except to indicate the basic mathematical relationships and design implications on leading edge liquid metal heat pipe applications.

An additional limit is typically encountered in the application of liquid metal heat pipes. This is due to the fact that at normal room temperature, the working fluid is solid and the pressure in the heat pipe a hard vacuum. With the working fluid initially in a frozen state, this first limit which will be encountered (Start-up) results from the fact that free molecular flow conditions will exist in the heat pipe at low temperatures. The heat pipe will be ineffective until the temperature and corresponding vapor pressure is increased to a level at which continuum flow conditions are present. Continuum flow will

be initiated at the region of highest heat input (i.e. at the stagnation point of a leading edge) and is assumed to occur when the mean free path ( $\psi$ ) of the vapor molecules is equal or less than one percent of the minimum vapor passage dimension. Figure 42 illustrates the temperature required for transition from free molecular to continuum flow as a function of vapor passage diameter for potassium, sodium, and lithium working fluids. The transition temperatures ( $T^*$ ) of Figure 42 were calculated from the following relationship per Reference 10.

$$T^* = \frac{\pi}{2} \frac{M}{g_c R} \left( \frac{\mu_v}{\rho_v \psi} \right)^2$$

It can be seen that the evaporator temperature of a typical sodium heat pipe, for example, must be heated to around 700K (800°F) (approximately 330K (594°F) above the melting point) before any significant axial heat transport can be provided. Transition temperatures of potassium are below those of sodium, while those of lithium are significantly above. Therefore, of these three working fluids, a heat pipe using potassium would become operative sooner. One of the main disadvantages of potassium for the leading edge application, however, is its higher vapor pressure at design operating temperature levels-e.g. 565 kPa (82 psia) for potassium, 221 kPa (32 psia) for sodium, and 4 kPa (0.6 psia) for lithium at 1256K (1800°F). The higher vapor pressure imposes higher structural requirements and thus larger container weights.

Sonic Limit - The sonic limit will also occur during startup when the vapor velocity at the exit of the evaporator reaches the velocity of sound. The sonic velocity limit represents the maximum heat transport capability physically possible and is influenced primarily by the cross-sectional area of the heat pipe vapor space, the type working fluid, and the temperature level. Although the sonic limit will limit axial heat transfer rates during startup, a failure will not necessarily occur, unless other limits are exceeded which result in fluid depletion or localized dryout in the evaporator. Higher sonic velocity limits are achieved with potassium, sodium, and lithium (i.e. in descending order). The following expression from Reference 15 is used for calculating the sonic limit:

$$Q_s = \frac{\rho_v \lambda A_v \sqrt{\frac{\gamma g RT}{M}}}{\sqrt{2(\gamma + 1)}}$$

Entrainment Limit - The entrainment limit is the result of a dynamic instability within the heat pipe which is caused by inertial forces of the vapor exceeding the surface tension forces of the capillary wick structure. The net result is fluid depletion and dryout in the evaporator, precipitated by stripping of liquid from the wick and entrainment of liquid droplets in the vapor as it flows toward the condenser. The basic expression from Reference 15 used for defining the onset of entrainment is:

$$Q_{e,m} = A_v \lambda \left( \frac{\sigma \rho_v}{2r_c} \right)$$

It can be seen that the heating rates at which entrainment occurs can be increased with larger vapor passages and smaller effective capillary pore sizes of the wick structure. In general, the assessment of entrainment effects is a good deal more complex than the above expression would indicate. The limiting failure mode resulting from entrainment is postulated as being related more to the



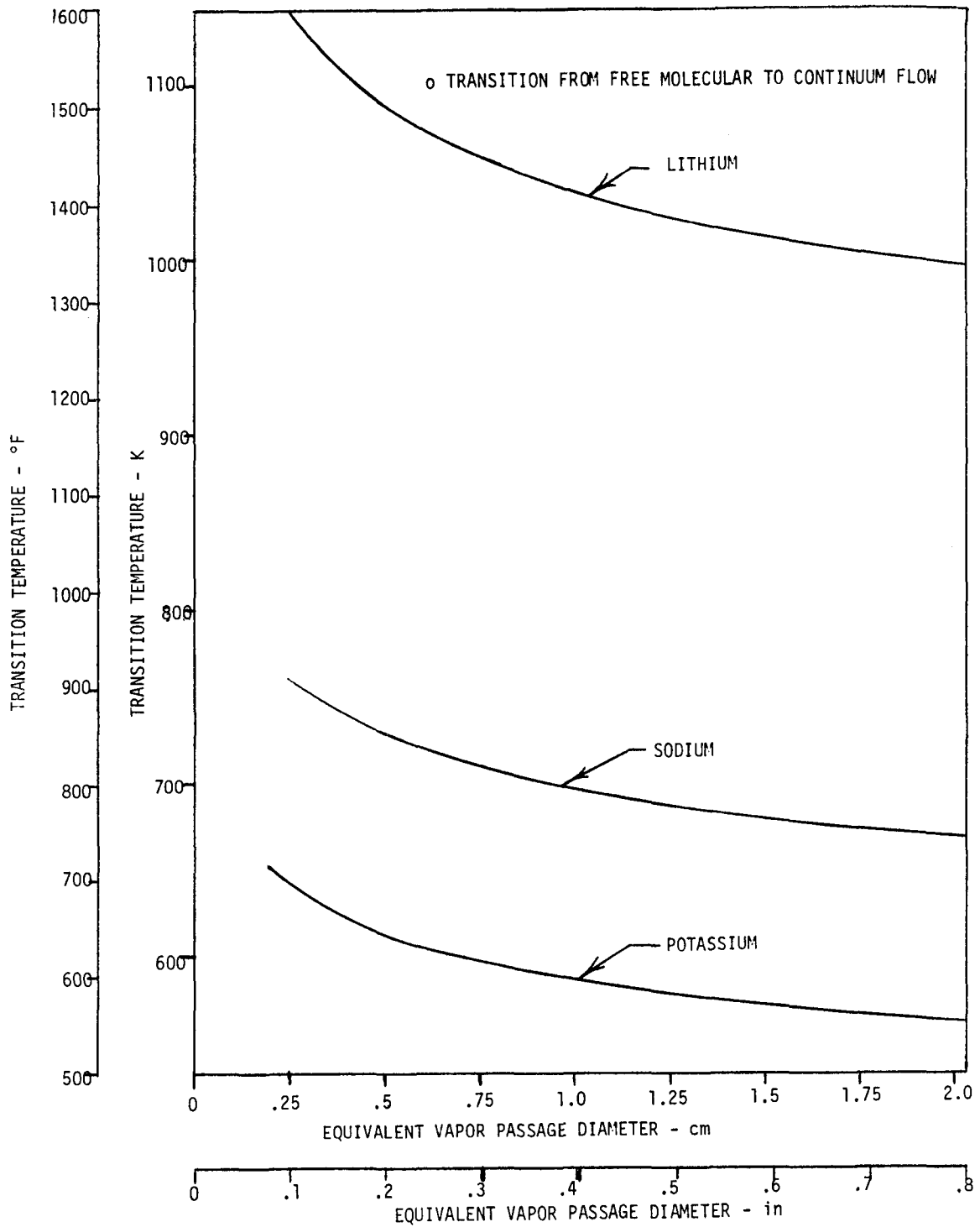


Figure 42. - Heat pipe working fluid transition temperatures.

role of entrainment and its ultimate influences on the overall system pressure balance, rather than to its onset. Thus, some amount of entrainment could likely be tolerated, but it is not clear at present as to the degree.

o Axial Dry-Out Limit - The axial dry-out limit for gravity assist heat pipes is described by Busse and Kemme in References 14 and 18. This limit is characterized by a lack of hydrostatic driving force, resulting in insufficient axial liquid return to all portions of the evaporator. The net result is localized and eventually complete dryout of the evaporator. The expression used for evaluation of this limit is:

$$Q_{d,m} = A_V \lambda \left[ \frac{\rho_V}{K_1} \left( \frac{\rho_L g h_e}{2} + \frac{\sigma}{r_c} \right) \right]^{1/2}$$

o Wick Limit - The wick limit is based on a pressure drop balance of the working fluid within the heat pipe. The sum of the pressure drop of the liquid in the wick structure ( $\Delta P_L$ ), the vapor pressure drop ( $\Delta P_V$ ), and the hydrostatic liquid adverse head ( $\Delta P_g$ ), is set equal to the capillary pumping capability of the wick structure ( $\Delta P_c$ ). Heat pipe failure will occur if the following expression is violated anywhere along the heat pipe:

$$\Delta P_L + \Delta P_V + \Delta P_g > \Delta P_c$$

The pressure drop terms are defined by:

$$\Delta P_L = \frac{1}{K_p A_w} \frac{\mu_L}{\rho_L} \int \dot{m}(X) dX$$

$$\Delta P_V = \frac{8}{A_V r_{v2}} \frac{\mu_V}{\rho_V} \int \dot{m}(X) dX$$

$$\Delta P_g = \frac{\rho_L}{g_c} \int g(X) dX$$

$$\Delta P_c = \frac{2 \sigma}{r_c}$$

The following relation was used for calculation of the axial heat transfer wick limit for conditions of either horizontal heat pipe operation (evaporator and condenser at the same elevation) or adverse gravity operation (evaporator above the condenser), assuming laminar vapor flow conditions.

$$Q_{w,m} = \frac{2FOM_0 \left[ 1 - \frac{\Delta Z r_c}{FOM_1} \right]}{r_c L_{eff} \left[ \frac{1}{K_p A_w} + \frac{32 \nu_v}{D_h^2 A_v \nu_L} \right]}$$

Where the zero g and 1 g figure of merits are functions of the working fluid properties and defined as:

$$FOM_0 = \frac{\sigma \lambda \rho_L}{\mu_L} \quad \text{and}$$

$$FOM_1 = \frac{2\sigma}{\rho_L g_c}$$

o Boiling Limit - Nucleate boiling of the working fluid in the wick adjacent to the heated surfaces of the evaporator will result in the formation of vapor bubbles, which will prevent flow of liquid to that area and cause local wick dryout. The following expression from Reference 15 is used to define the boiling limit.

$$Q_{b,m} = \frac{2\sigma k_e A_e T_v}{\Delta X_w \lambda \rho_v} \left[ \frac{1}{r_n} - \frac{1}{r_c} \right]$$

Local boiling is caused by a temperature gradient across the evaporator wick which is larger than the superheat tolerance of the working fluid. Since the thermal conductivity of liquid metals is very high, relatively small temperature gradients will occur in the wick and the boiling limit is seldom encountered, except at very high radial heat fluxes. Calculations using the above boiling limit equation show that boiling limits should not be encountered for the leading edge applications.

A2. Leading Edge Heat Pipe Design Parameters - Typical thermal environments which will be encountered by an advanced space transportation system are presented in this section. Peak heating rates during equilibrium glide trajectories are shown, along with a general discussion of heat pipe requirements necessary to limit leading edge temperatures to 1256K (1800°F), where superalloy construction could be used.

A.2-1 Stagnation Heating Rates - Peak stagnation heat fluxes which will occur during an equilibrium glide entry are depicted on Figure 43 as a function of the equilibrium glide parameter ( $W/SC_L$ ) for a reference sphere of 0.3048m (1.0 ft.) radius. Stagnation heating rates increase by a factor of  $\sqrt{2}$  as  $W/SC_L$  is doubled and the same amount for an equivalent decrease in spherical nose radius. The  $W/SC_L$  range anticipated for advanced space transportation systems is approximately 244 to 488  $kg/m^2$  (50-100  $lb/ft^2$ ), which would result in peak reference stagnation heat fluxes ( $q_0 \sqrt{R_0}$ ) of approximately 250 to 375  $kw/m^{3/2}$  (40 to 50  $Btu/sec-ft^{3/2}$ ).

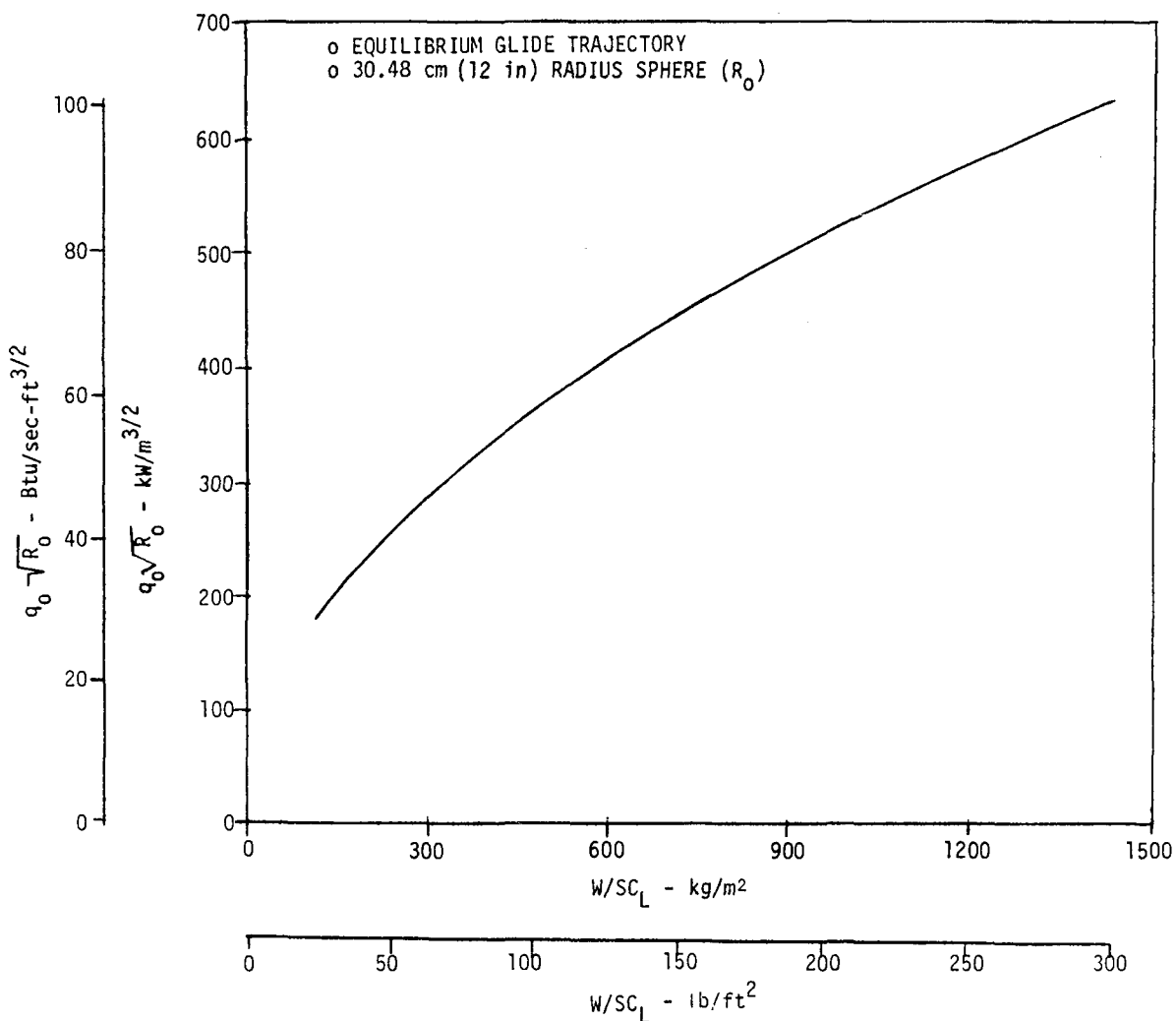


Figure 43. - Maximum reference stagnation heat flux.

The corresponding peak stagnation line heat fluxes for a cylindrically shaped leading edge, ratioed to the reference spherical heating rate, is shown on Figure 44 as a function of angle of attack and wing leading edge sweep angle. Typical leading edge sweep angles are expected to be around 60° and angles of attack 20° or higher. Lower angles of attack are addressed in subsequent paragraphs to illustrate the effects on leading edge heat pipe design requirements.

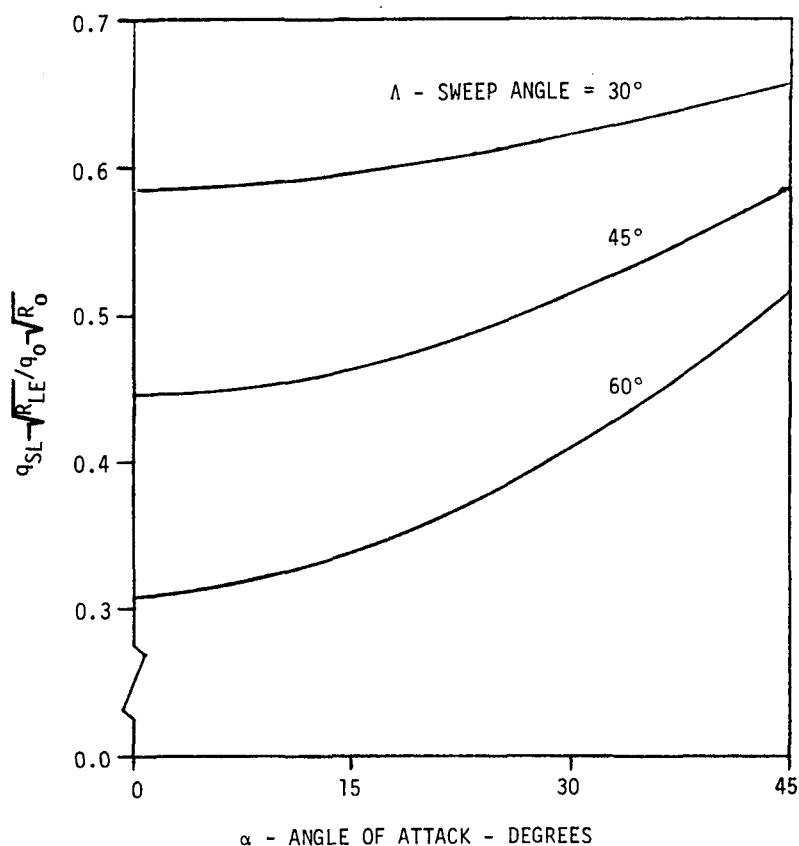


Figure 44. - Cylindrical leading edge stagnation line heat flux.

Maximum stagnation line radiation equilibrium temperatures that will be experienced by a cylindrical leading edge are shown on Figure 45 vs.  $W/SC_L$ , leading edge radius, and angle of attack. It can be seen that leading edge temperatures higher than 1256 K ( 1800°F) will be present in all cases. Even higher temperatures would occur at sweep angles lower than 60°.

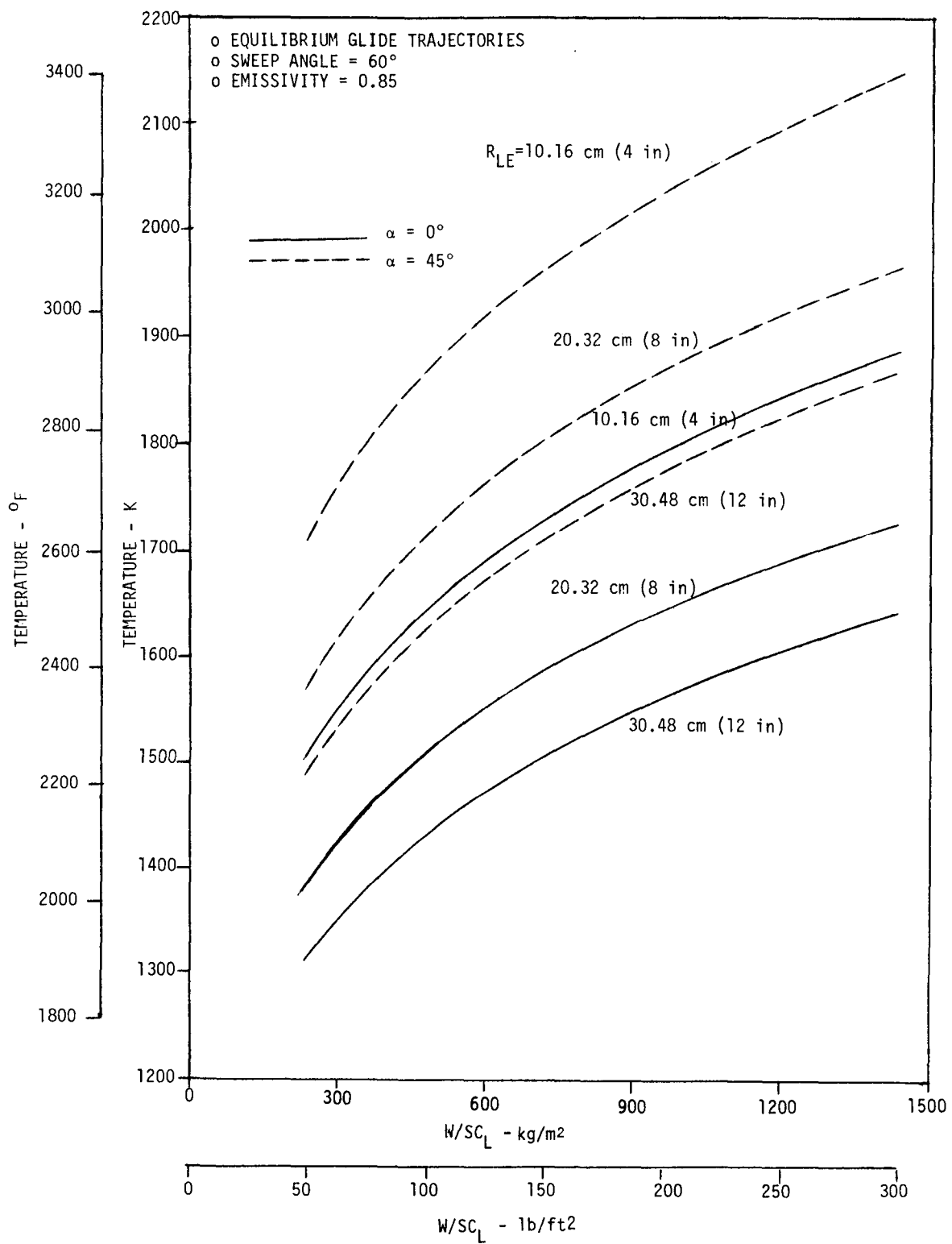


Figure 45. - Leading edge peak stagnation line temperatures.

A.2-2 Local Heating Rate Distribution - The normalized local heating rate distribution ( $\dot{q}_L/\dot{q}_{SL}$ ) over a hemi-cylindrical leading edge is shown on Figure 46 as a function of angle of attack and surface distance ratio (S/R) measured from the geometric centerline. Integration of the heating distribution data of Figure 46 with respect to S/R defines the average heating rate ratio ( $\dot{q}_{AVG}/\dot{q}_{SL}$ ) over the leading edge for various amounts of heat pipe coverage measured in terms of S/R. The leading edge average heating rate ratios are shown on Figure 47.

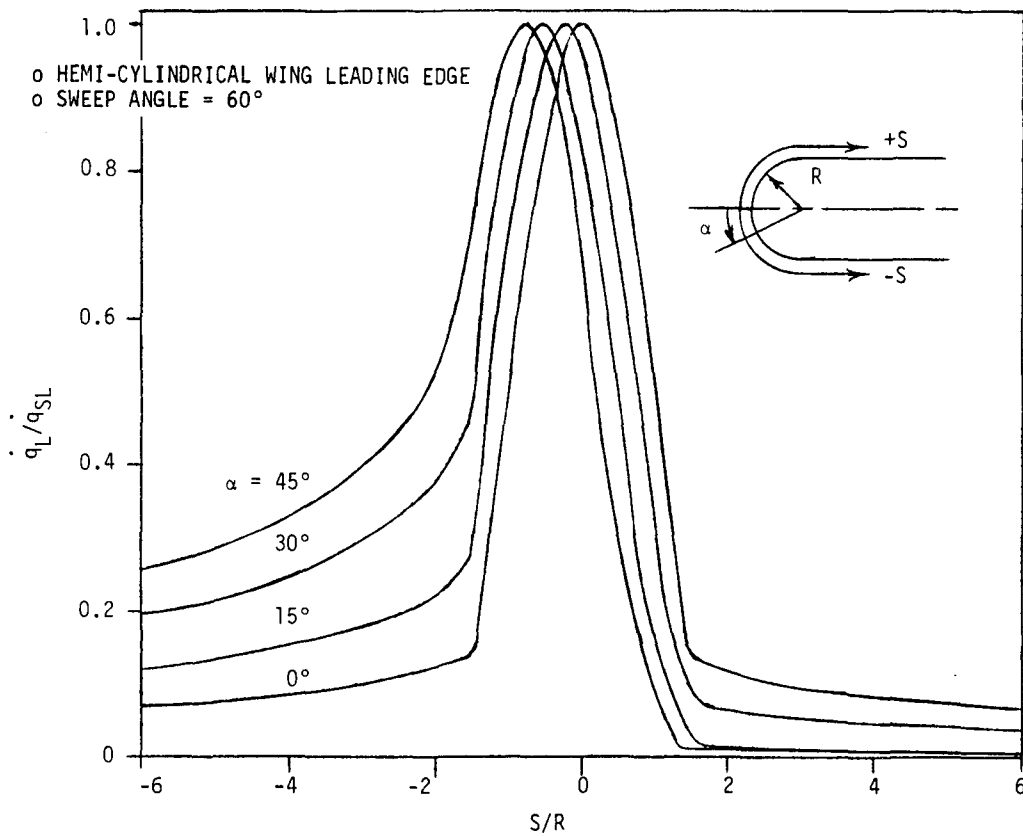


Figure 46. - Local heating rate distribution.

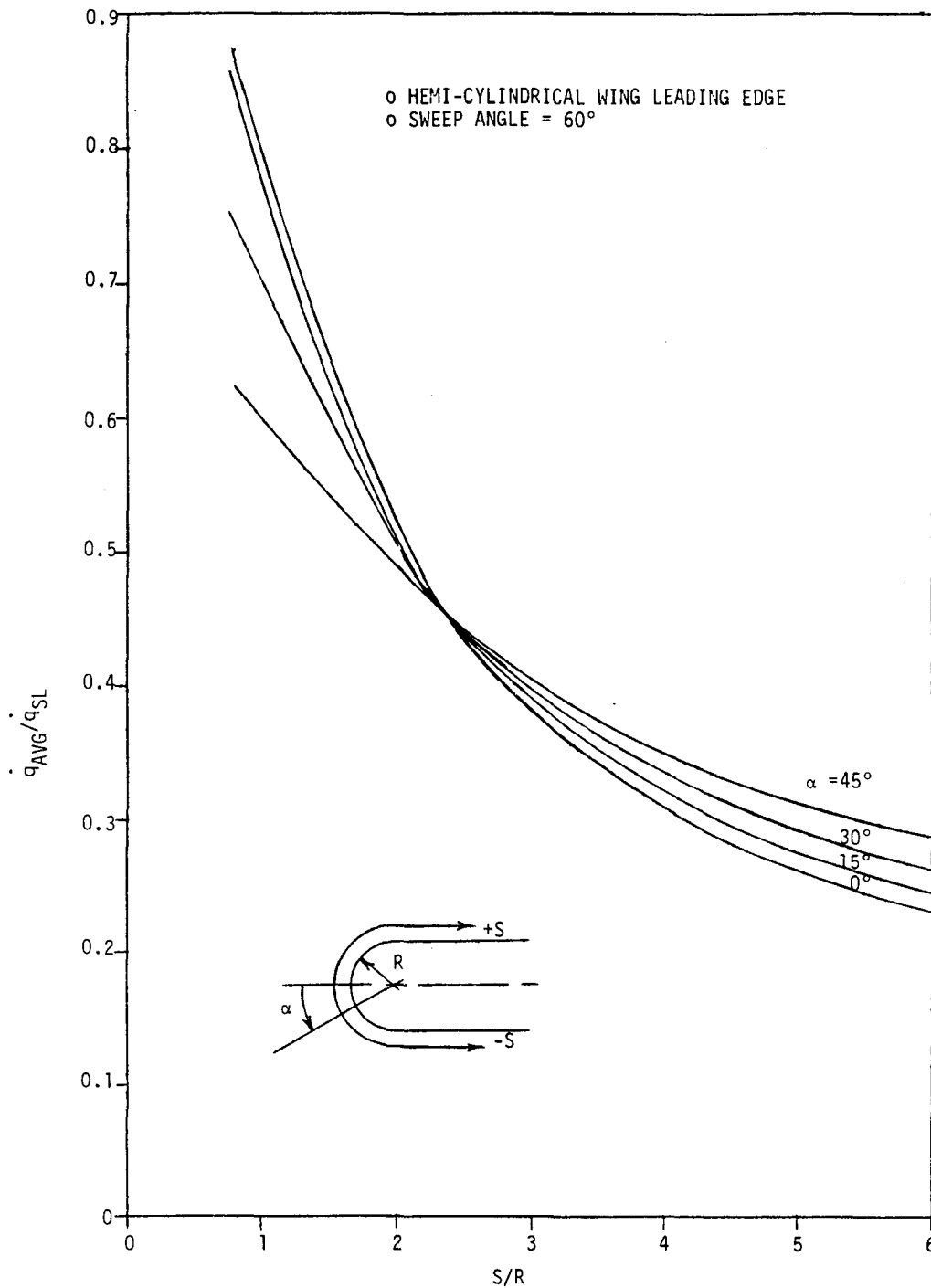


Figure 47. - Ratio of average to stagnation line heating rate.



A.2-3 Heat Pipe Axial Heat Loads and Length Requirements - The average integrated heating rate ratios shown on Figure 47, combined with the stagnation line heat transfer rates of Figure 44, are used to determine the required heat pipe chordwise lengths and total axial heat loads per unit span. Figures 48 and 49 show axial heat loads and required heat pipe lengths vs.  $W/SC_L$  and leading edge radius for designs which will limit leading edge peak temperatures to 1256 K (1800°F) and 1144 K (1600°F). Required heat pipe lengths and axial heat loads increase almost linearly with increasing values of  $W/SC_L$  at constant sweep angle and angle of attack, but are relatively insensitive to leading edge radius. Also, the heat pipe surface coverage required to limit leading edge temperatures to 1144 K (1600°F) is almost double that required for 1256 K (1800°F).

Effects of angle of attack on heat pipe loads and lengths required to maintain 1256 K (1800°F) are shown on Figures 50 and 51 for a  $W/SC_L$  of 488 kg/m<sup>2</sup> (100 lb/ft<sup>2</sup>). Minimal variation is evident for angles of attack up to 15°, but surface coverage requirements and heat loads increase substantially for higher values.

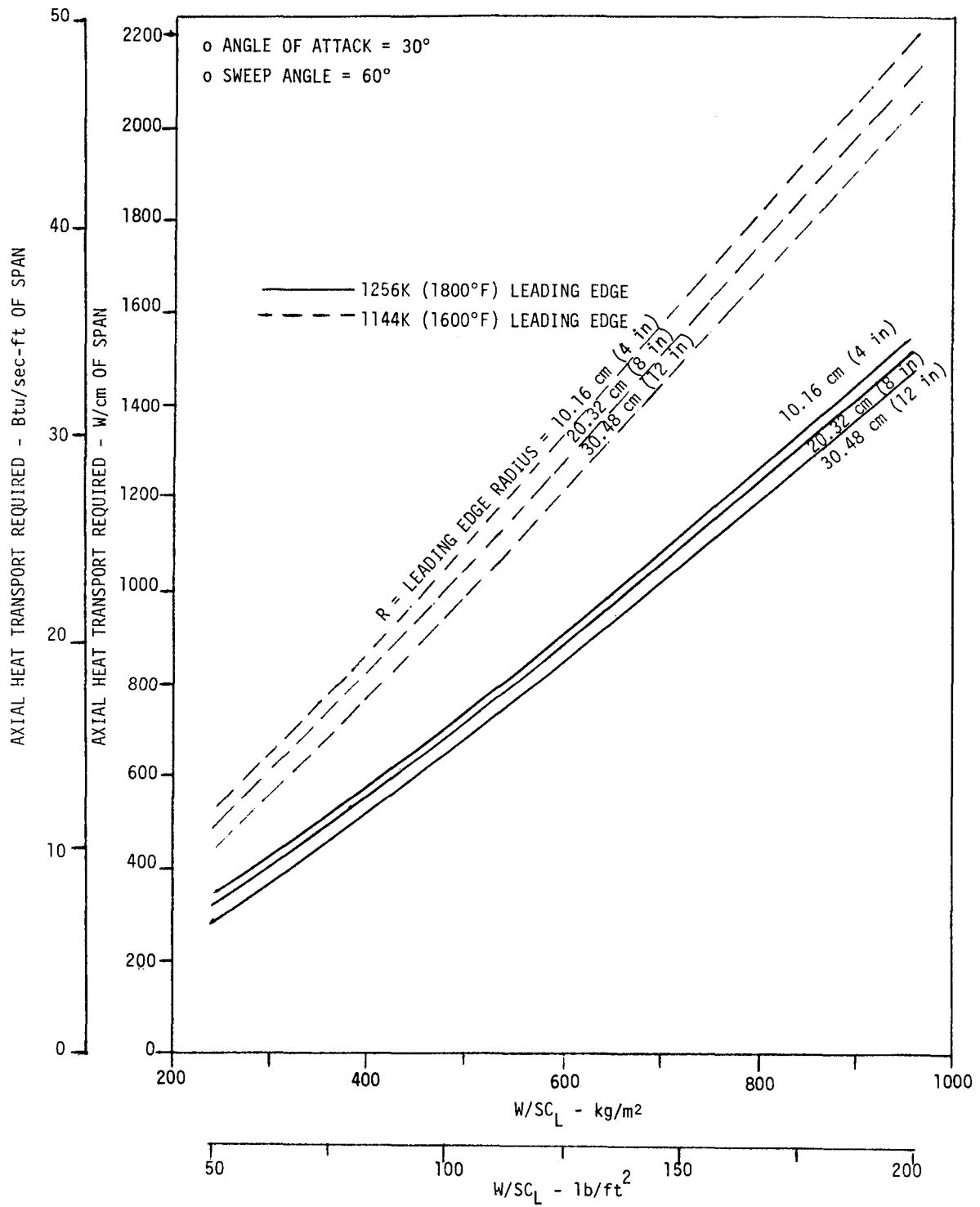


Figure 48. - Leading edge heat pipe axial load vs.  $W/SC_L$ .

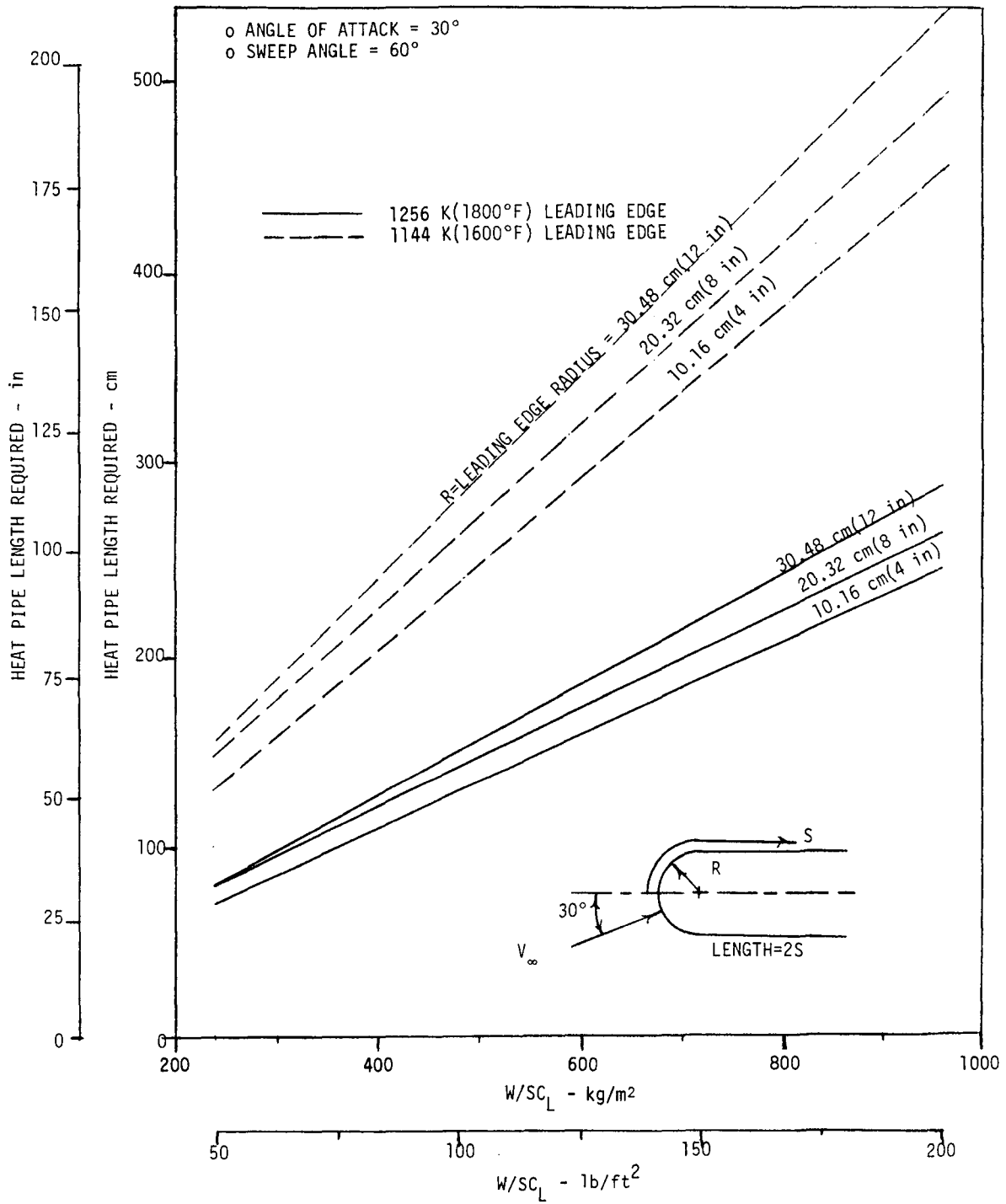


Figure 49. - Leading edge heat pipe length required vs.  $W/SC_L$ .

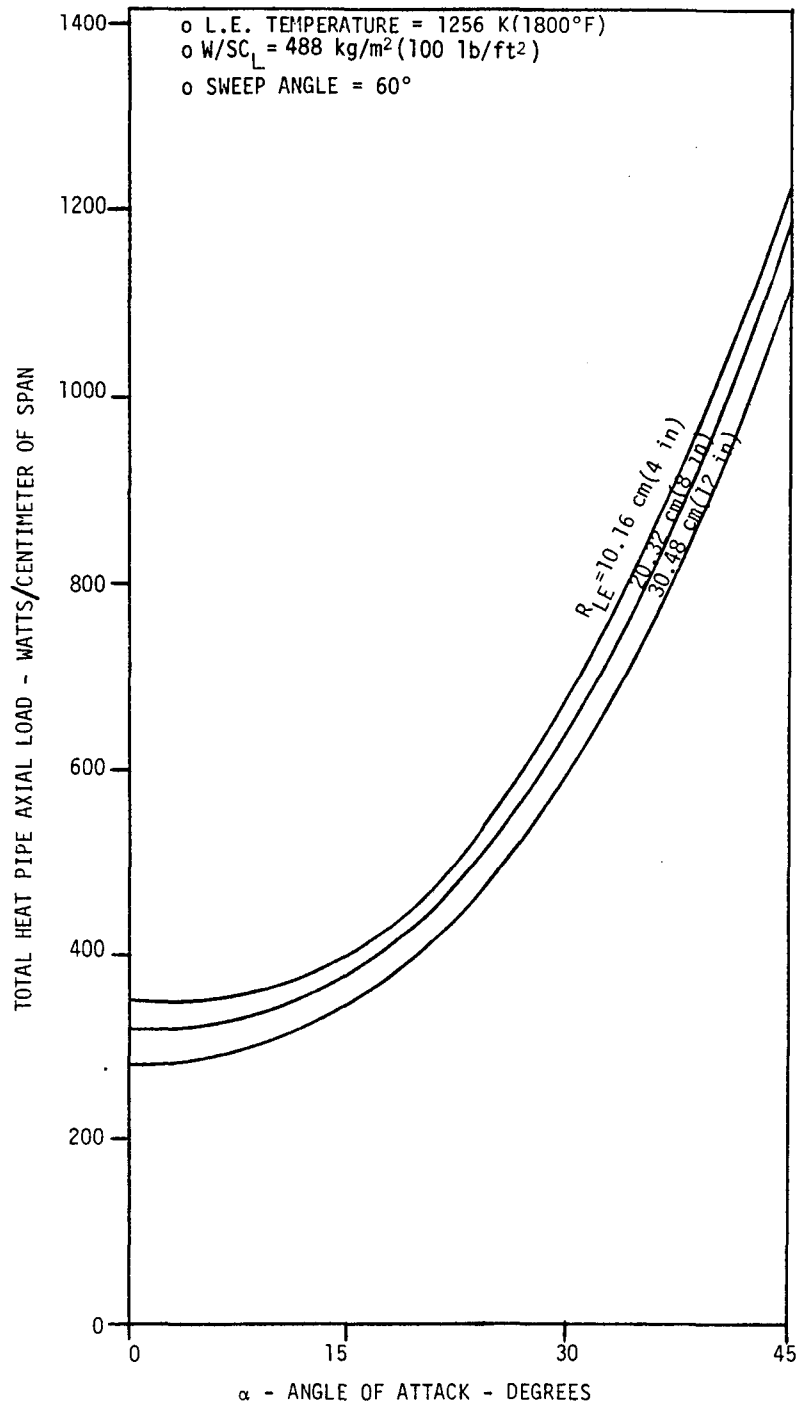


Figure 50. - Leading edge heat pipe axial load vs. angle of attack.

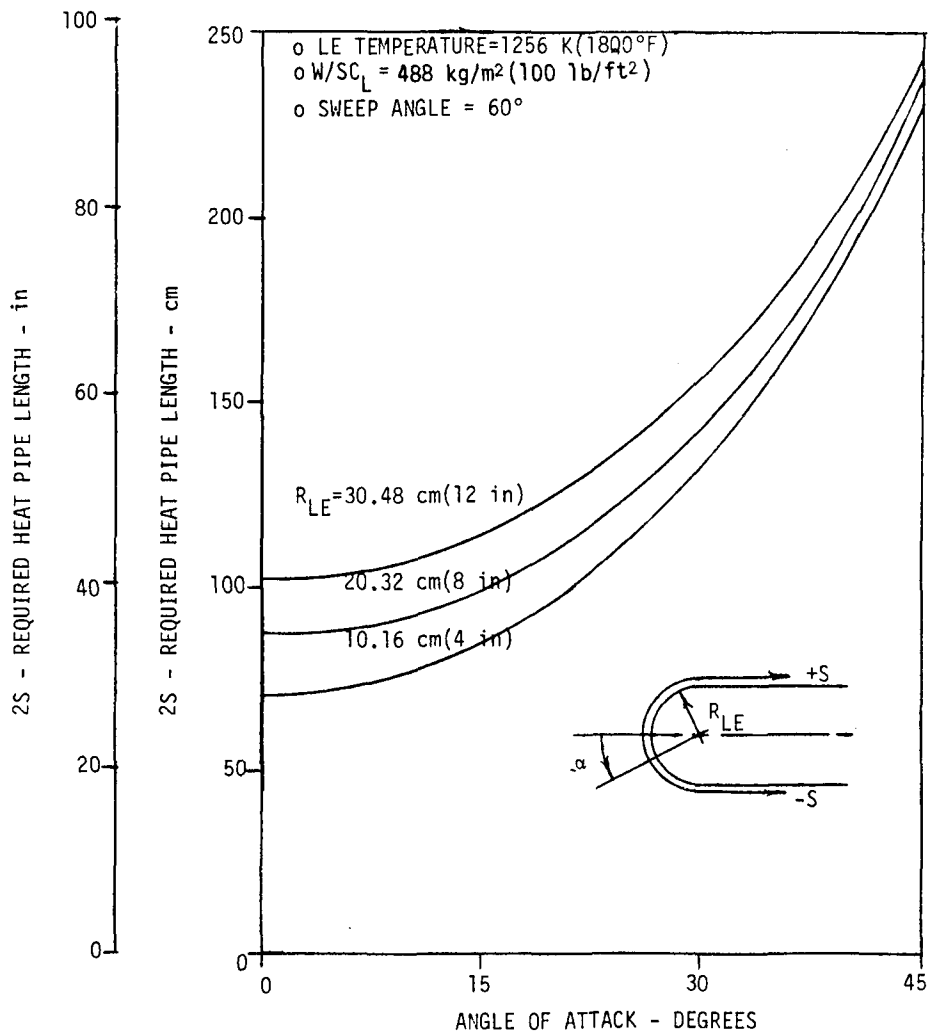


Figure 51. - Leading edge heat pipe length required vs. angle of attack.

A.2-4 Heat Pipe Wick Requirements - Wicking is generally required within heat pipes to provide surface tension forces necessary for circulation of liquid to the heated surfaces for re-evaporation. Heat pipe wick requirements and functional relationships with other elements of the system were generally described in Section A.1 and were shown to depend primarily on axial heat transfer rates and g forces or elevation heads.

Axial heat transfer rates for leading edge applications are related to the location and magnitude of radial heat flux. Radial heat flux distributions over a hemicylindrical leading edge are illustrated, for example, on Figures 52 and 53 for angles of attack of 0° and 30°, respectively. Resultant axial heat transfer rates are represented by the integral under the upper portion of the

curves which is bounded by zero radial heat flux. A net heat transfer into the heat pipe occurs for locations of positive values of radial heat flux, while a net heat transfer rate away occurs for negative values. Transition between adjacent evaporator and condensation regions is at zero radial heat flux.

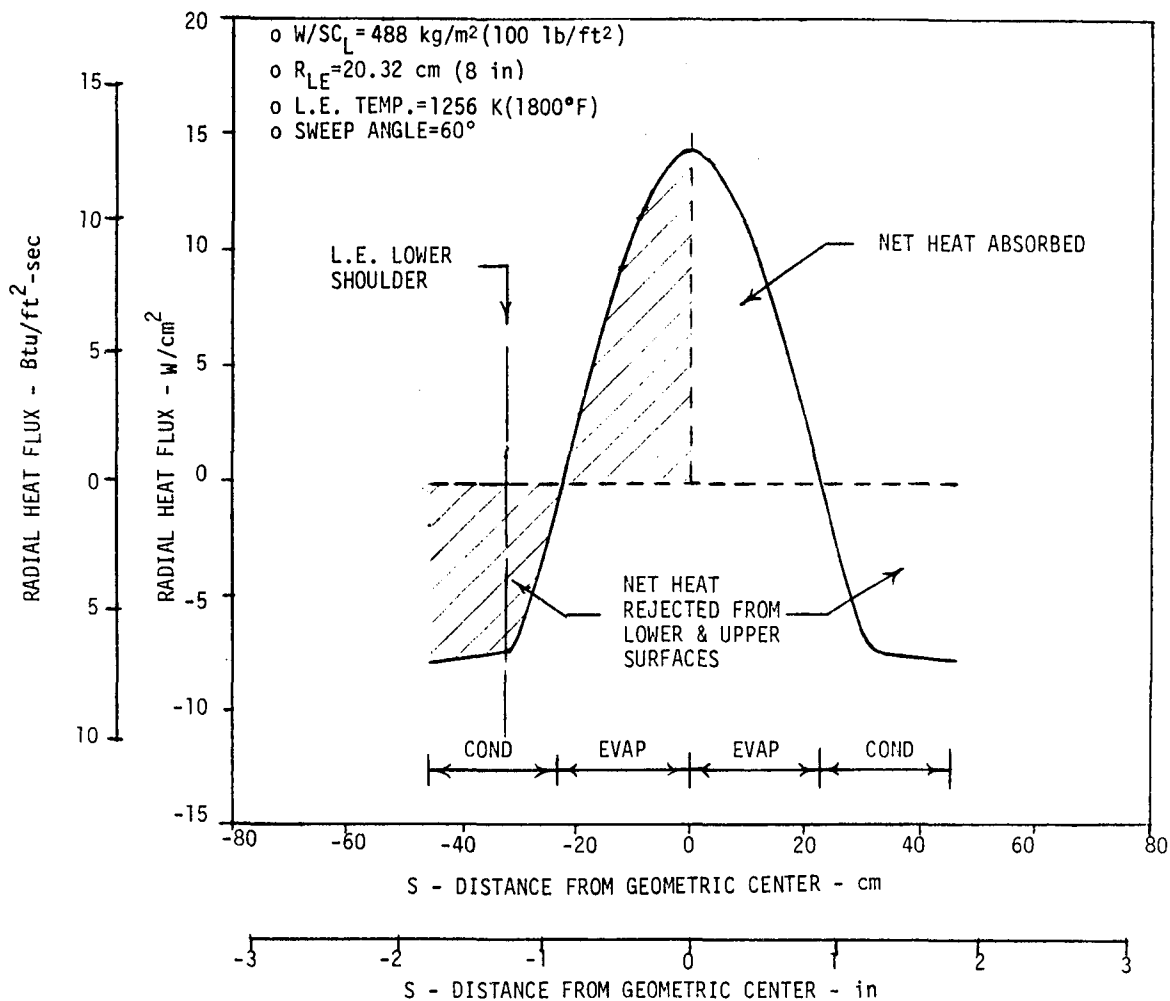


Figure 52. - Leading edge radial heat transfer rates for zero angle of attack.

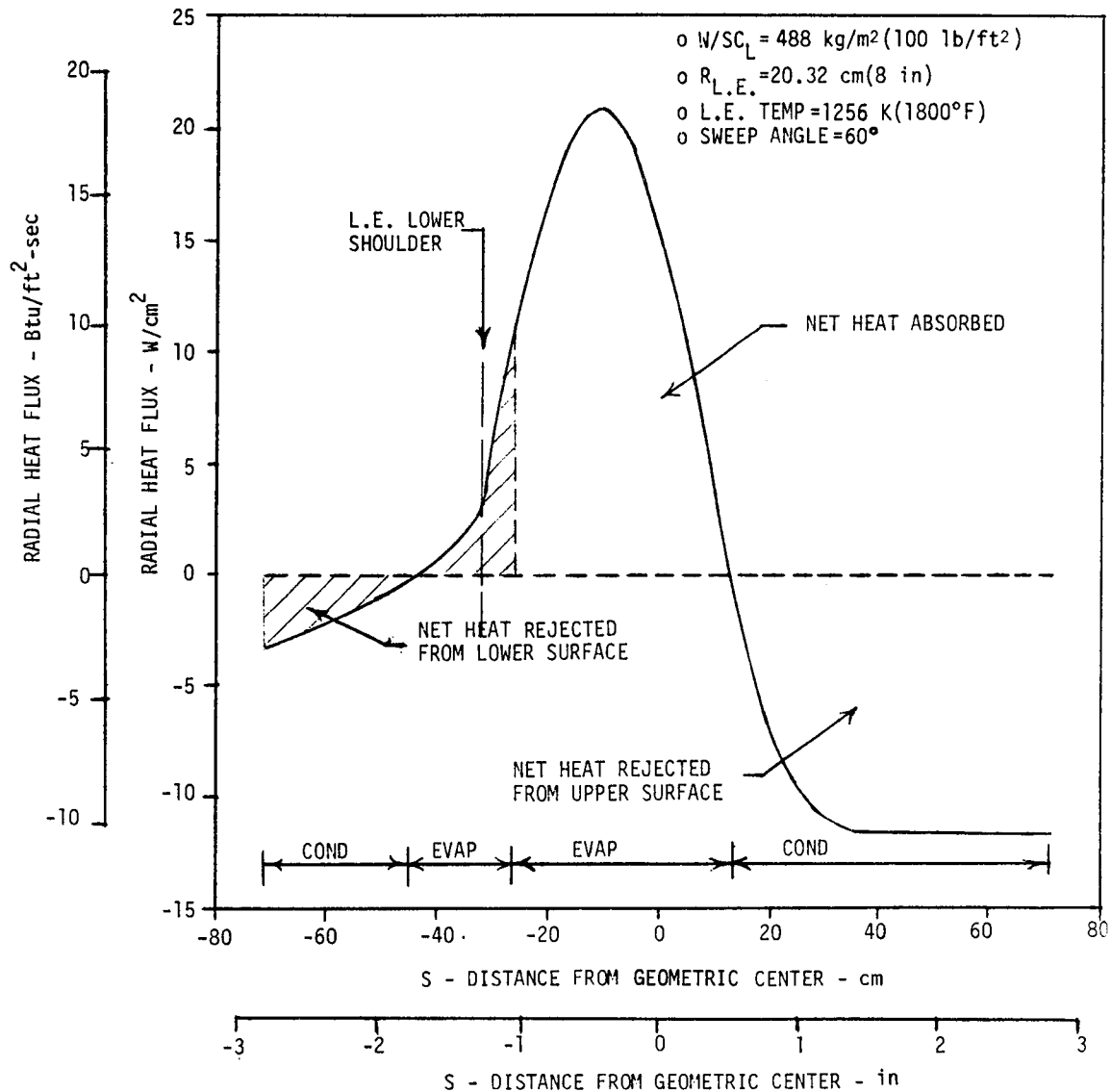


Figure 53. - Leading edge radial heat transfer rates for 30° angle of attack.

For the 0° angle of attack case (Figure 52), the heat transfer rates are symmetrical about the geometric centerline. Wick requirements are different for the upper and lower surfaces because of different elevation heads. The wick for the upper surface transports condensate horizontally back to the leading edge shoulder. Beyond that point, gravity assists the flow of condensate to the heated surfaces of the evaporator. The wick for the lower surface, however, must also be capable of delivering condensate up to the geometric centerline, but against an adverse hydrostatic gravity head. For zero angle of attack, the elevation head is equal to the leading edge radius. The adverse head is reduced for higher angles of attack and smaller leading edge radii, as shown by Figure 54.

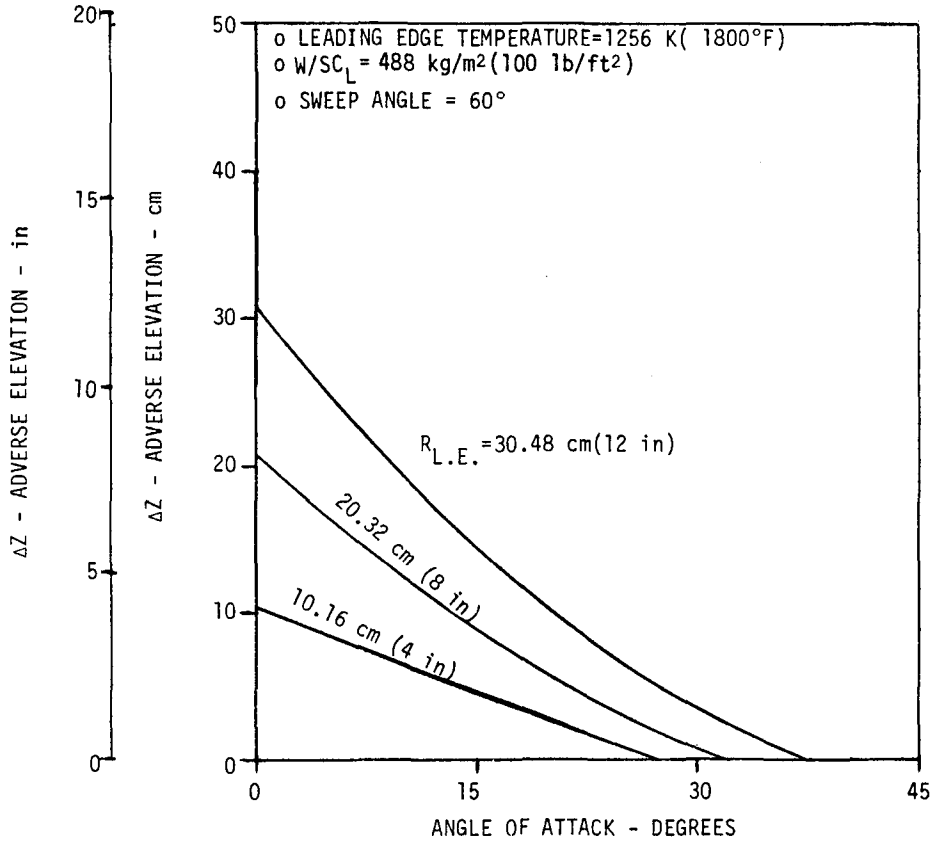


Figure 54. - Heat pipe lower surface adverse elevation.

The lower surface axial heat transfer rate which must be accommodated by wicking is also reduced for higher angles of attack as indicated by Figure 55. The reason for this is that the higher angles of attack result in greater lower surface aerodynamic heating rates, which reduces the ability that these locations can serve as areas of heat rejection or condensation. Thus the magnitude and length of the lower surface condensation and evaporation zones are reduced as angle of attack increases, while the opposite occurs for the upper surface. This is further illustrated by the curves on Figure 55, which define the lower surface axial heat transfer requirement ( $q_{ax} \cdot L_{eff}$ ) as a function of angle of attack. The term  $L_{eff}$  is an effective length which is approximately equal to half the required wicking distance.

The upper surfaces where wicking is required for axial return of condensate and the corresponding values of  $q_{ax} \cdot L_{eff}$  are shown on Figure 56. It is seen that the axial heat transfer rate per unit span required for the upper surface increases significantly at higher angles of attack, because of the increased magnitude and length of the upper surface evaporation and condensation zones.



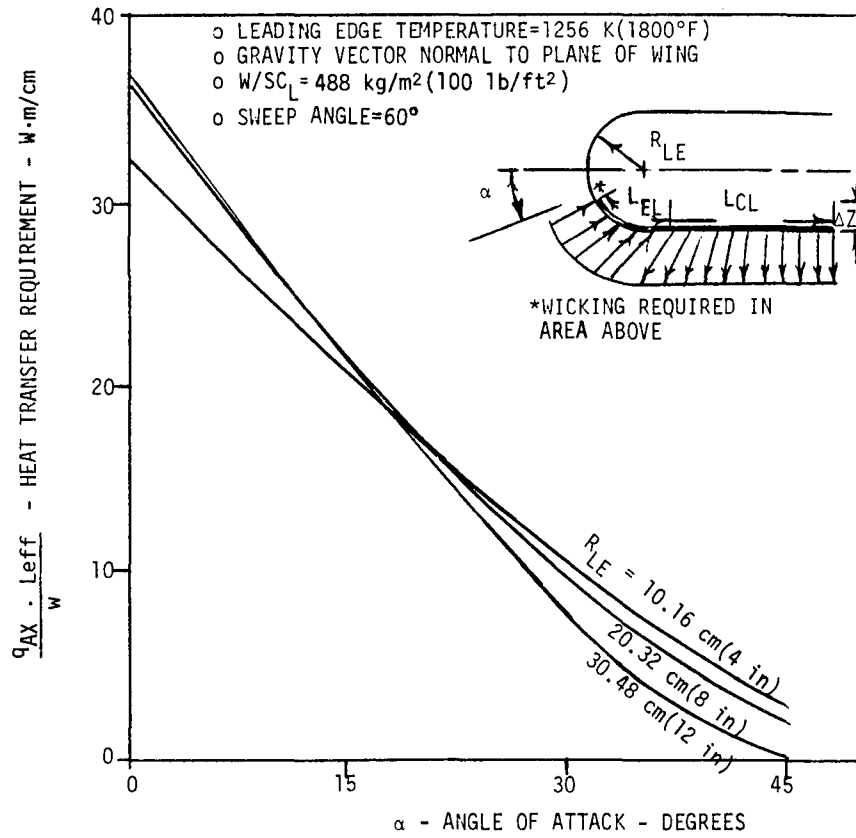


Figure 55. - Heat pipe lower surface heat transfer rates.

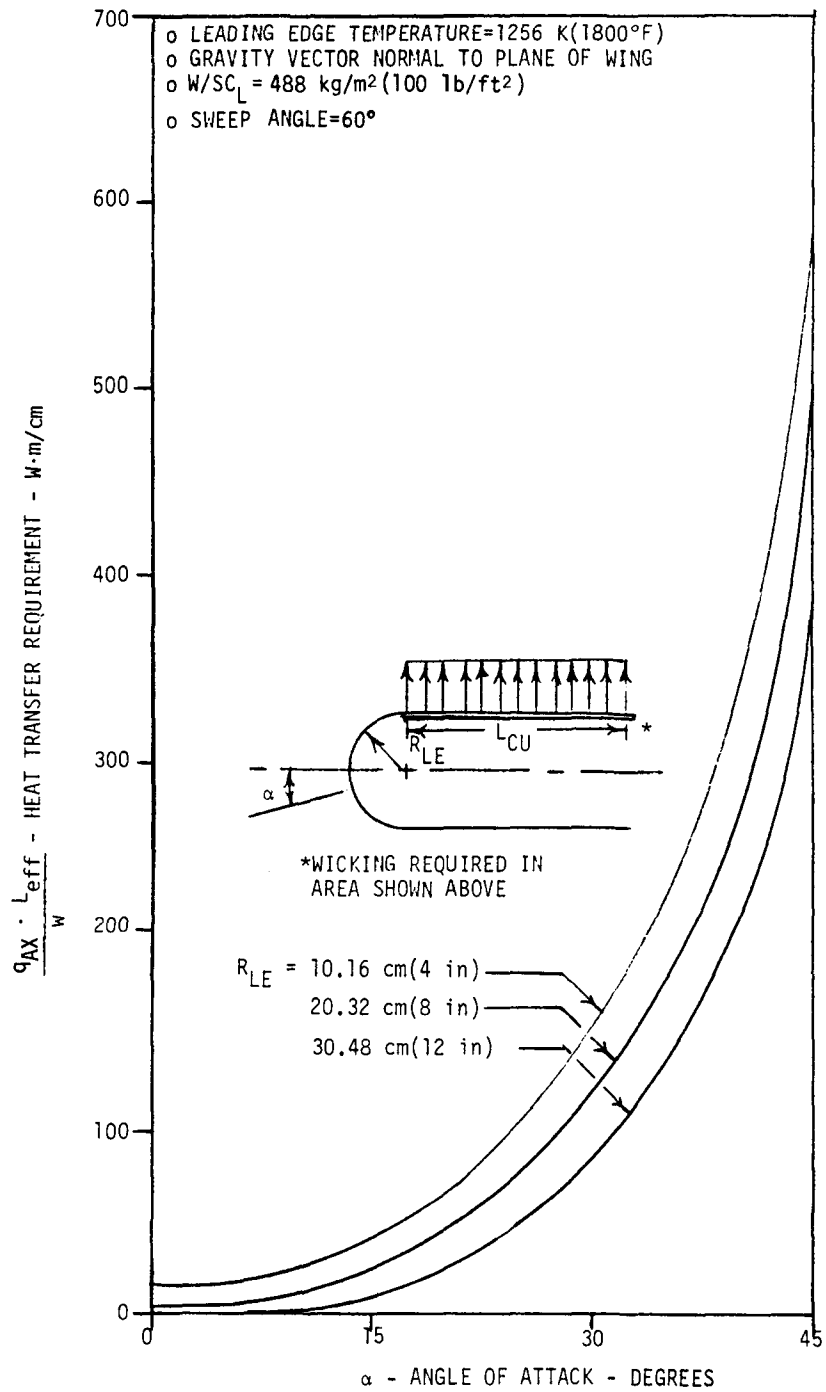


Figure 56. - Heat pipe upper surface heat transfer rates.

Leading edge wick requirements are presented as a function of angle of attack on Figures 57, 58, and 59 for assumed leading edge radii of 10.16 cm (4 in), 20.32 cm (8 in), and 30.48 cm (12 in), respectively. Required values of the wick parameter  $K_p A_w$  (product of wick permeability and wick cross-sectional area) are identified for both lower and upper surfaces. Effects of  $g$  levels normal to the plane of the wing are indicated as well as wick pore size, assuming standard square mesh screen wick. The analyses were based on a 1.27 cm (0.5 in) diameter D-tube heat pipe configuration like that described in Section 4 for the SST0 wing leading edge heat pipe design, but the data would also be applicable to a different shaped heat pipe with the same vapor cross-sectional area. It is seen that for all cases, lower surface wick requirements ( $K_p A_w$ ) are minimal for angles of attack of  $30^\circ$  and greater, requiring only a single layer of 100 mesh screen. As angle of attack is reduced and leading edge radius increased, wick requirements are shown to increase. For these cases, however, a homogeneous wick structure could still be used; but consisting of multiple screen layers. Fine screen would be used to provide higher capillary pumping pressures, combined with coarser screen to provide a higher  $K_p A_w$  for reducing viscous liquid pressure losses.

Upper surface wick requirements are shown on Figures 57, 58 and 59 to be relatively small at low angles of attack. As angle of attack increases, however, upper surface wick requirements also increase because of the higher axial heat loads and associated condenser lengths as depicted on Figure 56. If the upper surface configuration had been swept upward (i.e. like the SST0 wing configuration shown on Figure 19, wick requirements would diminish because of the assistance provided by gravity for condensate return.

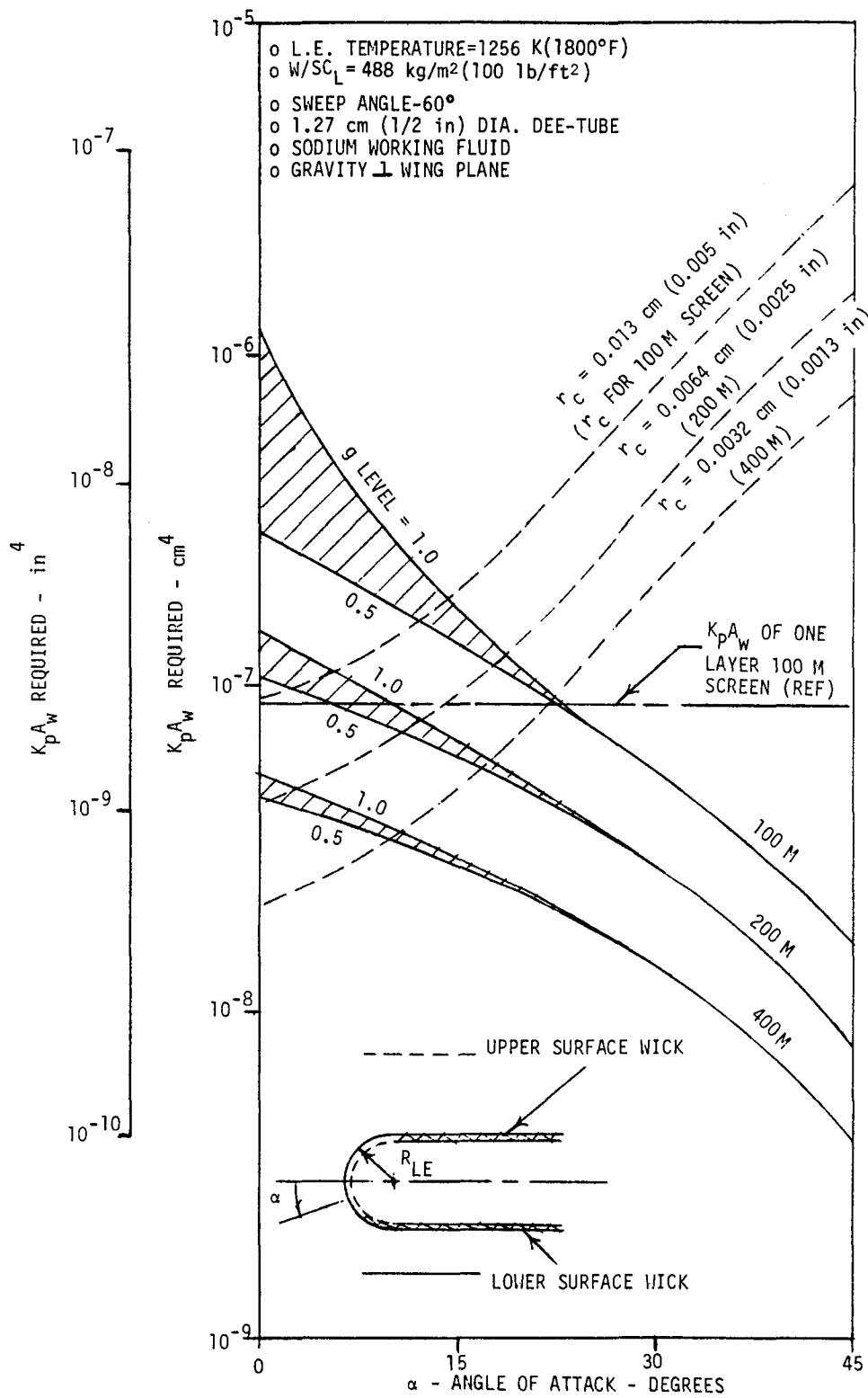


Figure 57. - Heat pipe wick requirements for  $R_{L.E.} = 10.16$  cm (4 in).

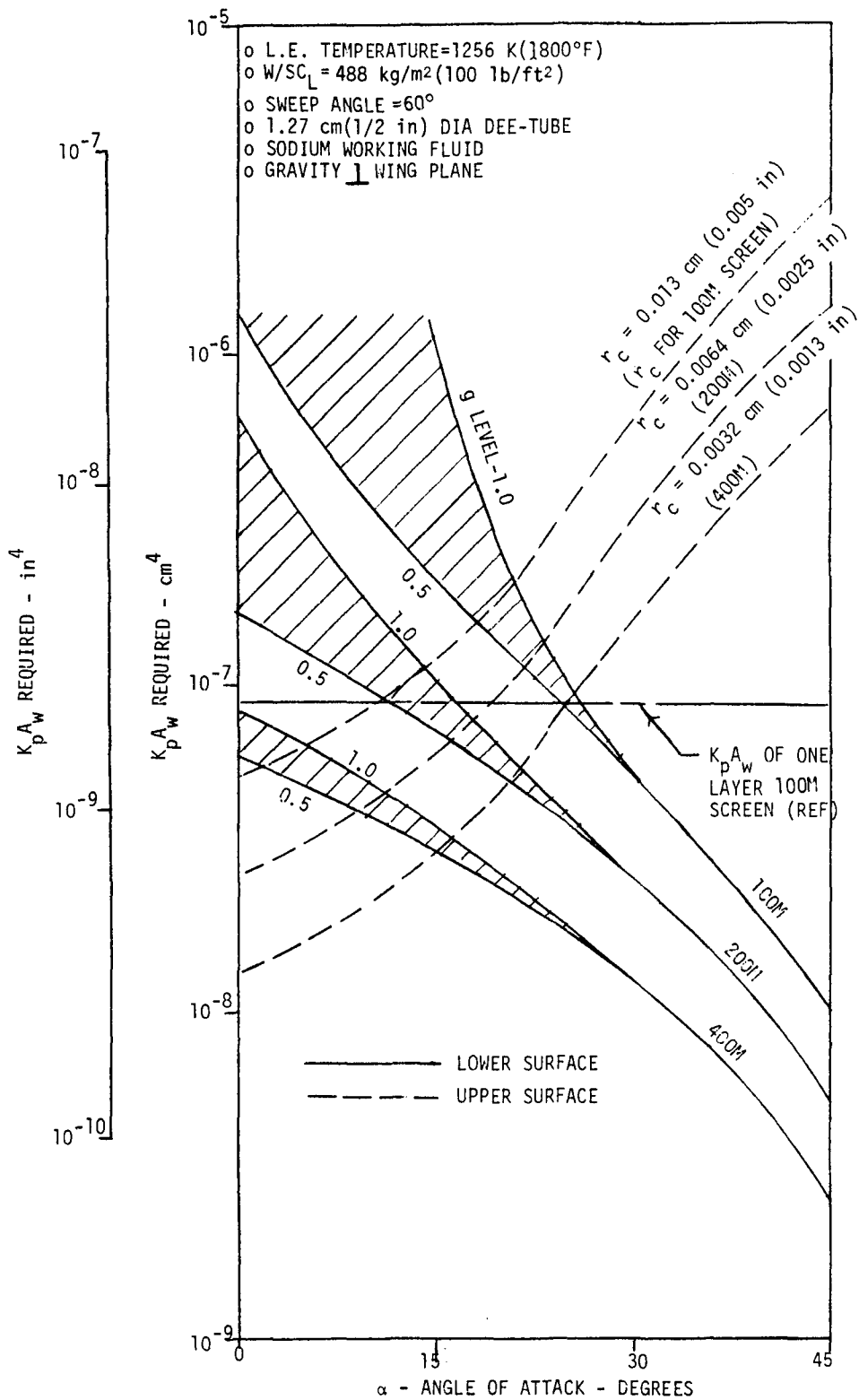


Figure 58. - Heat pipe wick requirements for R.L.E. = 20.32 cm (8 in).

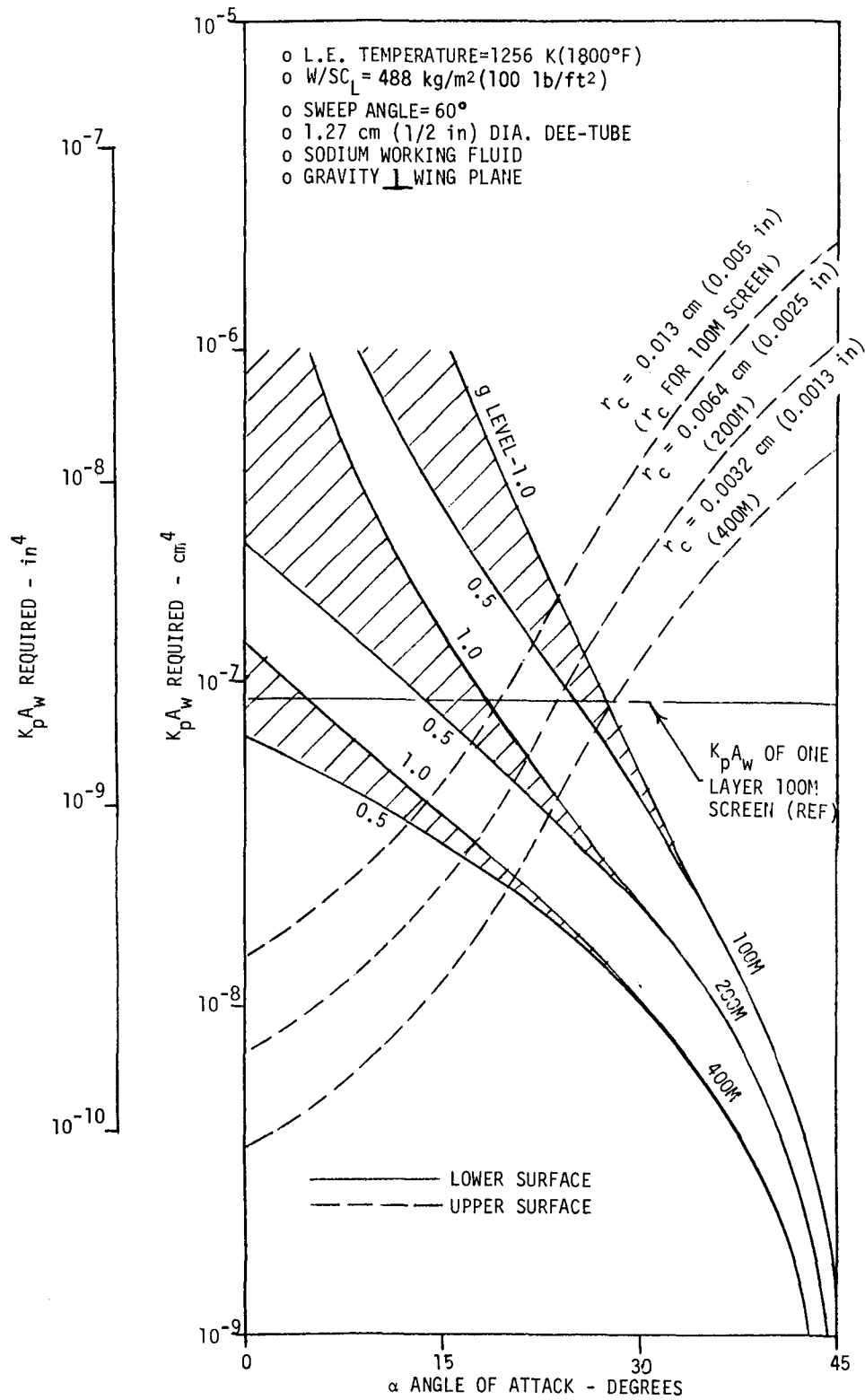


Figure 59. - Heat pipe wick requirements for  $R_{L.E.} = 30.48 \text{ cm (12 in)}$ .

A.2-5 Adverse Gravity Head Effects - The effect of adverse gravity heads on wicking requirements and axial heat transfer performance can be obtained from the curves in Figures 60, 61, and 62 for potassium, sodium, and lithium working fluids. Operation was assumed to be at 1256 K (1800°F) with a 1.27 cm (0.5 in) diameter D-tube heat pipe configuration (or one with an equivalent vapor cross-sectional area). The wick performance parameter  $q_{ax} \cdot L_{eff} / K_p A_w$  represents the axial heat transport capability for a particular wick configuration, and is shown to diminish with increasing adverse gravity heads and coarser screen wicks. Limiting values of adverse gravity heads which can be accommodated are apparent from the asymptotic vertical slope of the curves. For example, reference to Figure 61 shows that essentially no axial heat transport can be provided with a sodium heat pipe employing 400 mesh screen wick if the heat pipe must operate against an adverse gravity head ( $g/g_0 \Delta Z$ ) greater than approximately 45 cm (17.7 in). Performance sensitivity to gravity effects is most pronounced for potassium, sodium, and lithium - in that order.

An axial heat load range of 25 to 1000 W·m was assumed for the analyses of Figures 60, 61, and 62. This range encompasses those values found to be typical of leading edge heat pipe applications investigated in the current study. The upper curves bounding the cross-hatched regions for a particular screen mesh correspond to 25 W·m while the lower curves are for 1000 W·m. The differences between the upper and lower curves reflect the relative effects of vapor pressure losses on heat pipe performance. Vapor pressure losses are shown to be particularly significant for lithium working fluid for the assumed heat pipe configuration cross-section at higher axial heat loads, because of the low lithium vapor density. Only minor effects are shown for potassium and sodium.

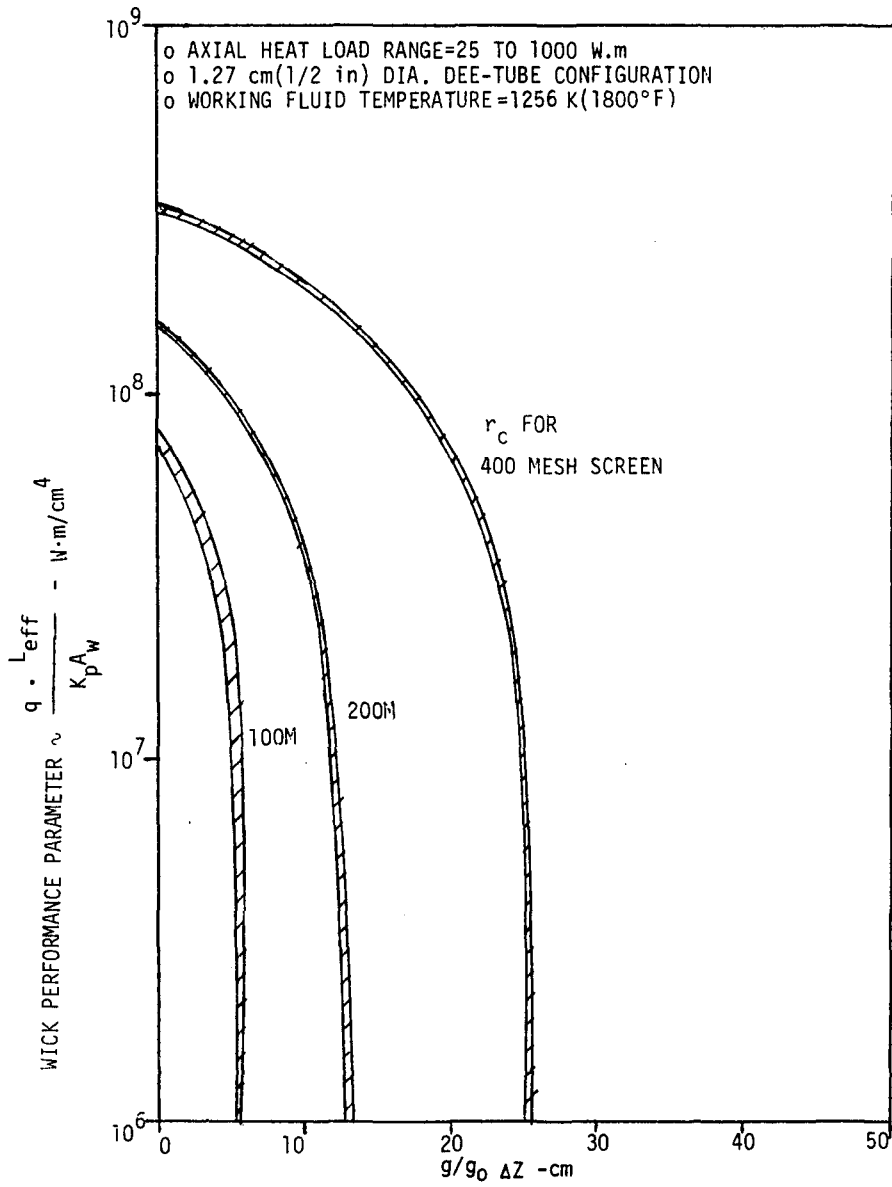


Figure 60 - Effect of adverse head on potassium wicking performance parameter



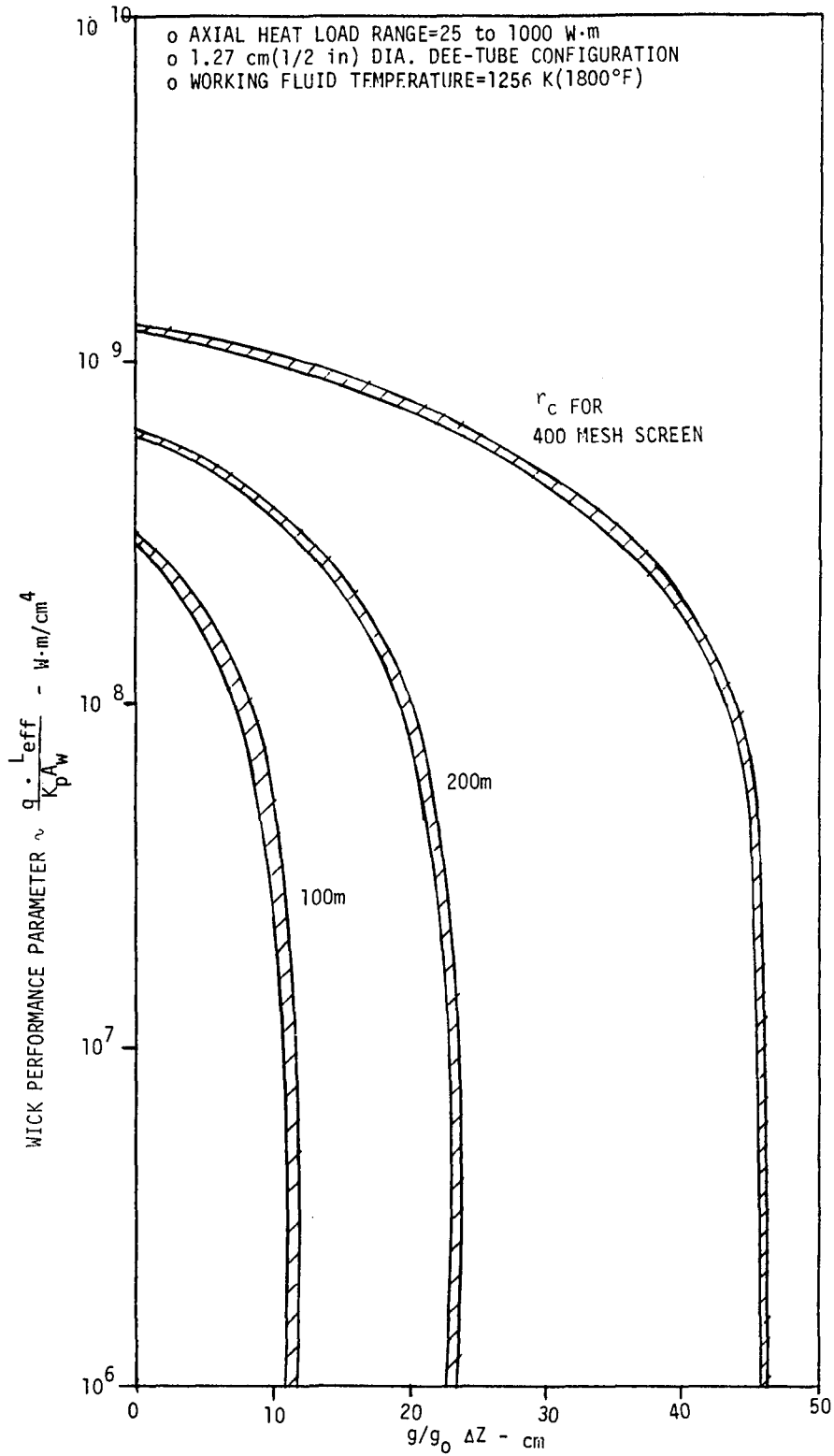


Figure 61 - Effect of adverse head on sodium wicking performance parameter

- o AXIAL HEAT LOAD RANGE=25 TO 1000 W.m
- o 1.27 cm (1/2 in) DIA. DEE-TUBE CONFIGURATION
- o WORKING FLUID TEMPERATURE=1256 K(1800°F)

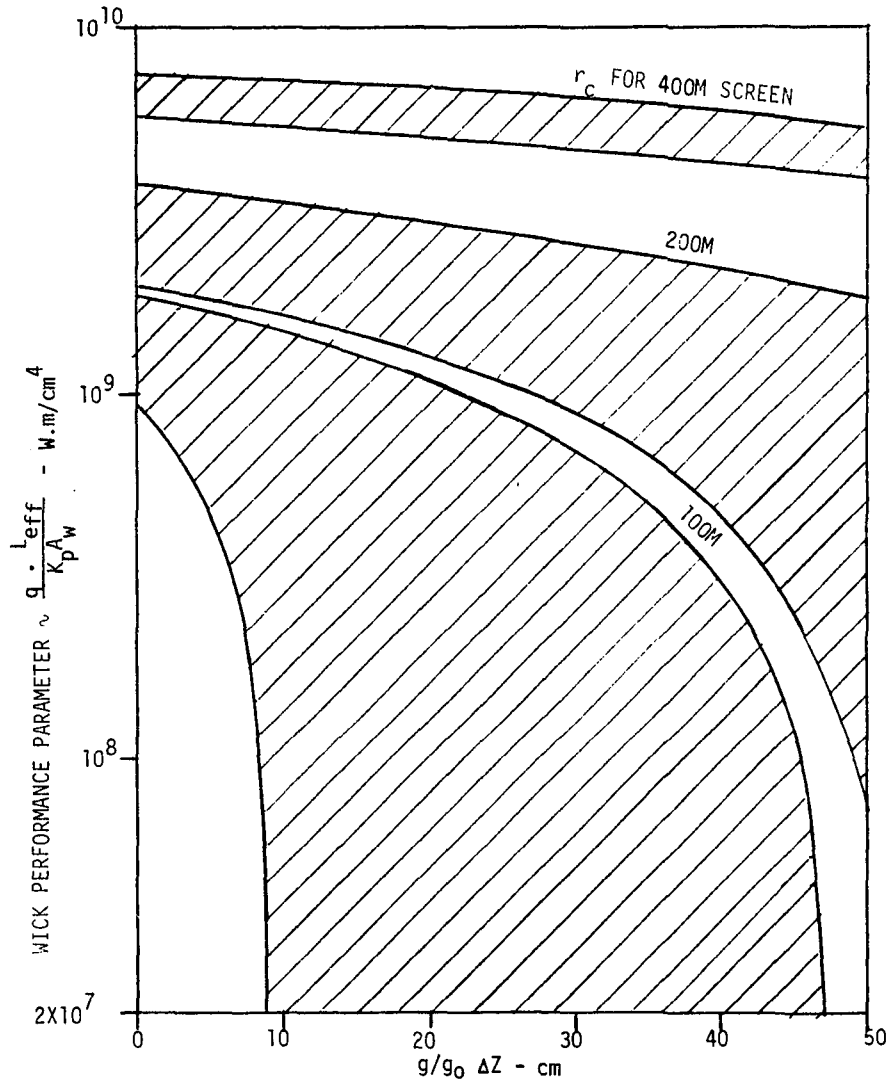


Figure 62 - Effect of adverse head on lithium wicking performance parameter

A.2-6 Heat Pipe Vapor Limits - Figures 63, 64, and 65 show axial heat transfer limits for potassium, sodium, and lithium working fluids as a function of D tube heat pipe diameter, assuming operation at 1256 K (1800°F). These analyses were based on the assumption of a homogeneous wick consisting of 100 mesh screen. The entrainment limit is shown to be lowest and therefore most critical for potassium and sodium. Use of a finer screen, however, would increase the entrainment limit as described in Section A.1. The sonic limit is most critical for lithium working fluid.

Peak axial heat transfer requirements corresponding to a configuration having a glide parameter ( $W/SC_L$ ) of 488 kg/m<sup>2</sup>(100 lb/ft<sup>2</sup>), a 60° wing sweep angle, and a hemicylindrical leading edge radius of 20.32 cm (8 in) are also shown for various angles of attack. Higher axial heat transfer rates are experienced at higher angles of attack as described previously. It can be seen that larger diameter heat pipe passages are required for both potassium and lithium than for sodium.

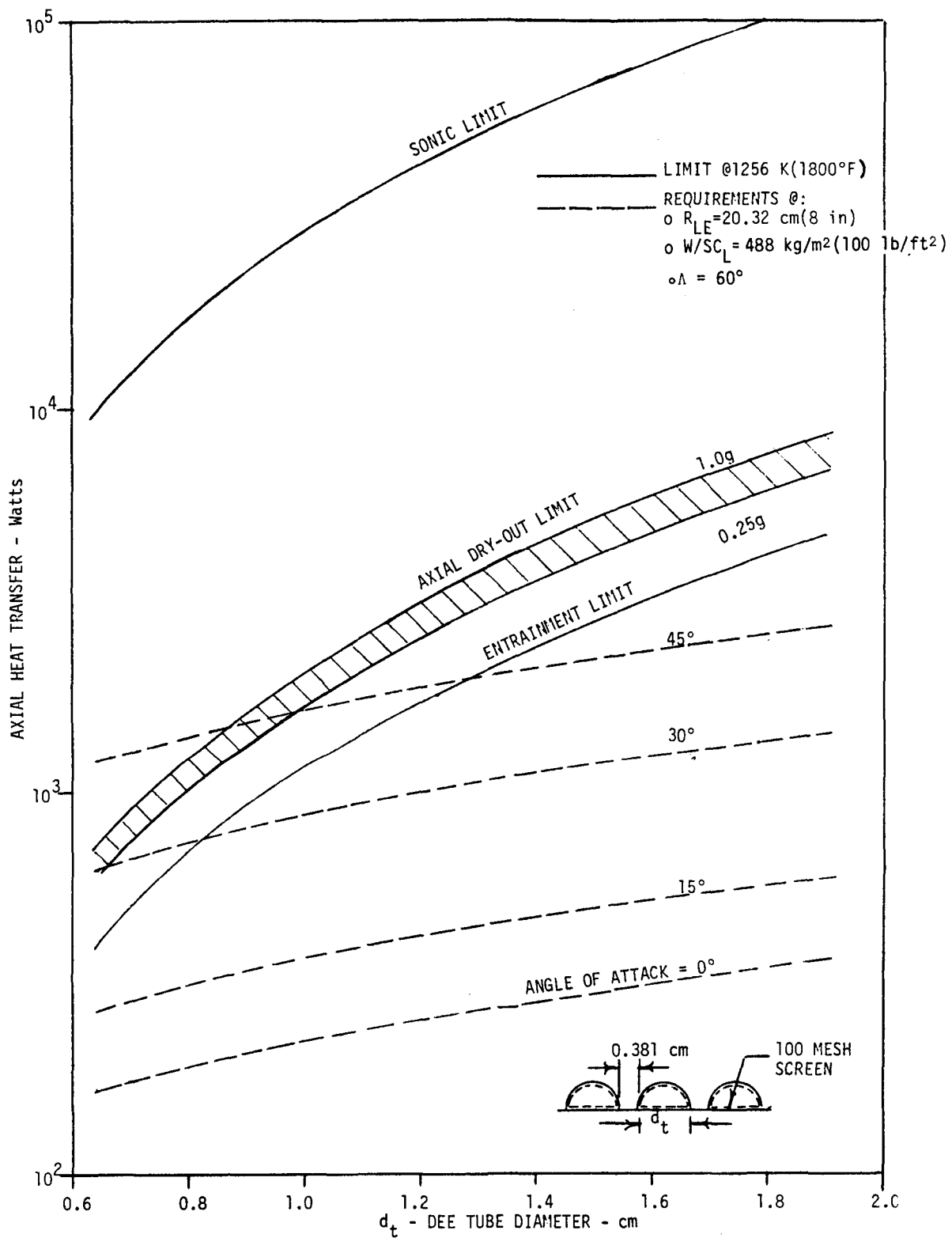


Figure 63. - Heat pipe vapor limits - potassium.

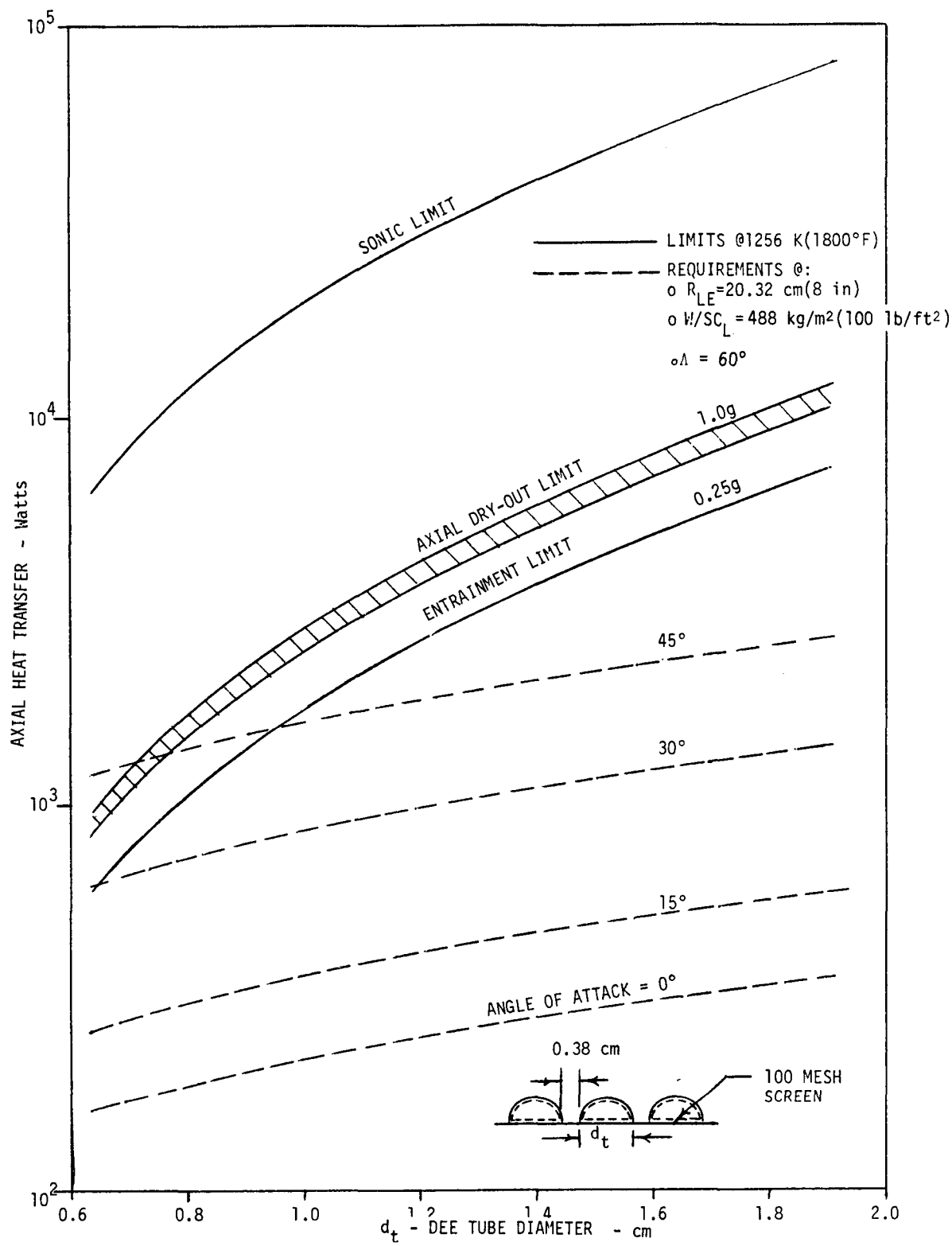


Figure 64. - Heat pipe vapor limits - sodium.

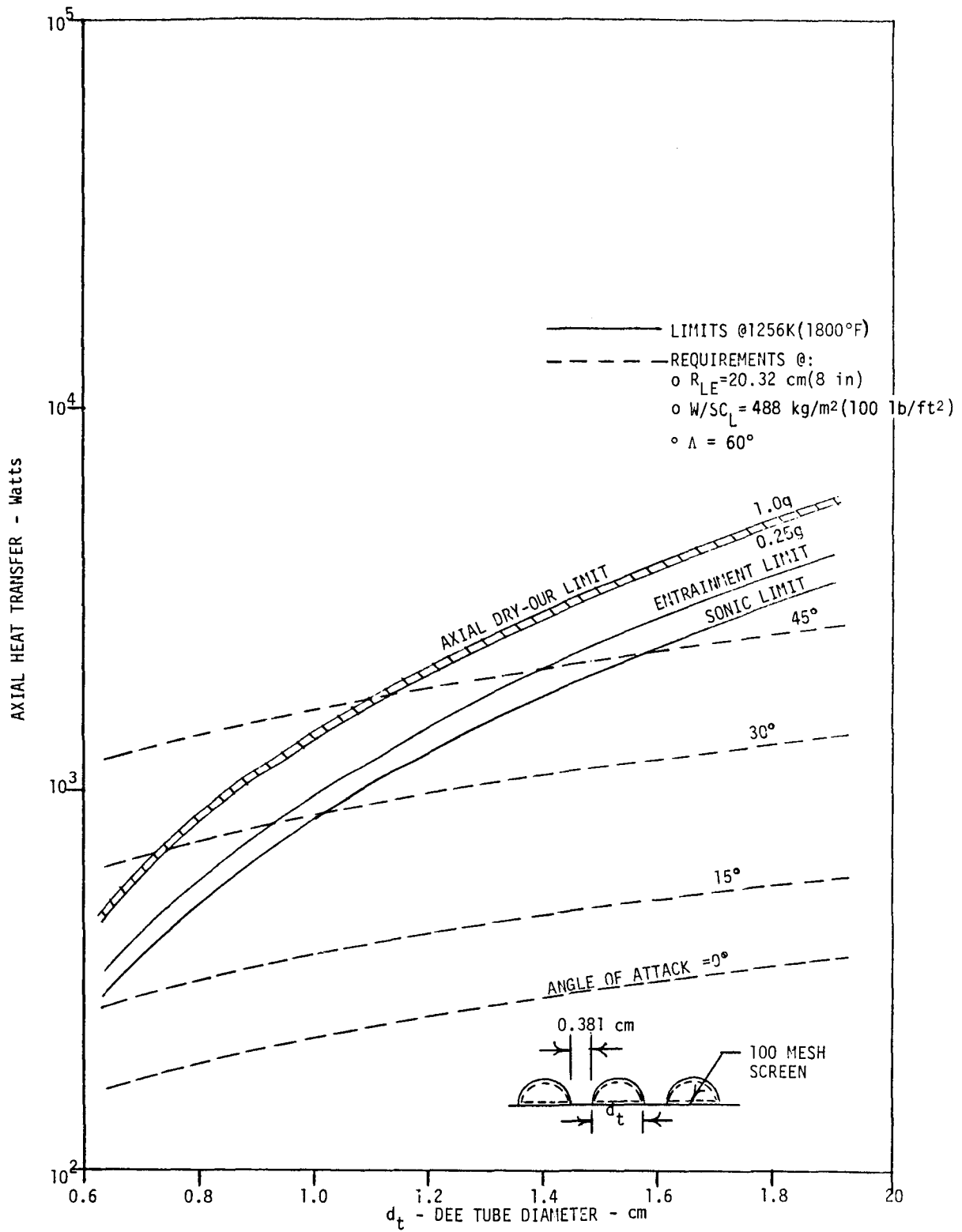


Figure 65. - Heat pipe vapor limits - lithium.

## 7.0 APPENDIX B - HEAT PIPE COOLED HONEYCOMB SANDWICH PANEL

Contractor preliminary design studies of the NASA Langley Airframe-Integrated Scramjet Engine (Reference 19) have recommended the use of a Hastelloy X or Inconel 718 honeycomb panel structure for the sidewall, topwall, and cowl of the engine. These studies have pointed out potential thermal stress problems resulting from high temperature gradients across the panels during the initial start-up upon exposure to high aerodynamic heat fluxes. Results of a transient thermal analysis reported in Reference 19 show the outer face sheet of the honeycomb panel reaching 889 K (1140°F) 125 seconds after start-up, while the inner face sheet rises to only 375 K (215°F). The high temperature differential of 514 K (925°F) across the honeycomb primary structure is of significant concern.

One way suggested by NASA Langley for reducing the temperature gradient is to employ heat pipes for more efficient conduction of heat from the outer to the inner face sheet of the honeycomb panel.

B.1 NASA Design Concept - The basic approach considered by NASA for using heat pipes for this application is illustrated on Figure 66. The honeycomb panel structure would be of a leak-proof design; containing either potassium or sodium working fluid and an internal wick structure consisting of either screen mesh inserts or grooves in the cell walls of the honeycomb core. Evaporation of the working fluid would occur at the face sheet exposed to aerodynamic heating. The fluid vapor would be condensed at the cooler inboard face sheet and the condensate returned, via capillary action of the wick structure, to the hotter face sheet for re-evaporation. The net effect of this design would be to reduce the temperature gradient across the panel to essentially zero, thus avoiding problems with thermal stresses.

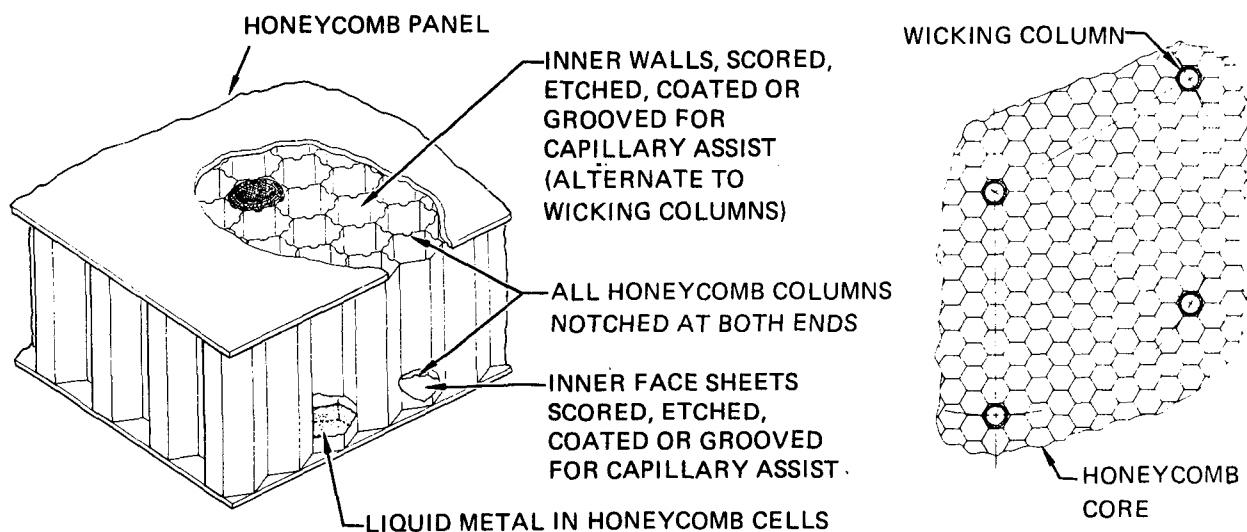


Figure 66. - Heat pipe application in honeycomb panel for low temperature gradient.

Possible design alternatives were explored by NASA in a preliminary manner, although no specific design was defined. Initial design and material options included the choice of the honeycomb container material, heat pipe working fluid, and wick and heat pipe designs. These are summarized as follows:

- o Container Material: Hastelloy X, Inconel 617, Haynes 188, and Nickel 200
- o Working Fluids: Cesium, Potassium, and Sodium
- o Wick Designs: Grooved honeycomb and face sheets, screen inserts, screened honeycomb and grooved face sheets, etc.
- o Heat Pipe Designs:
  - Complete Heat Pipe Cells (CHPC) - where each honeycomb cell is a complete heat pipe with wick, working fluid, and container.
  - Arbitrary Wicked HEAT Pipe Cells (AWHPC) - where selected honeycomb cells act as wicking columns for a designated area.

Concepts considered for the CHPC configuration included partially wicked cells, screen inserts, and node point vaporization as follows:

- o Partially Wicked cells - only part of a cell wall contains a wick (whether grooved, etched, coated or screen). Faces are etched, grooved, etc. The wicked surfaces are coated with a stop-off material.
- o Screen Inserts - small tubular screens are spot-welded to one face, long enough to be partially compressed by the opposite face. Braze sheets would then have holes cut out. The sodium would coat each of the faces and be solid prior to brazing.
- o Node-Point Vaporization - Do not etch faces. Coat the cell walls but not entirely to allow a section for filleting at the top and bottom of each cell.

Concepts considered for the AWHPC configuration included a thin cover foil, grooved wicking columns, and wicked slots as follows:

- o Thin Cover foil - Spot weld a thin cover foil (with holes over cells) to a grooved or etched face sheet to prevent braze alloy from filling the capillaries in the faces. Wicking columns would then be used, either screen or corrugated core type.
- o Grooved Wicking Columns - Use slotted core and do not apply braze alloy near wicking columns. Possible local buckling problems would have to be addressed.
- o Wicked Slots - Use very fine wicks in slots of above design to aid distribution of working fluid. A stop-off coating would be needed for this concept.



A cursory analytical evaluation conducted by NASA showed the general thermal performance feasibility of the heat pipe cooled sandwich using potassium as the working fluid. The analysis assumed the following panel configuration:

- o Hastelloy X material
- o Core depth - 4.57 cm (1.8 in)
- o Cell size - 0.635 cm (0.25 in) hexagonal
- o Cell wall thickness - 0.076 mm (0.003 in)
- o External face sheet thickness - 1.52 mm (0.06 in)
- o Internal face sheet thickness - 1.27 mm (0.05 in)

The peak heat transfer rate to each cell was calculated equal to 2.77 W (0.00263 Btu/sec). The entire surface of the cell walls was assumed to have parallel grooves either scribed or etched the full depth of the core. Groove dimensions equal to 0.114 mm (0.0045 in) wide and 0.0127 mm (0.0005 in) deep were found to satisfy the heat pipe wick requirements during an adverse gravity orientation (i.e. with the heated surface up). The entrainment limit and boiling limit was also calculated and found to be satisfactory.

Honeycomb panel fabrication techniques considered include isothermal solidification, liquid interface diffusion, and diffusion bonding. It was suggested that the honeycomb cell material be scribed or etched prior to fabrication and also be perforated to allow filling the sandwich panel with potassium vapor. The panel could be serviced with a prescribed amount of potassium, kept in a separate container, which was vaporized and allowed to solidify inside the honeycomb sandwich panel. A constant slow heat up of the filled sandwich would allow uniform distribution of the working fluid. The perforated core would facilitate vapor movement in three directions and provide capability for isothermalization in the in-plane direction.

B.2 Design Assessment - The heat pipe cooled honeycomb sandwich panel concept was reviewed and its design assessed on a cursory basis within the limits of available resources. The following aspects of the design are reviewed, with the major emphasis being placed on fabrication considerations:

- o Candidate working fluids
- o Candidate materials
- o Fabrication techniques
- o Servicing and fluid inventory considerations

Candidate Working Fluids - Of the candidate working fluids considered by NASA, potassium would seem to be the better choice for operation at the design maximum temperature of 889 K (1140°F). The transition temperature of potassium vapor from free molecular to continuum flow is approximately 600 K (620°F) vs 725 K (845°F) for sodium, which will provide better start-up characteristics. Performance parameters of potassium expressed in terms of zero g and one g figure of merit (Reference Section A.1) are superior to cesium, which results in higher heat transfer capability for a given wick design. Vapor pressure of potassium at 889K (1140°F) is only around 22 kPa (3.2 psia), which should not impose any significant problems on the honeycomb panel structural design. In addition, long term compatibility of potassium with super-alloy materials has been demonstrated (Reference 9).

Candidate Materials - Possible candidates cited by NASA are Hastelloy X Inconel 617, Haynes 188, or Nickel 200. All of these materials exhibit excellent high temperature strength and creep rates. Corrosion and oxidation resistance to 1311 K (1900°F) are all similar in each material with machinability, weldability, and ease of fabrication being generally about the same. Availability, strength, and creep rate are the selection criteria between the candidate materials.

Fabrication Techniques - In bonding thin gauge sections of the various superalloys together, there are four possible methods of fabrication. These are, tack welding, brazing, diffusion bonding, and a combination of both brazing and diffusion bonding. Each of these possible techniques is discussed as follows:

- o Resistance Welding - Honeycomb cores can be obtained from the Astech Corp (Santa Ana, CA) in Inconel 625, a non-heat-treatable alloy, and Inconel 718, a heat treatable alloy. Cores with cell sizes ranging from 0.735 cm (0.25 in) to 1.095 cm (0.75 in) and depths up to 5.08 cm (2.0 in) can be provided. According to Astech, the addition of capillary grooves to the cell walls poses no large technical problems. The primary development that needs to be done is in the tooling to form the grooves. Specific groove geometries would have to be studied in more detail in order to assess development times and associated costs. The fabrication process employed is one of tack welding; both for joining the cell sheets to each other and also to the face sheets. This method of construction has been demonstrated in the buildup of a titanium honeycomb panel, which is currently being investigated for use as a control fin for the Advanced Harpoon Missile. The core material for this design is corrugated to add stiffness to the overall panel. Similar corrugations might serve as liquid return channel wicks, if they can be made small enough to wick against an adverse gravity head.
- o Brazing - Brazing of Ni-based superalloys is a well established practice. Braze temperatures start at about 1111 K (1540°F) and extend to 1389 K (2040°F). There are a range of braze alloys (most notably in the Ni-Au group) with excellent compatibility and adhesion to the

superalloys. In brazing operations, to limit the flow of the braze alloy and provide an adequate fillet, a stop-off coating is used. These coatings will work by depositing an oxide surface (normally either  $Al_2O_3$ ,  $TiO_2$ ,  $Y_2O_3$ , or some combination of the three) that is tightly adherant to the base metal. These oxide coatings are non-wettable by the braze alloy and prevent flow of the alloy past the edge of the stop-off coating. The oxide coatings are normally then stripped off after the brazing operation. In fabrication of a closed cell honeycomb, the stop-off oxide would remain and be subjected to the liquid alkali metal environment. The liquid metals will, it is suspected, strip the oxygen from the various oxides leading the pure metal on the base and form oxides of the liquid metal. If the stop-off coating sees the liquid metal environment before the flow part of the brazing operation begins, it will cease to function as an effective coating to prevent excessive flow of the braze alloy. Excessive flow results in weak bonds and incomplete sealing. In addition, with the excessive flow, the braze alloy will in all probability fill the capillaries in the heat pipe wick.

- o Diffusion Bonding - Diffusion bonding of Ni-based superalloys has been demonstrated as being feasible, but, except for some aircraft turbine components, it is not currently being used in production. Diffusion bonding of the core to the face sheets holds several advantages. There is no problem with containing excessive run-off, both sheets can be done at the same time, no additional contaminants are introduced into the working fluid, no large fillet is formed, and metallurgical properties are continuous. These somewhat impressive advantages are offset by problems encountered in producing the diffusion bond itself. These include incomplete bonding, necessity for contaminant-free surfaces, and high pressure on the bond surface. Bonding assembly is required under vacuum, with elevated bonding temperatures in the 1167 K - 1389 K (1640°F-2040°F) range.

In diffusion bonding of the honeycomb structure, it would be preferable to bond the face sheets on before charging the system with liquid metal. This requires inter-connecting cells in the honeycomb structure. This method of fabrication allows leaks to be found and repaired in addition to eliminating contamination problems during the bonding process. By performing the diffusion bonding with the core under partial vacuum, trapped gasses in the bond area can be reduced along with some slight reduction of the plan area pressure. After bonding, leak detection can be performed to ensure complete sealing under at least one atmosphere pressure differential. A hard vacuum and heating could then be induced in the core to remove all contaminants before charging with the desired liquid metal.

- o Combination bonding - If it proves to be too difficult to obtain a leak-free bond in the honeycomb core sandwich, a combined brazing/diffusion bonding process has been patented by Rohr Industries under the name Rohrbond.® This consists of diffusing a lower melting temperature metal into the base material and then using the alloyed

surfaces to bond together. Because the alloyed surfaces can be made to flow at temperatures lower than diffusion bonding temperatures, braze type joints can be made to form at lower temperatures and pressures than are required by diffusion bonding. Although the bond is produced by diffusion bonding processes, it is referred to as a braze joint due to its formation of a small fillet and transition at the bond line to a different alloy, both characteristics of brazed bonds. Rohrbond has been demonstrated and used in bonding titanium together, but it has not yet been proven on superalloys. In theory, the process should work on superalloys, albeit at higher temperatures than those at which titanium bonding is performed. Another unknown factor in using the Rohrbond processes on superalloys is the effect the diffusion into the base material will have on the strength properties of the base material.

Based on information provided by Astech as previously indicated, fabrication of the honeycomb panel via tack welding would seem to offer more flexibility to the design. This method might lend itself more to providing capillary grooves in the cell walls for wicking, although additional investigation is needed. Use of screen insert wicks does not appear practical from either a production or cost standpoint.

If only fabrication techniques which have already been proven on superalloys are considered as viable candidates, the honeycomb sandwich should be fabricated by diffusion bonding each face sheet separately using inserts to help maintain core dimensions when bonding the first face sheet onto the core. Bonding should be performed on parts which have been cleaned according to MIL-S-5002 and all bonding surfaces should have a fine surface finish. Vacuum during bonding should be at least  $7 \times 10^{-3}$  torr. Minimum bonding pressure should be 290 kPa (2000 psi) over the plan area of the bonding surfaces. After bonding, the bonded core sandwich should be helium leak checked under a pressure of at least 7.25 kPa (50 psig) for any edge leaks. Leaks can be repaired by brazing or welding the outside edge surface of the core. When repaired and passed by helium leak check, the panel should be heated and the interior subjected to a hard vacuum. The honeycomb sandwich should then be charged and sealed.

Servicing and Fluid Inventory Considerations - Servicing the honeycomb panel with working fluid in the manner suggested by NASA appears to be a reasonable approach. This method would require interconnecting the individual cells by perforations in the cell walls or by some other means. The question of whether all cells can be serviced uniformly cannot be answered without tests. However, it would seem that if sufficient time for servicing is allocated and the panel is evenly heated, near uniform servicing of the cells could be achieved.

The number of cells interconnected would have to be limited though because during operational flight the panel will be subjected to variable heating rates which are both width and axially dependent. Due to the unequal heating rates in flight, working fluid could be deposited non-uniformly among the connected cells (i.e. tending to collect in the cooler regions).

The panel should be serviced with sufficient working fluid to fill the capillaries in the cells as well as any fillets formed at adjoining surfaces. However, from the standpoint of heat capacity requirements during operational flight, the quantity of potassium needed per cell is relatively small. Only 127 J (0.12 Btu) is required to be transferred to the 1.27 mm (.05 in) thick inboard face sheet of each cell in order to increase its temperature to the same level as the exposed outboard face sheet - i.e. from 222 K (-60°F) to 889 K (1140°F). This represents only 0.03 g of potassium per cell which would have to be evaporated at the hot face sheet and condensed on the cooler inboard face sheet.



## 8.0 REFERENCES

1. Camarda, C. J. and Masek, R. V., "Design, Analysis, and Tests of a Shuttle-Type Heat-Pipe-Cooled Leading Edge," ASME 79-ENAs-20, Ninth Intersociety Conference on Environmental Systems, San Francisco, California, July 16-19.
2. Camarda, C. J., "Analysis and Radiant Heating Tests of a Heat-Pipe-Cooled Leading Edge," NASA TN D-8468, August 1977.
3. Niblock, G. A. and Holmgren, J. S., "Study of Structural Active Cooling and Heat Sink Systems for Space Shuttle," MDC Report E0638, June 1972.
4. Hepler, A. K. and Bangsund, E. L., "Technology Requirements for Advanced Earth Orbital Transportation System, Volume 3: Summary Report - Dual Mode Propulsion," NASA Contractor Report 3037, July 1978.
5. Space Shuttle Aerothermodynamic Data Report, "Results of Heat Transfer Test of A 0.017-Scale Space Shuttle Orbiter 140 B Model (Modified 22-0) in the NASA Ames Research Center 3.5-Foot Hypersonic Wind Tunnel (Test OH26)," DMS-DR-2193 NASA CR-151,380, October 1977.
6. Peeples, M. E. and Herring, R. L., "Study of a Fail-Safe Abort System for an Actively Cooled Hypersonic Aircraft," NASA CR-144920, Volume II, January 1976.
7. Herring, R. L. and Stone, J. E., "Thermal Design for Areas of Interference Heating on Actively Cooled Hypersonic Aircraft," NASA CR2828, January 1978.
8. Scuderi, L. F., "Expressions for Predicting 3-D Shock Wave-Turbulent Boundary Layer Interaction Pressures and Heating Rates," AIAA 78-162, Presented to the AIAA 16th Aerospace Sciences Conference in Huntsville, Alabama 16-18 January 1978.
9. Heat Pipe Design Handbook, Part I, NASA-CR-134264, August 1972.
10. Silverstein, C. C., "A Feasibility Study of Heat-Pipe-Cooled Leading Edges for Hypersonic Cruise Aircraft," NASA CR-1857, November 1971.
11. Roark, R. J., Formulas for Stress and Strain, Third Edition, McGraw-Hill Book Company Inc., 1954.
12. Timoshenko, S., Strength of Materials, Part II, Third Edition, D. Van Nostrand Company Inc., March 1956.
13. Structures Handbook, McDonnell Aircraft Company Report 339, Revised 1 June 1973.
14. Kemme, J. E., Keddy, E. S., and Phillips, J. R., "Performance Investigations of Liquid-Metal Heat Pipes for Space and Terrestrial Applications," Proc. 3rd International Heat Pipe Conference, Palo Alto, California, May 22-24, 1978.

15. Chi, S. W., Heat Pipe Theory and Practice: A Sourcebook, Hemisphere Publishing Corporation, 1976.
16. Dunn, P. D. and Reay, D. A., Heat Pipes, Pergamon Press Ltd., 1976.
17. Kemme, J. E., "Vapor Flow Considerations in Conventional and Gravity-Assist Heat Pipes," Proc. 2nd International Heat Pipe Conference, Bologna, Italy, March 31-April 2, 1976.
18. Busse, C. A. and Kemme, J. E., "The Dry-Out Limits of Gravity Assist Heat Pipes with Capillary Flow," Proc. 3rd International Heat Pipe Conference Palo Alto, California, May 22-24, 1978.
19. Killackey, J. J., Katinsky, E. A., Tepper, S., Vuigner, A. A., "Interim Summary Report Thermal - Structural Design Study of an Airframe-Integrated Scramjet," NASA CRI45368, December 1978.





